Universidad Autónoma de Madrid
Department of Biochemistry

Autonomic cholinergic regulation of bone marrow stem cell niches

Doctoral Thesis

Andrés García García

Madrid, 2017

Department of Biochemistry
Faculty of Medicine
Universidad Autónoma de Madrid

Autonomic cholinergic regulation of bone marrow stem cell niches

Doctoral Thesis

Andrés García García
Licenciado en Biología

Director:
Dr. Simón Méndez Ferrer

Centro Nacional de Investigaciones Cardiovasculares - CNIC
Instituto de Salud Carlos III – ISCIII
University of Cambridge

…A toda la gente que confió en mis posibilidades…

Acknowledgements

Más de cuatro años ha sido la duración de esta montaña rusa llamada doctorado. Un buen puñado de días que han dado para muchas horas de intenso trabajo, pero también para incontables experiencias junto a magníficas personas. Mucha gente que me ha dado minutos de su vida, algo que yo no dudo ni un segundo en agradecerles.

Empezando por la persona que ha hecho esto posible. Quiero darle las gracias a Simón por depositar en mí toda su confianza desde aquella primera llamada en la primavera de 2011. Han sido muchos años cargados de muchos buenos momentos y alguno que otro no tan bueno. Si bien los primeros han hecho que disfrutara de esta aventura científica, son los segundos los que me han hecho crecer como persona con la consigna de que rendirse no es una opción. Entre otras muchas cosas, él me ha enseñado que la perseverancia es el camino de una carrera científica, que el sentido debe ser el de la mejora y que el tiempo es muy valioso. Gracias por cambiar mi vida en todos los sentidos.

En segundo lugar quiero agradecer a todas aquellas personas que algún momento formaron parte de nuestro laboratorio en el CNIC. Para describir lo que Joan me ha enseñado necesitaría otra tesis. Por ello sencillamente le doy las gracias por ser como es y por enseñarme la curiosidad científica. Ana Martín completaba aquel primer equipo, y me enseñó que primero somos personas y luego científicos. Ambos me acogieron desde el primer día y me cuidaron como a un hijo. Eternamente agradecido.

Pero no me puedo olvidar de todos aquellos que vinieron después. Gracias a Abel por enseñarme que el rigor y el sentido crítico es la única magia que hace la ciencia. Qué decir del "Doctorsito y la morita", como el agua y el aceite pero miscibles para formar el tándem perfecto. De Dani aprendí que la calma y el razonamiento hacen al buen profesional (gustos musicales aparte). Sandra me mostró que la espontaneidad y los sentimientos sin filtros son atributos de las mejores personas (risas aparte). Mil gracias. Para nosotros quedan esos descansitos… A Lorena le agradezco que me enseñase que en ciencia, al igual que en la vida, no hay recompensa sin sacrificio. A Raquel le doy las gracias por su naturalidad y por su contagiosa alegría.

Gracias al maestro Xavi por convencerme que la histología es un arte. También a Oliver y Carmen, dos magníficos valientes con las ideas muy claras. A Carlos le agradezco todos esos días en los que paliamos el duro trabajo a base de risas. Finalmente, gracias a Sara por enseñarme que pase lo que pase la dignidad y la autenticidad es innegociable.

Este excelente grupo humano era un órgano más del organismo llamado CNIC. Gracias a todas las "células" de esta institución por ayudarme de una u otra manera. De la nutrición se encargaba "multiusos" Ángel. Gracias por esa alegría día tras día y por esos señores desayunos. Mención especial también para Sergio, gran compañero de piso y mejor persona. Pero también agradezco a todos esos nombres propios que formaron parte de la 3 sur, pues ellos me confirmaron que en el sur se vive muy pero que muy bien.

El traslado a Cambridge me trajo nuevas aventuras y me demostró que la calidad humana es universal. Desde España vino María, a ella le agradezco su optimismo ante la adversidad y toda la ayuda en la "mudanza". A los "locales" Anne, Claire y Tom les doy las gracias por mostrarme toda la riqueza y tradiciones del Reino Unido. Adicionalmente, a Claire le agrezco toda su dedicación, compromiso y ayuda experimental cuando más lo necesitaba. También tengo que agradecer a Dorian y a Flavia de Italia. El primero me hizo entender que el trabajo en el cuarto de cultivos es importante, pero ambos me confirmaron que el café lo es más. Igualmente gracias a Justyna de Polonia, por ser la coordinadora de fiestas; a Antony de Taiwán, por su dedicación; a Chrysa de Grecia, por su amabilidad y generosidad; a Cora de Suiza, por su entusiasmo y alegría; y a Araceli de Méjico por su positividad. A todos les agradezco que me hayan dejado aprender de ellos y su importante contribución para la culminación de esta tesis.

También le doy las gracias a todas las personas de la Universidad de Cambridge que me han ayudado a desarrollar mis proyectos con la máxima calidad científica posible durante los dos últimos años, y también por su acogida, apoyo y estímulo constante para la carrera científica de excelencia.

Ahora bien, la aventura en Cambridge estaría incompleta sin la gran familia de los "Survivors". Gracias al apoyo de Aihnoa, Cesar, Dani, Jon, Manu, María, Mikel, Quique y de todos aquellos que ya se fueron, no me he sentido solo ni un solo segundo durante estos años. "El Cherry" permanecerá siempre en mi recuerdo.

Igualmente gracias a George y Cay por tratarme como a un hijo desde el primer día.

Y volviendo a los orígenes, tengo que agradecer a todos esos amigos "biólogos sexis": Adri, Álvaro, Ana S, Ana V, Cha, Cris, Elena, Inma, Olga, Rosa y Yasir. Ellos no solo me recuerdan lo grande que fue la promoción 2012/2017 de biología en Málaga, sino que demuestran que los amigos de la universidad son para toda la vida.

Sería imposible citar a todos aquellos amigos que me han acompañado a lo largo de estos años, pero especialmente me siento en deuda con la familia Infantes Lorenzo. Ellos me enseñaron que la familia, al igual que los amigos, también se puede elegir. No hay palabras para describir todo el amor que me han dado durante tantos años. A Alberto, que lo vi crecer; a Laura, por tantos momentos nuestros; y a José Antonio, porque contigo empezó todo…

Agradezco a todos los miembros de mi familia sencillamente por eso, porque son familia y como tal siempre me han animado a perseguir y pelear por mis sueños. Abuelos, tíos y primos que en mayor o menor medida me han ofrecido su apoyo incondicional. Especialmente agradecido estoy a mi abuela María porque no necesita entender bien lo que hago para hacerme saber que está orgullosa de mí. También gracias a mis "germanos" Juan y Jesús pues da igual con qué frecuencia hablemos pues el tiempo se detiene entremedias.

A Claudia, la persona que llena de felicidad e ilusión cada uno de mis días, no basta con agradecerle todo lo que ha hecho para que esta tesis sea una realidad. Sencillamente sin ella no hubiese sido posible y solo espero poder devolverle día a día todo lo bueno que se merece. Nichts ist unmöglich. Gemeinsam sind wir stark.

Por último y porque no somos nadie sin nuestras raíces, agradezco a las dos personas que me dieron la vida y me educaron en los valores del respeto, la constancia y la superación, mis padres. Ellos me enseñaron que no hay virtud sin humildad, como no hay éxito a largo plazo sin esfuerzo. A ellos les debo todo lo que fui, soy y seré; y simplemente eso ya se merece el mayor de los agradecimientos.

Summary

Haematopoietic stem cells (HSCs) reside in specialized microenvironments in the bone marrow (BM) called “niches”. BM HSC niches comprise different stromal cell types that directly or indirectly contribute to maintain and regulate HSCs and, in turn, haematopoiesis.

In the last two decades, multiple studies have revealed the importance of numerous BM stromal cell types as modulators of different HSC functions, like migration/trafficking and proliferation/quiescence. Many studies have suggested that specific niches close to the bone surface (endosteal) or around sinusoids (perisinusoidal) can regulate distinct HSC states. How these different niches cooperate to coordinate various HSC activities according to organismal demands remains unclear.

In this thesis, novel neural signals have been found to regulate different HSC functions in spatially separated niches during circadian time cycles. Central cholinergic signals from the parasympathetic nervous system antagonise BM sympathetic noradrenergic activity during the nocturnal phase. Cholinergic inhibitory signals indirectly diminish β3-adrenergic signalling in perisinusoidal niches, reducing HSC egress at a specific circadian time. Cholinergic signals also appear to contribute to bone remodelling via unknown mechanisms. In addition, a specific type of sympathetic neuron that switches from noradrenergic to cholinergic fate during the first postnatal weeks has been identified in endosteal niches. Sympathetic cholinergic fibres might promote BM colonisation of HSC through Cxcl12 induction in immature BM niches. In adult mice, sympathetic cholinergic innervation targets bone-associated nestin^{+} BM stromal cells and promotes *Cxcl12* expression, favouring HSC quiescence and long-term maintenance.

In summary, neural signals from both branches of the autonomic nervous system cooperate to orchestrate and integrate different HSC features in a spatiotemporal context. While sympathetic noradrenergic signals activate HSCs and favour their trafficking, parasympathetic and sympathetic cholinergic activity promote HSC maintenance signals that counterbalance the first. This precise regulation might help to adjust stem cell functions to meet physiological requirements.

Resumen

Las células madre hematopoyéticas (HSCs) residen en microambientes especializados de la médula ósea llamados “nichos”. Los nichos de HSCs de la médula ósea engloban a las células estromales y moléculas que directa o indirectamente contribuyen a mantener y regular las HSCs y, así, la hematopoyesis.

En las dos últimas décadas, múltiples estudios han demostrado la importancia de distintos tipos de células estromales como reguladores de las propiedades de las HSCs, como su migración/tráfico y su proliferación/quiescencia. Muchos de estos estudios han sugerido que determinados nichos próximos a la superficie ósea (endostiales) o alrededor de los sinusoides (perisinusoidales) están especializados en regular distintas funciones de las HSCs. Pero aun queda por aclarar como esos nichos pueden coordinarse entre sí de acuerdo a las necesidades del organismo.

En esta tesis se han encontrado nuevas señales neurales capaces de regular diferentes funciones de las HSCs en nichos separados y en distintos momentos del día. Señales parasimpáticas colinérgicas centrales antagonizan la actividad simpática noradrenérgica durante la noche. Estas señales disminuyen la señalización adrenérgica β3 en nichos perisinusoidales, y reducen la salida circadiana de las HSCs hacia la sangre. Además, las señales colinérgicas parecen contribuir al remodelado óseo por vías aun desconocidas. Por otra parte, en los nichos endostiales se ha identificado un tipo específico de neurona simpática que cambia de fenotipo noradrenérgico a colinérgico. Estas fibras podrían contribuir a la colonización de la médula por parte de las HSCs durante el desarrollo postnatal al estimular la producción de Cxcl12. En estadío adulto, estas fibras inervan algunas células estromales nestina^{+}, incrementando su expresión de *Cxcl12* y favoreciendo la quiescencia y mantenimiento a largo plazo de las HSCs.

En resumen, este trabajo sugiere que la señales neurales procedentes de ambas ramas del sistema nervioso autónomo coordinan distintas funciones de las HSCs en un contexto espacio-temporal. Mientras que las señales simpáticas noradrenérgicas activan a las HSCs y estimulan su tráfico, la señalización parasimpática y simpática colinérgica promueve señales de mantenimiento que equilibran las primeras. Esta regulación precisa podría ayudar a ajustar las funciones de las células madre de acuerdo con las necesidades fisiológicas.

Table of Contents

List of Figures

List of Tables

Abbreviations

µCT	Micro computer tomography
5-FU	5-fluoruracil
6-OHDA	6-hydroxydopamine
ABC	Avidin-Biotin complex
Ach	Acetylcholine
AchE	Acetylcholinesterase
Adrb	Adrenergic receptor beta
AGM	Aorta gonad mesonephros
Ang1	Angiopoietin-1
ANOVA	Analysis of variance
ANS	Autonomic nervous system
APC	Allophycocyanin
Artn	Artemin
BM	Bone marrow
Bmal1	Brain and muscle ARNT-Like 1
BMP	Bone morphogenetic protein
BMSC	Bone marrow-derived mesenchymal stem and progenitor cell
BSA	Bovine serum albumin
BV	Brilliant violet
$CaCl_2$	Calcium chloride
CAR	Cxcl12-abundant reticular
CD"x"	Cluster of differentiation "x"
cDNA	Complementary deoxyribonucleic acid
CFU	Colony-forming unit
CFU-C	Colony-forming unit culture
CFU-F	Fibroblastic colony-forming-unit
CFU-OB	Osteoblastic colony-forming unit
ChAT	Choline acetyltransferase
Chrm1	Muscarinic receptor type-1
Chrna	Cholinergic receptor nicotinic alpha

Clec-2	C-type lectin-like receptor 2
CNS	Central nervous system
CNTF	Ciliary neurotrophic factor
CT-1	Cardiotrophin-1
Ctg	UDP-galactose;ceramide galactosyl-transferase
Cxcl4	C-X-C motif chemokine 4
Cxcl12	C-X-C motif chemokine 12
Cxcr4	C-X-C chemokine receptor type 4
Cy	Cyanine
DAPI	4’,6-diamidino-2-phenylindole
DBH	Dopamine-b-hydroxylase
dH_2O	Distilled water
Dhh	Desert hedgehog
DNA	Deoxyribonucleic acid
dNTP	Deoxynucleotide
DPD	Deoxypyridinoline
E”x”	Embryonic day “x”
EDTA	Ethylenediaminetetraacetic acid
ELISA	Enzyme-linked immunosorbent assay
FBS	Foetal bovine serum
FDR	False discovery rate
FITC	Fluorescein isothiocyanate
FL	Foetal liver
GAP-43	Growth associated protein 43
G-CSF	Granulocyte-colony stimulating factor
GDNF	Glial cell line-derived neurotrophic factor
GFP	Green fluorescence protein
Gfra	GDNF family receptor alpha
Gs	G protein subunit
GSEA	Gene set enrichment analysis
H42	Hoechst 33342
HCl	Hydrochloric acid

HEPES	Hydroxyethyl piperazineethanesulfonic acid
hi	High
HRP	Horseradish peroxidase
HSC	Haematopoietic stem cell
HSPC	Haematopoietic stem and progenitor cell
i.p	Intraperitoneously
i.v	Intravenously
IT-MPP	Intermediate multipotent progenitor
KCl	Potassium chloride
Kitl	KIT ligand
KO	Knock-out
Lepr	Leptin receptor
LIF	Leukemic inhibitory factor
LIN	Lineage
LMPP	Lymphoid-primed multipotent progenitors
lo	Low
LSK	$LIN^-SCA1^+cKIT^+$
LT-HSC	Long-term haematopoietic stem cell
LTR	Long-term repopulation
Ly-6A/E	Lymphocyte antigen 6A-2/6E-1
Ly-6G	Lymphocyte antigen 6 complex, locus G
MCAM	Melanoma cell adhesion molecule
MMP-9	Matrix metalloproteinase-9
Mpl	Myeloproliferative leukaemia protein
MPP	Multipotent progenitor
mRNA	Messenger ribonucleic acid
NaCl	Sodium chloride
Nes	Nestin
NES	Normalized enrichment scores
NG2	Neuron-glial antigen 2
NPY	Neuropeptide Y
Nr3c1	Nuclear receptor subfamily 3 group C member 1

Nrtn	Neurturin
Opn	Osteopontin
P/S	Penicillin-streptomycin
PBS	Phosphate-buffered saline
PCR	Polymerase chain reaction
PDGFr	Platelet-derived growth factor receptor
PE	Phycoerythrin
PerCP	Peridinin chlorophyll protein complex
PFA	Paraformaldehyde
PGP 9.5	Protein gene product 9.5
Pf4	Platelet factor 4
PNS	Parasympathetic nervous system
Pspn	Persephin
PY	Pyronin Y
qPCR	quantitative polymerase chain reaction
RCF	Relative centrifugal force
RNA	Ribonucleic acid
Rpm	Revolutions per minute
RT	Room temperature
s.c	Subcutaneously
SCA1	Stem cells antigen 1
Scf	Stem cell factor
Sdf-1	Stromal cell- derived factor 1
SDS	Sodium dodecyl sulphate
SEM	Standard error of the mean
SLAM	Signalling lymphocyte activation molecule
SNS	Sympathetic nervous system
Sp1	Specificity protein 1
ST-MPP	Short-term multipotent progenitor
TE	TRIS-EDTA
Tgf-β	Transforming growth factor β
TH	Tyrosine hydroxylase

Tie	Tyrosine kinase with immunoglobulin-like and EGF-like domains
TMB	Tetramethylbenzidine
TNB	TRIS-NaCl-blocking buffer
Tpo	Thrombopoietin
TRAP	Tartrate-resistant acid phosphatase
TRITC	Tetramethylrhodamine isothiocyanate
TZ	Transition zone
UDP	Uridine diphosphate
VAChT	Vesicular acetylcholine transporter
VIP	Vasoactive intestinal peptide
VPAC1	Vasoactive intestinal peptide receptor type 1
WT	Wild type
ZT	Zeitgeber time

“Ever tried. Ever failed. No matter. Try again. Fail again. Fail better”

Worstward Ho - Samuel Beckett

1 Introduction

1.1 The haematopoietic system

Haematopoiesis - the production of blood cells – primarily takes place in the bone marrow (BM), which is located inside the bones (Fig. 1). Two types of BM have been described: red marrow and yellow marrow. All haematopoietic cells (including erythrocytes and leukocytes) and platelets ultimately arise from haematopoietic stem cells (HSCs) allocated in the red marrow, whereas the yellow marrow contains fat tissue (adipocytes). The red marrow represents the BM at birth, but starts to decrease with age, when the yellow marrow becomes predominant. As a consequence, the efficiency of haematopoiesis decreases with ageing and can eventually lead (under pathological conditions) to BM failure.

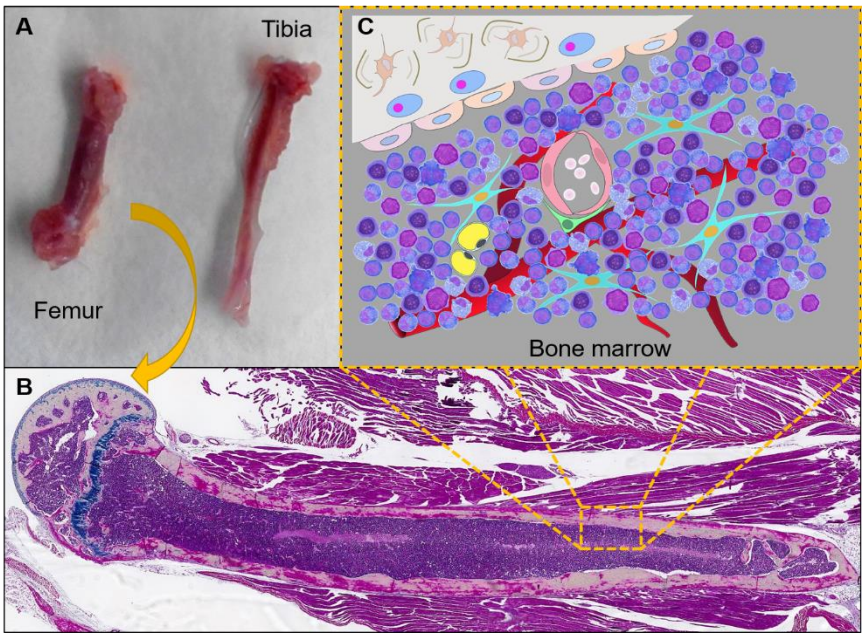

Figure 1. The BM is the main haematopoietic organ and is located in the bone cavity. *A, Murine tibia and femur are two long bones with high BM content. B, Azan trichrome staining of a 10 µm femur section. C, Scheme illustrating the complexity of the BM, which includes many different types of haematopoietic and stromal cells.*

1.2 Bone marrow stem cell niches

The HSC is one of the best characterized adult stem cell types, partly due to the fact that it was the first one discovered in the early 1960s. HSCs have the capability to self-renew and differentiate to progenitors cells, which in turn give rise to committed blood cells of multiple “lineages”. Under homeostatic conditions, many HSCs exhibit a quiescent state, ensuring the long-term repopulation (LTR) of blood cells

throughout life (Cheshier, Morrison, Liao, & Weissman, 1999). During differentiation, a hierachy of haematopoietic cells with progressively decreasing self-renewal and increasing proliferative capacity is established. However, intense research over the last decades has suggested that HSCs are heterogeneous. The SLAM family markers CD150 and CD48, together with many other markers, have been used to identify distinct subpopulations of HSCs (Fig. 2A) (Kiel et al., 2005; Oguro, Ding, & Morrison, 2013). Whereas intrinsic mechanisms controlling HSC quiescence, self-renewal and differentiation have been investigated with more detail, the role of external cues in regulating haematopoiesis is still an emerging field of research.

HSCs and haematopoietic cells are surrounded by bone, cartilage and multiple types of bone marrow stromal cells. Some of these stromal cells share markers and *in vitro* features with mesenchymal stem cells isolated from different tissues. These are the BM-derived mesenchymal stem and progenitor cells (BMSCs). In contrast to the HSC hierarchy, in which several populations of haematopoietic stem and progenitor cells (HSPCs) have been defined and are broadly accepted in the field, BMSC lineages are still poorly understood (Fig. 2B) (Bianco, Robey, & Simmons, 2008). Research in the past few years has characterised BMSCs by combining *in vitro* assays with *in vivo* fate-mapping experiments. These studies have shed light on different BMSC populations that can be identified with specific markers (Chan et al., 2015; Kunisaki et al., 2013; Mendez-Ferrer, Michurina, et al., 2010; Zhou, Yue, Murphy, Peyer, & Morrison, 2014).

BMSCs and HSCs have originally been described, in the context of regeneration, as the cells responsible for BM reconstitution after mechanical depletion of the marrow cavity (Patt & Maloney, 1975). Since Friedenstein *et al.* identified BMSCs as fibroblastic-colony-initiating cells giving rise to the haematopoietic stroma in culture (Friedenstein, Chailakhjan, & Lalykina, 1970), multiple indications have pointed at the important role of BMSCs in supporting haematopoiesis through direct and indirect mechanisms. Dexter *et al.* proposed a method of obtaining murine long-term cultures of BMSCs which maintain haematopoiesis *in vitro* (Dexter, Wright, Krizsa, & Lajtha, 1977). Although the concept of the stem cell niche was first introduced three decades ago in the haematopoieitc system (Schofield, 1978), only very recently experimental evidence has been gathered which demonstrates the critical BMSC role in the HSC nice.

Besides BMSCs, other haematopoietic and non-haematopoietic cells regulate HSCs directly or indirectly. This include osteoblasts, macrophages, megakaryocytes, endothelial cells, T-regulatory cells, peripheral neurons and Schwann cells (Fig. 3) (Morrison & Scadden, 2014).

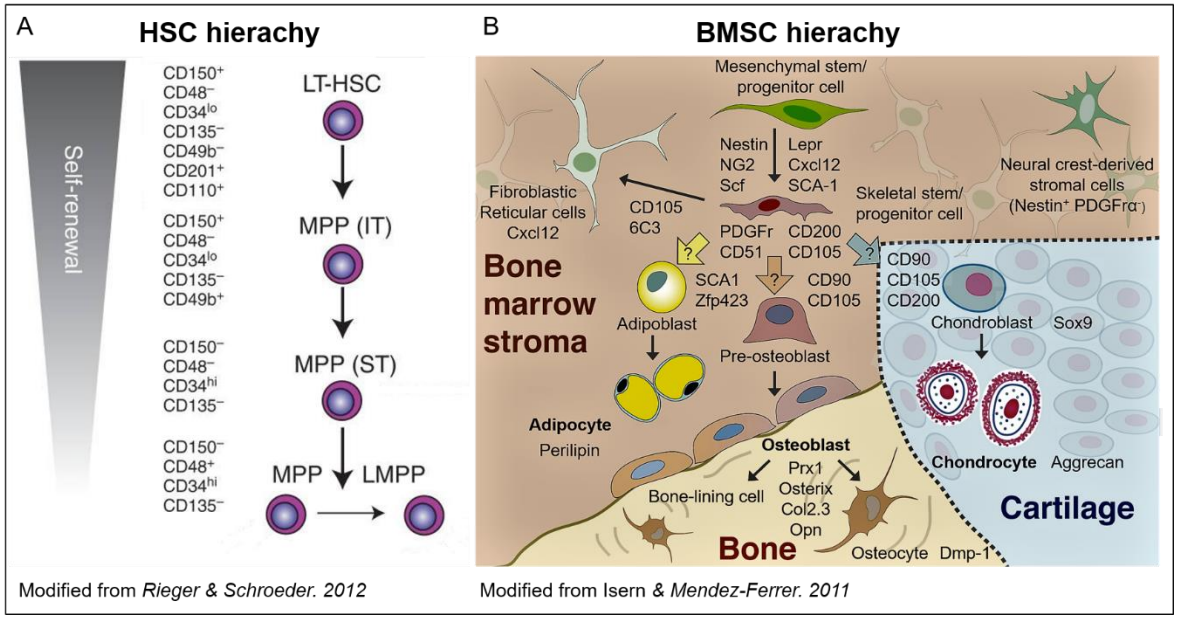

Figure 2. HSC (A) and BMSC (B) hierarchies have been determined based on functional assays and on surface membrane antigen expression (immunophenotype). *A, Different surface membrane antigens have been used to distinguish between long-term HSC (LT-HSC) and different multipotent progenitor (MPP) populations including intermediate (IT), short-term (ST) and lymphoid-primed multipotent progenitors (LMPP). B, Specific BMSC populations have been well characterised but the existence of subpopulations and their relationships is currently subject of debate and study in the field.*

1.2.1 Osteoblasts

Osteoblasts are short-lived bone-forming cells. The ones in contact with the bone matrix are also named “bone-lining” cells, which can over time be trapped in the bone matrix and become osteocytes. HSPCs have initially been detected close to the inner bone surface (“endosteum”). For this reason bone-lining osteoblasts have been proposed to play an active role in regulation of haematopoiesis (Gong, 1978; Lord, Testa, & Hendry, 1975; Nilsson, Johnston, & Coverdale, 2001). Calvi *et al.* provided the first *in vivo* evidence of osteoblasts as candidate HSC niche cells that control endosteal HSCs through Notch signalling (Calvi et al., 2003). At the same time, BMP signalling in bone-lining osteoblasts appears to regulate the BM HSC niche size (Zhang et al., 2003). Angiopoietin-1 (Ang1) produced by osteoblasts and

other stromal cells as well as HSC contributes to Tie-mediated HSC quiescence and endosteal localization (Arai et al., 2004; Zhou, Ding, & Morrison, 2015). Thrombopoietin (Tpo)/Mpl signalling has also been proposed to regulate primitive HSCs in osteoblastic niches (Yoshihara et al., 2007). However, it seems that megakaryocytes, instead of osteoblasts, might be the major source of Tpo in the BM (Nakamura-Ishizu, Takubo, Fujioka, & Suda, 2014).

Osteopontin (Opn), produced by osteoblasts of the endosteal bone surface, has been proposed as a relevant component of the osteoblastic HSC niche by attracting and retaining HSPCs, while inhibiting HSC proliferation (Nilsson et al., 2005).

In summary, these studies highlight the osteoblast as one of the first non-haematopoietic defined cell types that can regulate HSCs. Later studies have suggested that osteoblasts have a more prominent role in the regulation of lymphoid progenitors, although they participate in the regulation of HSC traffic. Contemporarily, BMSCs have been increasingly recognised as key HSC niche cells.

1.2.2 BMSCs

Studies both in human (Sacchetti et al., 2007) and murine (Mendez-Ferrer, Michurina, et al., 2010) BMSCs suggested the possibility that two different somatic stem cell types (haematopoietic and mesenchymal stem cells) share the same niches in the BM. The intermediate filament protein nestin has been used to identify in *Nestin-gfp* transgenic mice this BMSC population with high fibroblastic colony-forming-unit (CFU-F) activity and self-renewal capacity in serial transplantations. Nestin$^+$ BMSCs have been shown to express high levels of HSC maintenance genes, like Cxcl12 (Nagasawa et al., 1996), Stem cell factor (Scf) and Ang1. In addition, sympathetic nervous system stimulation or nestin$^+$ BMSC depletion reduces the expression of HSC maintenance genes resulting in HSC activation and trafficking (Mendez-Ferrer, Michurina, et al., 2010).

Shortly thereafter, Omatsu et al. also concluded that the stromal HSC niche population in the BM that they had previously characterised by a reticular shape and high expression of Cxcl12 contained BMSC-like cells. These cells are called Cxcl12-abundant reticular (CAR) cells and are highly enriched in mesenchymal progenitor activity. Similar to nestin$^+$ BMSC depletion, ablation of CAR cells reduces HSPC numbers and impairs HSC function (Omatsu et al., 2010; Sugiyama, Kohara, Noda,

& Nagasawa, 2006), albeit larger depletion of stromal cells using the CAR model also causes loss of multiple haematopoietic progenitors. Subsequent studies have shed more light on the importance of Cxcl12-expressing cells in HSPC regulation; however, the role of different Cxcl12-expressing cells has become controversial depending on their source and location. While Cxcl12 expression in osteoblasts has been shown to be relevant for B-cell lymphopoiesis and progenitor retention in the BM, perivascular Cxcl12 has been reported to directly target HSCs (Ding & Morrison, 2013; Greenbaum et al., 2013). Part of the controversy might be explained by partial overlap of stromal cell populations identified with different markers and differences of cell-type specificity and recombination efficiency, depending on the Cre line used.

All these studies have highlighted the Cxcl12-Cxcr4 axis as one key molecular pathway in HSPC regulation by BMSCs. Rac GTPases, activated by Cxcl12 in nestin^{+} perivascular BMSCs, have been shown to control several aspects of HSC maintenance (Ciuculescu et al., 2015; Sanchez-Aguilera et al., 2011). However, other signals different from Cxcl12 also importantly regulate HSCs. Long-term activation of Gs signalling in osteoblastic cells negatively affects HSC maintenance (Adams et al., 2009; Schepers, Hsiao, Garg, Scott, & Passegue, 2012), and Wnt signalling has been involved in the survival, self-renewal and differentiation of HSPCs (Florian et al., 2013; Reya et al., 2003).

In the last few years intense efforts to characterise primary BMSCs have provided different markers for partially-overlapping cell populations (Fig. 2B). Perivascular leptin receptor (Lepr) positive and Scf-expressing cells contain HSC niche-forming BMSCs (Ding, Saunders, Enikolopov, & Morrison, 2012). Whereas Lepr mainly marks Nes-GFP^{lo} cells associated with sinusoidal vessels, the Frenette laboratory has proposed NG2^{+} cells as a Nes-GFP^{hi} BMSC population forming an arteriolar HSC niche. Depletion of NG2^{+} cells triggers HSPC proliferation and dampens HSC LTR-capacity *in vivo* (Kunisaki et al., 2013). This study has been disputed by the Morrison laboratory, which has found that Lepr^{+} cells contain all BMSC populations (Zhou et al., 2014). However, it remains unclear to which degree BMSCs labelled in a transgenic *LeprCre;tdTomato* mouse model overlap with other BMSC subpopulations. Lepr^{+} cells and HSPCs themselves have been proposed as the major BM source of Ang1 required for BM HSC niche regeneration. These findings

are in contrast to previous studies suggesting that osteoblasts are major Ang1-producing cells (Arai et al., 2004; Zhou et al., 2015). Recently, the relevance of each factor produced by different cells in the HSC niche has been investigated. Whereas HSCs mainly depend on Scf produced by Lepr^{+} Nes-GFP^{lo} BMSCs cells, HSCs mainly require Cxcl12 produced by Lepr^{-} Nes-GFP^{hi} NG2^{+} BMSCs (Asada et al., 2017). Nevertheless, since all these cell populations express these factors, it remains unclear why they are biologically relevant only in one niche, but not in the other.

Human BMSCs have been identified using the melanoma cell adhesion molecule (MCAM; also known as CD146) as a marker that highly enriched BMSCs and cells with HSC-niche features (Sacchetti et al., 2007). However, the Scheding group has also found CD146^{-}CD271^{+} BMSCs preferentially associated with the endosteum (Tormin et al., 2011). A recent study has demonstrated that CD146^{+} BMSCs support long-term persistence of human lymphomyeloid HSPCs through cell-contact dependent Notch signalling (Corselli et al., 2013). CD105 (endoglin) is another surface antigen used to label human BMSCs (Lv, Tuan, Cheung, & Leung, 2014). Along these lines, non-adherent cultures of BMSCs in enriched medium that favoured their self-renewal (mesenspheres), originated from CD146^{+}CD105^{+}nestin^{+} cells, promote HSC expansion. Indeed, increased long-term human haematopoietic engraftment in serial transplantations, from HSCs previously expanded in the presence of mesenspheres, has highlighted the relevance of primitive BMSCs in HSC maintenance (Isern et al., 2013). Similarly, PDGFrα^{+}CD51^{+} nestin^{+} cells have been shown to highly enrich for BMSCs capable of HSC support (Pinho et al., 2013). In contrast, adult human BMSCs are enriched in the PDGFrα^{-}CD271^{+} cell fraction (Li et al., 2014). Therefore, ressembling CD34 expression on HSCs, murine and human BMSCs also differ in marker expression. Overall, significant advances over the last years now allow for the isolation and prospective identification of primary BMSCs. These studies have also highlighted the relevance of primitive BMSCs in the HSC niche.

1.2.3 Endosteal vs perisinusoidal BM niches

Beyond the ongoing debate about different markers to identify BMSCs with HSC niche function, the distribution of BMSC subpopulations within the BM cavity and

their differential impact on different HSPC populations/functions is a topic of intense research in the field.

To address this question it is essential to identify HSCs in the BM. HSCs have been immunophenotypically defined based on the expression of SLAM family receptors by the Morrison's laboratory. The majority of primitive HSCs are enriched in the Lineage^{-}Sca1^{high}ckit^{+}CD34^{-}CD48^{-}CD150^{hi} population, which is more abundant around sinusoids in the BM, defined as perisinusoidal niches (Kiel et al., 2005; Oguro et al., 2013). However, small subsets of HSPCs were initially found by others in close association with the bone, near the endosteal surface of the diaphyseal bone, but more abundantly in the trabecular BM. This, together with the fact that the first *in vivo* studies suggested a relevant role for osteoblasts in the regulation of HSC quiescence, has prompted the idea that endosteal niches harbour quiescent HSCs (Arai et al., 2004; Nilsson et al., 2005; Yoshihara et al., 2007).

Scf-expressing Lepr^{+} cells are located adjacent to sinusoidal endothelial cells in the highly vascularized area in the central part of the BM. Interestingly, Scf deletion in endothelial or perivascular Lepr^{+} cells drastically reduces HSCs numbers in the BM (Ding et al., 2012). Recent studies originated from the angiogenesis field have characterised the BM vasculature and identified markers for vessel subtypes (sinusoids, endosteal arterioles and arteries) with different functions and associated perivascular cells. The grade of vessel permeability, highly conditioned by the surrounding perivascular cells and extracellular matrix, has been suggested to regulate HSC quiescence. While less permeable arterial-like vessels contribute to keep HSCs quiescent, the higher permeability of sinusoids favours HSPC activation and trafficking (Itkin et al., 2016; Kusumbe et al., 2016). However, quiescent HSCs are abundant in the sinusoids (Acar et al., 2015), where other mechanisms might promote HSC quiescence. For instance, megakaryocytes, which are very abundant near sinusoids, have been proposed to promote HSC quiescence by secretion of Pf4/Cxcl4, transforming growth factor β (Tgf-β), Tpo and Clec-2 (Bruns et al., 2014; Nakamura-Ishizu et al., 2014; Zhao et al., 2014).

The improvement of imaging techniques has allowed tracing single HSCs in their niches. Taking advantage of high-resolution confocal two-photon intravital imaging, some authors have found enrichment of primitive HSCs in endosteal areas, arguing for a non-random distribution of transplanted HSCs in the BM (Nilsson et al., 2001).

This different HSC location has been linked to HSC differentiation status, with primitive cells located closer to bone (Lo Celso et al., 2009). Furthermore, HSCs tend to home to endosteal areas in irradiated mice, from where they expand to regenerate the damaged BM (Xie et al., 2009).

Previous studies have suggested that functionally distinct HSCs (quiescent and active) occupy different BM niches (endosteal and perisinusoidal, respectively). Interestingly, HSCs can reversibly switch between dormant and activated status based on their needs during homeostatic conditions or after haematopoietic stress (Wilson et al., 2008). More recently, Acar *et al*. has used tissue clearing techniques to perform deep confocal imaging of the BM. In contrast to previous studies, they have reported that most of HSCs (independently if they were active or inactive) are located close to $Lepr^{+}$ BMSC in perivascular niches and distant from endosteal niches (Acar et al., 2015). It has to be noted that sinusoids occupy over 90% of the BM volume of long bones, and it remains possible that the much lower number of endosteal HSCs might be especially important under stress/regenerative settings, as suggested from the studies in lethally-irradiated mice, in which the sinusoids are largely damaged, whereas endosteal vessels are spared (Hooper et al., 2009).

Other studies have recognised the relevance of both niches. CAR cells, which are in contact with most HSCs, are distributed around sinusoidal endothelial cells but also near the endosteum. Thus, Cxcl12-Cxcr4 signalling seems to regulate both vascular and endosteal niches in the murine BM (Sugiyama et al., 2006).

Importantly, the original dichotomy between endosteal and vascular niches is no longer valid because the endosteum is also highly vascularised. Endosteal vessels have been found near N-$cadherin^{+}$ pre-osteoblastic cells (Xie et al., 2009). More recently, a new BM vessel subtype formed of $CD31^{high}Endomucin^{high}$ endothelial cells has been described. These vessels, called transition zone (TZ) vessels as they connect lowly permeable arterioles with highly permeable sinusoids and have mixed properties, are exclusively found in endosteal areas and in the growth plate (Kusumbe, Ramasamy, & Adams, 2014).

However, despite many advances in the understanding of the BM HSC niche in the last years (Boulais & Frenette, 2015; Ehninger & Trumpp, 2011; Kiel & Morrison, 2008; Morrison & Scadden, 2014), the impact of each niche on haematopoietic fate

and its precise composition are not fully clear. In fact, it is reasonable to argue that different types of niches co-exist and house HSCs with different features and functions. Another interpretation supports the concept that HSCs circulate between different niches according to the needs required in a dynamic system (Trumpp, Essers, & Wilson, 2010) (Fig. 3).

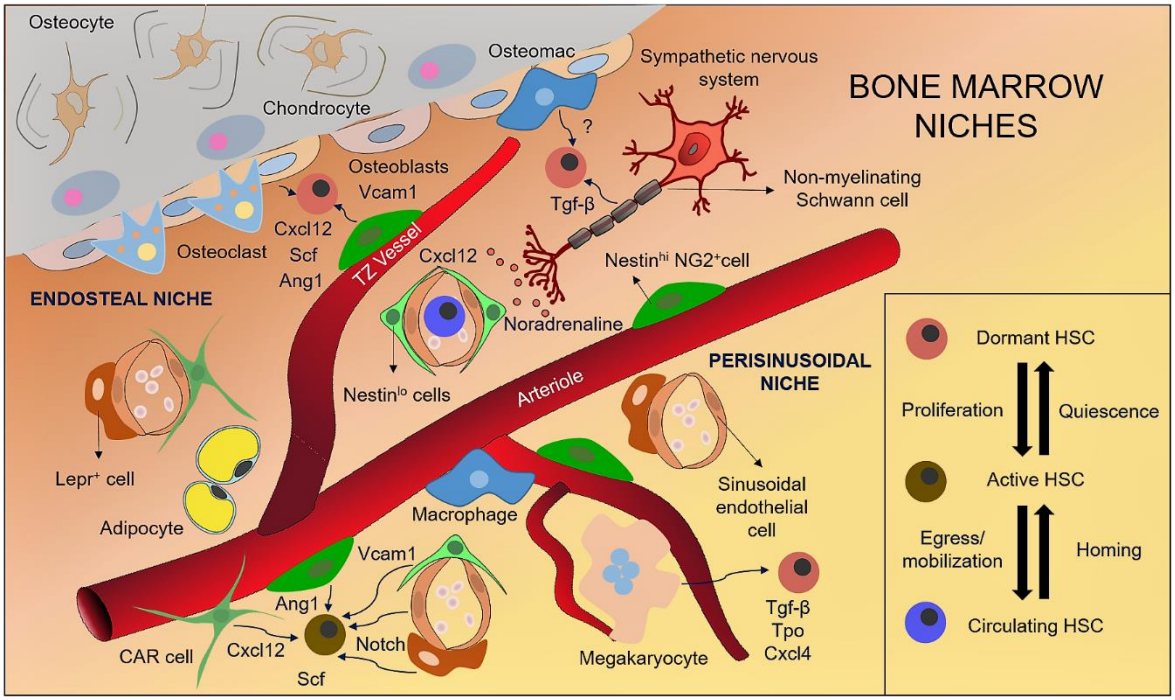

Figure 3. HSCs reside in different specific BM microenvironments called "niches". *In homeostasis HSCs are in a dynamic balance in which distinct niches provide signals that regulate HSC behaviour and function. However, in stress situations this balance is altered to meet the needs and recover homeostasis.*

1.3 The autonomic nervous system

In addition to the contribution of mesenchymal stromal elements, other cells with a neural crest origin control the BM HSC niche. The autonomic nervous system has been proposed to play an important role in regulating HSCs.

The peripheral nervous system connects the central nervous system (CNS, brain and spinal cord) with the target organs in the periphery. The peripheral nervous system is divided into the somatic nervous system and the autonomic nervous system (ANS). The somatic nervous system is responsible for voluntary movements of the body and is comprised of motoneurons that innervate the skeletal muscle to activate muscle contraction and sensory fibres that innervate the skin to transmit sensory signals to the CNS.

The ANS is responsible for modulating involuntary actions that ensure proper functioning of our body and contributes to its homeostasis. Therefore, the ANS innervates multiple internal organs such as the heart to control the heart rate or the bladder to influence the urination process. Moreover, haematopoietic organs, such as the BM or the spleen, are innervated by the ANS (Calvo, 1968).

The ANS is divided into two branches: the sympathetic nervous system (SNS) and the parasympathetic nervous system (PNS). SNS and PNS are both structured as "two-step efferent pathways" containing ganglions in which a preganglionic neuron forms a synapse with a postganglionic fibre that eventually innervates the peripheral organ (Richins & Kuntz, 1953).

The sympathetic branch, which has its preganglionic origin in the thoracolumbar region of the spinal cord, has traditionally also been called "noradrenergic". The parasympathetic branch, which originates from cranio-sacral areas, has been described as "cholinergic". This alternative nomenclature is based on the type of neurotransmitter released by postganglionic terminals in each system: catecholamines (adrenaline/noradrenaline) in the SNS, and acetylcholine in the PNS. However, acetylcholine can also act as preganglionic neurotransmitter in both branches of the ANS (Burnstock, 1981).

Although classical concepts present both branches with opposing effects, many exceptions have been described, which contradict this general rule. Yet, sympathetic signalling is associated with rapid activating responses, while parasympathetic signals are more related to slow, dampening responses. In the context of the immune response, the SNS triggers the inflammatory response at initial steps of an injury, while the PNS activates anti-inflammatory pathways at the end of the process to resolve inflammation (Olofsson, Rosas-Ballina, Levine, & Tracey, 2012; Pongratz & Straub, 2014).

Despite recent studies on the parasympathetic innervation of haematopoietic organs, little is known about the possible relevance of the PNS as regulator of haematopoiesis beyond its anti-inflammatory properties. However, the SNS has been more extensively studied and associated with multiple physiological haematopoietic functions (Fig. 4).

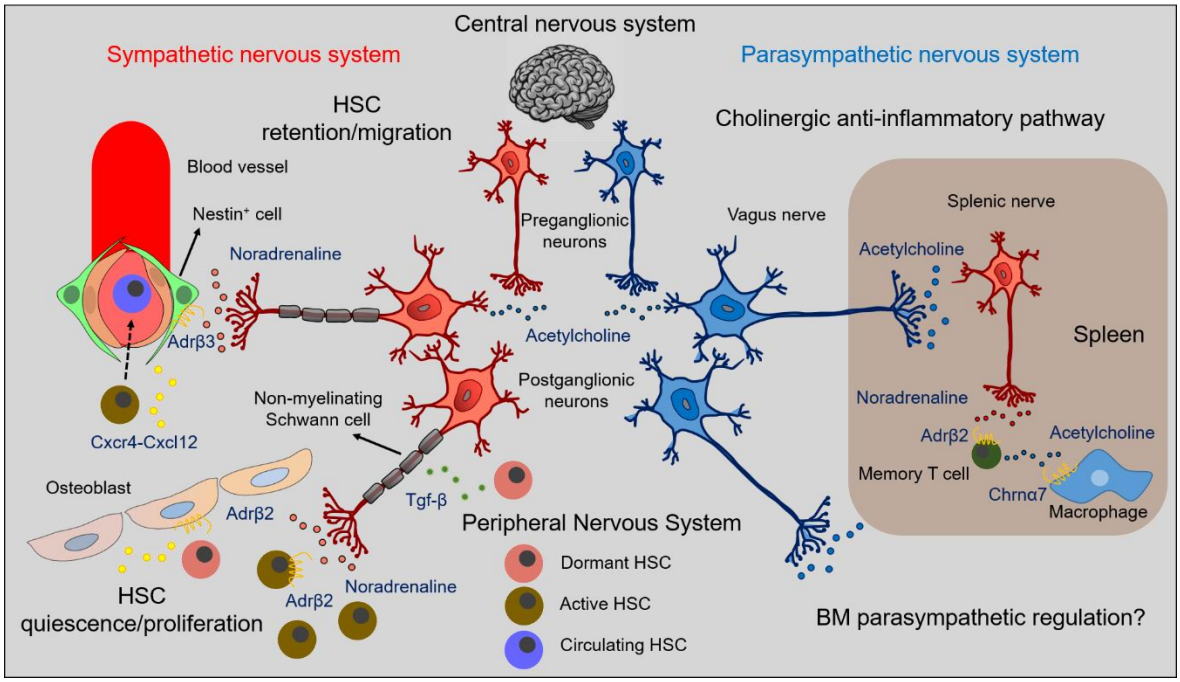

Figure 4. Neural regulation of haematopoietic organs. *SNS signalling modulates HSC trafficking and maintenance in the BM by activating β-adrenergic receptors in BMSCs and HSCs. PNS anti-inflammatory signalling has been described in the spleen, but the cholinergic contribution to the BM has not been explored.*

1.3.2 Sympathetic innervation of haematopoietic organs

Sympathetic postganglionic terminals innervate haematopoietic organs where they release catecholamines as neurotransmitters. Catecholamines are synthesized from tyrosine, which is first transformed to dihydroxyphenylalanine by tyrosine hydroxylase (TH), and then converted to dopamine. Dopamine is loaded into vesicles inside sympathetic terminals and transformed into noradrenaline by Dopamine-b-hydroxylase (DBH) (Nagatsu, Levitt, & Udenfriend, 1964). Although noradrenaline is the main neurotransmitter released by sympathetic fibres in haematopoietic organs, it is eventually converted into adrenaline. Adrenaline has an important role as sympathetic effector in the humoral pathway of the immune response. The two main enzymes involved in noradrenaline synthesis, TH and DBH, are useful markers to label sympathetic fibres.

The splenic nerve is the only widely accepted innervation of the spleen and has been shown to contain almost exclusively postganglionic sympathetic axons in several species (De Potter, Kurzawa, Miserez, & Coen, 1995; Felten, Ackerman, Wiegand, & Felten, 1987; Fried et al., 1986; Kinney, Cohen, & Felten, 1994; Saito, 1990). Noradrenergic terminals of the splenic nerve emerge from the celiac/superior

mesenteric plexus ganglion (Rosas-Ballina et al., 2008) and penetrate within the spleen associated with the vasculature (Bellinger, Felten, Lorton, & Felten, 1989).

Similarly, sympathetic fibres enter the BM in association with blood vessels. Arteries penetrate the BM, where they branch within the central cavity. Some radial arteries connect with the venous sinuses broadly distributed in the marrow through smaller arterioles (Travlos, 2006). There are also some radial arteries which connect with specific arterioles located in the endosteum: the TZ vessels (Kusumbe et al., 2014), which connect arteriolar with sinusoidal vessels. Some periosteal arteries irrigating the periosteum can eventually cross through the bone to also supply the TZ vessels. Immunostainings against the TH enzyme reveal large noradrenergic fibres around arteries and smaller isolated varicosities scattered throughout the BM (Mach et al., 2002; Tabarowski, Gibson-Berry, & Felten, 1996). The close association of endothelial cells, nerve terminals and BMSCs, tightly jointed through gap junctions, has given rise to the concept of the “neuroreticular complex” in the BM functioning as a syncytium-like unit (K. Yamazaki & Allen, 1990).

Some sympathetic terminals can also release neuropeptide Y (NPY) in addition to noradrenaline; however, the role of NPY in haematopoietic organs is not clear yet. Chemical sympathectomy to deplete NPY^+ fibres have failed to significantly decrease NPY content in the spleen, suggesting a non-neuronal splenic source of NPY (Ericsson et al., 1987; Romano, Felten, Felten, & Olschowka, 1991).

Some studies have described the presence of residual NPY^+ fibres in the BM (Mach et al., 2002; Tabarowski et al., 1996; K. Yamazaki & Allen, 1990). However, those fibres have not been fully characterized and, more importantly, their functional relevance in the haematopoietic context is very controversial. Some studies have suggested that NPY signalling modulates osteoblastic function (Lee et al., 2015; Lundberg et al., 2007; Teixeira et al., 2009), helps to restore BM dysfunction after chemotherapy-induced neural damage (M. H. Park et al., 2015) and induces HSPC mobilisation (M. H. Park et al., 2016).

In summary, sympathetic fibres regulate different HSC functions via direct and indirect mechanisms involving primarily noradrenaline.

1.3.3 First functional evidences of adrenergic neural regulation of haematopoiesis

Although multiple histochemical studies had illustrated sympathetic BM innervation, the functional relevance of these fibres in haematopoiesis remained elusive until the 1990s. A first link between immune and neural signalling was identified by Maestroni *et al.* showing that circadian release of melatonin enhances immune function (Maestroni & Conti, 1990; Maestroni, Conti, & Pierpaoli, 1988). Subsequent studies by the same group have demonstrated that leukocyte reconstitution after BM transplantation is dependent on dark/light cycles (Maestroni, Conti, & Pedrinis, 1992). Chemical sympathectomy with 6-hydroxydopamine (6-OHDA) have identified the importance of noradrenaline released from local sympathetic terminals in the BM to control leukocyte levels in the peripheral blood (Maestroni et al., 1992). Likewise, noradrenaline has been described to exhibit protective effects against the chemotherapeutic agent carboplatin (Maestroni, Togni, & Covacci, 1997). Adrenergic control of haematopoietic cells has been demonstrated to be mediated via cell-autonomous α1-adrenergic receptor signalling in haematopoietic cells. Treatment with adrenergic antagonists (α1-adrenergic and β-adrenergic blockers) enhances myelopoiesis in BM and spleen, whereas it interferes with lymphopoiesis (Maestroni & Conti, 1994a, 1994b; Maestroni et al., 1992). Although most of these experiments have been performed *in vitro* or under myeloablative conditions, the same group has also measured catecholamines in the BM of mice over 24 h and has suggested that noradrenaline levels follow circadian oscillations. These first evidences by Maestroni *et al.* lay the basis of all subsequent studies investigating the neural regulation of haematopoiesis.

1.3.4 Neural regulation of HSPC trafficking

Haematopoietic cells, including HSPC, are in constant circulation between the BM and the periphery. This haematopoietic trafficking does not only help to equally distribute haematopoietic cells among peripheral organs, but it also helps to regenerate the HSPC pool contributing to the maintenance of haematopoiesis throughout life (Abkowitz, Robinson, Kale, Long, & Chen, 2003; Smith, Weissman, & Heimfeld, 1991). Importantly, some studies at the beginning of this century have reported that this “normal traffic” can be altered using certain cytokines and factors (T. Ahmed, Wuest, & Ciavarella, 1992). This knowledge has been used to “artificially

move" HSPCs into the bloodstream (a process known as mobilisation, in contrast of the physiological HSPC egress) and facilitate HSPC collection by apheresis (J. Chen et al., 2006).

Among several mobilising agents granulocyte-colony stimulating factor (G-CSF) has been studied for many years and is now broadly used to mobilise HSPCs for transplantation purposes (Molineux, Pojda, Hampson, Lord, & Dexter, 1990). However, subsequent experiments using chimeras have demonstrated that G-CSF does not act directly on HSPCs, but targets stromal components of the BM (Liu, Poursine-Laurent, & Link, 2000). Initially, G-CSF has been proposed to increase the levels of proteases such as matrix metalloproteinase-9 (MMP-9), cathepsin G, and other serine proteases in the BM. These proteases contribute to degrade key chemoattractant molecules involved in HSC maintenance like Cxcl12 and its receptor Cxcr4 (Kollet et al., 2006; Levesque, Hendy, Takamatsu, Simmons, & Bendall, 2003). However, inhibition of protease activity is not sufficient to abrogate G-CSF-induced Cxcl12 reduction and subsequent HSPC mobilisation (Levesque et al., 2004), suggesting that other stromal elements are required to mediated the G-CSF-induced drop of Cxcl12. According to this, it has been shown that a population of trophic endosteal macrophages named "osteomacs" are also depleted upon G-CSF administration. Osteomacs depletion is associated with loss of osteoblasts, decreased HSC chemoattractant factors in endosteal niches and HSC mobilisation (Winkler et al., 2010).

Some stromal components targeted by G-CSF have their origin in the nervous system. Galactocerebrosides are glycolipids present in myelin sheaths of Schwann cells in myelinating fibres of the peripheral nervous system. The enzyme UDP-galactose;ceramide galactosyl-transferase (Ctg) is responsible for the transfer of UDP-galactose to ceramide forming galactosylceramide, which is the main galactocerebroside of myelin. G-CSF-induced mobilisation is impaired in *Ctg*$^{-/-}$ mice despite normal protease activity. β2-adrenergic signalling has been identified to participate in G-CSF-mediated HSPC mobilisation by inducing osteoblast suppression and decreasing osteoblastic Cxcl12 level (Katayama et al., 2006). This work expands the previously described adrenergic regulation of osteoblasts during bone remodelling (Fu, Patel, Bradley, Wagner, & Karsenty, 2005) and provides more evidences supporting a relevant function for sympathetic fibres in modulating

HSPC chemoattraction in endosteal niches. β2-adrenergic signalling also directly targets human $CD34^+$ cells to stimulate human HSPC proliferation, migration and engraftment. Thus, β2-adrenergic signalling in HSPCs cooperates with stromal cell-mediated β2-adrenergic mechanisms during G-CSF-induced mobilisation (Spiegel et al., 2007).

Circadian oscillations in DNA synthesis rate and progenitor activity (measured *in vitro* as colony-forming units in culture) have been reported in murine and human BM (Aardal & Laerum, 1983; Smaaland, Sothern, Laerum, & Abrahamsen, 2002). Evidence for the direct involvement β-adrenergic signalling in these circadian fluctuations (Byron, 1972) have been proposed, but the underlying mechanisms have remained unexplored. Likewise, catecholamine levels in the blood undergo circadian fluctuations, suggesting that sympathetic control of haematopoietic cells might follow circadian rhythms (Sauerbier & von Mayersbach, 1977). Subsequently, levels of sympathetic metabolites (noradrenaline and dopamine) have been shown to follow daily fluctuations in the murine BM with maximum values during the night, suggesting a circadian regulation of haematopoiesis (Maestroni et al., 1998). Central circadian rhythms generated by the suprachiasmatic nucleus have also been described to be transmitted to other peripheral organs, such as the liver, via the SNS (Terazono et al., 2003).

Along these lines, it has been shown that HSC egress from the BM to the bloodstream follows circadian oscillations dependent on sympathetic signalling (Mendez-Ferrer, Lucas, Battista, & Frenette, 2008). Light signals received in the suprachiasmatic nuclei at central level are processed and translated into HSC egress at peripheral level. Postganglionic sympathetic terminals innervate the BM periphery to release noradrenaline and transmit the adrenergic signal to stromal cells expressing β3-adrenergic receptor. This leads to the degradation of Sp1 nuclear transcription factor and Cxcl12 suppression in BMSCs. Circulating HSPCs fluctuate in antiphase with *Cxcl12* expression and both oscillations are dramatically altered when light periods and/or sympathetic signalling are disrupted (Mendez-Ferrer et al., 2008).

These circadian oscillations are also present in HSPC human trafficking but inverted in time. While the highest HSC accumulation in circulation occurs 5 hours after the light stimulus in the murine system, the peak of HSC egress in humans is observed

in absence of light during the evening (Lucas, Battista, Shi, Isola, & Frenette, 2008). Other species promote HSC release into the bloodstream during their resting period independent of light/dark phases. This highlights the importance of molecular clocks such as Bmal1 to precisely synchronize circadian oscillations and sustain them in the absence of light. The fact that circulating HSC peak coincides with the resting phase in both species has been interpreted as a cyclical way to regenerate the BM microenvironment and other haematopoietic tissues in a coordinated manner (Abkowitz et al., 2003; Smith et al., 1991). Moreover, regeneration of other peripheral organs during the resting phase might correlate with higher demands of haematopoietic cells (Massberg et al., 2007).

1.3.5 Neural regulation of haematopoietic ontogeny

During late stages of murine embryonic development, nerve fibres colonize limb buds along with blood vessels in the developmental BM cavity (Calvo & Haas, 1969; Miller & McCuskey, 1973). Stainings for pan-neuronal markers like PGP 9.5 and GAP-43 have shown the presence of nerve fibres in the perichondrium and periosteum of rodent limb buds around birth. Both cholinergic and adrenergic fibres have been found in periosteal regions and inside the marrow space during postnatal stages (Gajda, Adriaensen, & Cichocki, 2000; Gajda et al., 2010).

Adult HSCs originate in the aorta gonad mesonephros (AGM) region of the embryo at early stages of embryonic development (around embryonic day 10 (E10)). Sympathetic signals have been described to contribute to HSC emergence in the AGM region (Fitch et al., 2012). After leaving the AGM, HSCs colonize the foetal liver (FL) in which they expand to finally engraft the BM at E15 (Dzierzak & Speck, 2008). HSC migration to the BM initiates at pre-natal stages but extends until two weeks after birth (Wolber et al., 2002). During this period, HSCs switch from their proliferative FL state to a quiescent phenotype found in the adult BM. Stromal components including nerve fibres and Schwann cells, which are still undergoing maturation during these postnatal stages, might contribute to the regulation of HSC colonisation and quiescence in the developing BM. For instance, a neural crest-derived BMSC population has been proposed to be important for HSC niche-formation in the developing BM. These neural crest-derived BMSCs give rise to (or even contain) Schwann cell precursors. In contrast to mesoderm-derived BMSCs controlling foetal skeletogenesis, quiescent neural crest-derived BMSCs secret

higher levels of Cxcl12 and contribute to HSC attraction and BM niche maturation (Isern et al., 2014). Thus, the neural crest, as a source of peripheral neurons, Schwann cells and BMSCs, might contribute to the regulation of HSC microenvironments in the BM.

During postnatal development, some sympathetic neurons innervating the sternum have been reported to switch their neurotransmitter properties upon receiving signals from the outer bone surface ("periosteum"). Transplantation of periosteum tissue onto skin innervated by sympathetic fibres resulted in neurotransmitter switch in some fibres from noradrenergic to cholinergic fate. Interestingly, these sympathetic cholinergic fibres are generated mainly during the first two postnatal weeks around the time of HSC BM colonisation and niche maturation (Asmus, Parsons, & Landis, 2000; Asmus, Tian, & Landis, 2001). Whether these sympathetic cholinergic fibres have a role in HSC migration or adult haematopoiesis is still unexplored.

Neurotrophic factors are essential to support growth, survival and differentiation of nerve fibres (Henderson, 1996). Three different families of neurotrophic factors including neutrophins, the ciliary neurotrophic factor (Cntf) family and the glial cell line-derived neurotrophic factor (GDNF) family have been described. The GDNF family, which is composed of the ligands GDNF, Nrtn (neurturin), Artn (artemin) and Pspn (persephin), has been implicated in the control of immune functions (Vega, Garcia-Suarez, Hannestad, Perez-Perez, & Germana, 2003). Although each of these specific neurotrophic ligands binds preferentially to a specific co-receptor in the Gfrα1-4 family, it is possible some low-affinity bindings to other co-receptors because their structural homology. Gfra co-receptors are associated with the tyrosine kinase RET-receptor that mediates downstream signalling (Baloh, Enomoto, Johnson, & Milbrandt, 2000). GDNF/Gfrα1 is especially important for dopaminergic neurons survival (Airaksinen & Saarma, 2002). Additionally, RET-receptor is expressed in developmental HSCs and neurotrophic factor/RET signalling has been shown to promote HSC survival and proliferation (Fonseca-Pereira et al., 2014). This study pointed neurotrophic factors as novel components of BM microenvironments and suggested that Gfra/RET signalling is another potential pathway by which ANS might regulate haematopoiesis in the BM.

1.3.6 Sympathetic regulation of HSC cell cycle status: quiescence vs proliferation

SNS is not only involved in the dynamic processes that allow HSC migration between haematopoietic organs, but also controls HSPC proliferation through cell-autonomous effects mediated by β2-adrenergic receptor signalling (Spiegel et al., 2007). Nestin^{+} BMSC, which mediate sympathetic fibre-controlled HSC traffic to extramedullary sites via Cxcl12, also express other HSC maintenance genes such as Scf or Ang1 (Mendez-Ferrer, Michurina, et al., 2010). Non-myelinating Schwann cells, which unsheathe sympathetic nerve fibres, contribute to maintain HSC quiescence. Schwann cells release Tgf-β in the BM, which binds to Tgf-β type II receptor in HSCs and triggers Smad-mediated quiescence. Sympathetic denervation resulting in Schwann cell loss leads to a quick reduction of BM HSCs (S. Yamazaki et al., 2011). Therefore, peripheral sympathetic neurons and their associated Schwann cells appear to have the capacity to directly and indirectly regulate HSC proliferation.

1.3.6 Parasympathetic innervation of haematopoietic organs

The presence of parasympathetic innervation in haematopoietic organs has remained debated for many years. Retrograde tracing experiments performed in rodents and cat has suggested the existence of parasympathetic innervation in the spleen (Branen et al., 2004; Buijs, van der Vliet, Garidou, Huitinga, & Escobar, 2008; X. H. Chen, Itoh, Sun, Miki, & Takeuchi, 1996). Still, most groups working in this field doubt the existence of parasympathetic fibres in the spleen and argue for interspecies differences. (Bellinger, Lorton, Hamill, Felten, & Felten, 1993; Cano, Sved, Rinaman, Rabin, & Card, 2001; Nance & Sanders, 2007). Recently, cholinergic fibres with spinal origin have been detected around arterioles in the white pulp of the spleen (Gautron et al., 2013).

However, there is strong evidence for a cholinergic anti-inflammatory reflex in the spleen initiated by the PNS (Huston et al., 2006; Rosas-Ballina et al., 2008; Vida, Pena, Deitch, & Ulloa, 2011). This pathway involves an indirect regulation by the parasympathetic vagus nerve via the celiac plexus, from where the splenic nerve emerges to innervate the spleen. The splenic nerve is catecholaminergic and innervates an Ach-producing T cell population via β2-adrenergic signalling in the

spleen. Upon stimulation by noradrenaline, these T cells produce Ach to activate α7-nicotinic receptors on macrophages resulting in the downregulation of pro-inflammatory cytokines and dampening of the immune response (Rosas-Ballina et al., 2011). Whereas this study describes the importance of cholinergic immune control in the spleen despite the absence of direct PNS innervation, other groups have reported the existence of splenic PNS fibres with anti-inflammatory function (Kooijman et al., 2015). These studies have fostered the significant controversy in the field regarding parasympathetic innervation of the murine spleen (Anderson, McKinley, Martelli, & McAllen, 2015).

Besides the controversial parasympathetic innervation of the spleen, neuroanatomical evidence of a parasympathetic supply to the BM is scarce (Nance & Sanders, 2007). Immunohistochemistry studies of the enzyme choline acetyltransferase (ChAT) has been used to label parasympathetic fibres in the BM of the rat (Artico et al., 2002). Another study has used the cholinergic marker vesicular acetylcholine transporter (VAChT) and retrograde tracing with pseudorabies virus to suggest the presence of PNS terminals transmitting bone-anabolic signals from the brain. The sacral intermediolateral cell column and the central autonomic nucleus has been identified as origin of PNS fibres in the bone (Bajayo et al., 2012). However, the possibility of an indirect vagal input (as it occurs in the spleen) through sympathetic postganglionic terminals innervating the BM cannot be excluded. Hence, another group has reported bone-anabolic PNS signals regulating bone mass indirectly through the inhibition of central sympathetic tone (Shi et al., 2010). Sympathetic fibres that regulate bone remodelling also innervate the BM, suggesting the possibility of haematopoietic regulation by the PNS at the central level.

Recently, central cholinergic signals have been shown to control G-CSF-mediated HSPC mobilisation in the BM through a glucocorticoid signalling relay. Cholinergic signalling mediated by muscarinic receptor type-1 (Chrm1) is transmitted from the hypothalamus to the hypothalamic-pituitary-adrenal axis, where it promotes glucocorticoid hormones release. Physiological levels of corticosterone lead to HSC mobilisation via the glucocorticoid receptor Nr3c1-dependent signalling and reorganization of actin cytoskeleton in HSPCs (Pierce et al., 2017).

Vasoactive intestinal peptide (VIP) is a neurotransmitter mostly associated with parasympathetic signalling which has been identified in nerve fibres supplying the spleen and the BM. Only residual VIP-immunoreactive fibres have been found along the splenic vasculature, where they might modulate lymphocyte function during the inflammatory response (Chevendra & Weaver, 1992). VIP^+ fibres have also been found in the BM and the periosteum in rats with particular abundance in the growth plate and intervertebral discs (M. Ahmed, Bjurholm, Kreicbergs, & Schultzberg, 1993). The VIP receptor (VPAC1) has been detected in human megakaryocytes (S. K. Park, Olson, Ercal, Summers, & O'Dorisio, 1996), in which autocrine VIP-signalling has been suggested to inhibit megakaryocyte proliferation and differentiation (Nam, Case, Hostager, & O'Dorisio, 2009). However, VIP/VPAC1-signalling exhibits opposite effects on proliferation and clonogenic capacity of HSPCs isolated from human BM or human umbilical cord blood (Kawakami et al., 2004; Rameshwar et al., 2002). It is also important to note that VIP is not exclusively present in parasympathetic terminals, but a net of sympathetic VIP-immunoreactive nerve fibres has been described to innervate the periosteum and bone in several species (Hohmann, Elde, Rysavy, Einzig, & Gebhard, 1986). In contrast, VIP^+ fibres in the spleen are not affected by sympathectomy (Bellinger et al., 1997), suggesting that these fibres are parasympathetic.

In conclusion, the evidence for cholinergic fibres in haematopoietic organs remains very limited and controversial, highlighting the urgent need to study the possible cholinergic regulation of haematopoiesis to improve the current understanding of neural control mechanisms in the HSC niche.

2 Aims

A considerable number of studies in the last decades has revealed the importance of the nervous system as a master regulator of haematopoiesis. The autonomic nervous system relays signals from the CNS to haematopoietic organs. Although several studies have suggested that the innervation of BM and spleen might derive from both branches of the autonomic nervous system (SNS and PNS), only the sympathetic regulation of haematopoiesis has been validated at the peripheral level by functional studies. Whereas the SNS is an established regulator of HSC maintenance and trafficking, parasympathetic innervation has not been studied in detail in haematopoietic organs and the evidence of cholinergic regulation at this level is limited to the orchestration of the cholinergic anti-inflammatory reflex.

Despite significant advances in the field of BM niche regulation and the description of numerous “niche elements”, an integrated vision of how these different components ultimately regulate HSC function is lacking. Different BM niches have been described in spatially distinct locations in the BM. While endosteal niches mainly contribute to the maintenance of dormant/quiescence HSCs, perisinusoidal niches in the central part of the marrow have been demonstrated to harbour the vast majority of active HSCs. However, how these spatially separated niches physiologically and coordinately regulate haematopoiesis is still elusive. It remains to be shown whether these niches harbour different HSC populations or if they work as a dynamic system in which HSCs are exchangeable between niches and show different behaviours depending on the niche they occupy over time.

In this study, we propose that the other branch of the autonomic nervous system, the PNS, might also regulate the BM stem cell niche. To address this question, it is important to dissect whether the PNS directly contributes to haematopoiesis through cholinergic signalling, or whether it indirectly modulates HSC function by antagonizing sympathetic activity, as it occurs in other peripheral organs. Thus, the aims of this study are:

1) Investigation of the pathways by which the PNS might transmit cholinergic signals to the BM.
2) Characterization of the roles of cholinergic signalling in regulating HSC function in different BM stem cell niches in a spatiotemporal context.

“Siempre hay que buscar la perfección.
Para mí significa: de una tela a otra, ir siempre más lejos, más lejos.”
Pablo Picasso

3 Materials and Methods

3.1 Materials

3.1.1 Mouse strains

Table 1 Mouse strains

MOUSE STRAIN	SOURCE	IDENTIFIER
Mouse: *Gfra2*$^{-/-}$	Rossi *et al*., 1999	N/A
Mouse: *Nes-gfp*	G.E.Enikolopov ; Mignone *et al*., 2004	N/A
Mouse: *Adrb2tm1Bkk/J*	G. Karsenty ; Chruscinkski et al., 1999	N/A
Mouse: FVB/N-*Adrb3*^{tm1Lowl}	The Jackson Laboratory	JAX: 006402
Mouse: B6.129S7-*Chrna7*^{tm1Bay}/J	The Jackson Laboratory	JAX: 003232
Mouse: *Th-IRES-Cre*	T. Ebendal ; Lindeberg *et al*., 2004	N/A
Mouse: *Dhh-IRES-Cre*	gift	N/A
Mouse: *ChAT-IRES-Cre*	gift	N/A
Mouse: B6.Cg-Gt(ROSA)26Sortm14(CAG-tdTomato)Hze/J	The Jackson Laboratory	JAX: 007914
Mouse: B6.SJL-Ptprca Pepcb/BoyJ	The Jackson Laboratory	JAX: 002014
Mouse: C57BL/6J	The Jackson Laboratory	JAX: 000664

3.1.2 Cell lines

Table 2 Cell lines

CELL LINE	SOURCE	IDENTIFIER
MS-5 murine stromal cell line	ATCC	N/A
ST-2 murine stromal cell line	ATCC	N/A
MC3T3-E1 murine osteoblastic cell line	ATCC	CRL-2593
MLO-Y4 osteocyte-like cell line	ATCC	N/A

3.1.3 Antibodies

Table 3 Antibodies list

ANTIBODY	SOURCE	IDENTIFIER
PE-Cy™7 Mouse Anti-Mouse CD45.1 Clone A20	BD Biosciences	Cat#560578
APC-Cy™7 Mouse Anti-Mouse CD45.2 Clone 104	BD Biosciences	Cat#560694
FITC Rat Anti-Mouse CD45R/B220 Clone RA3-6B2	BD Biosciences	Cat#553088
APC Rat Anti-Mouse CD11b Clone M1/70	BD Biosciences	Cat#553312
PerCP-Cy™5.5 Hamster Anti-Mouse CD3e Clone 145-2C11	BD Biosciences	Cat#561108
PE Rat Anti-Mouse Ly-6G Clone 1A8	BD Biosciences	Cat#561104
PE Rat Anti-Mouse CD90.2 Clone 53-2.1	BD Biosciences	Cat#553005
PE Rat Anti-Mouse Ly-6A/E Clone E13-161.7	BD Biosciences	Cat#553336
FITC Rat anti-Mouse CD34 Clone RAM34	BD Biosciences	Cat#560238
APC Rat Anti-Mouse CD135 Clone A2F10.1	BD Biosciences	Cat#560718
Biotin Mouse Lineage Panel (CD11b, Gr-1, Ter119, B220, CD3e)	BD Biosciences	Cat#559971
Anti-Mouse CD117 (c-Kit) PE-Cyanine7	eBioscience	Cat#25-1171-82
APC anti-mouse CD150 (SLAM) Antibody Clone TC15-12F12.2	BioLegend	Cat#115910
PerCP/Cy5.5 anti-mouse CD41 antibody Clone MWReg30	BioLegend	Cat#133918
Streptavidin APC-Cy™7	BD Biosciences	Cat#554063
Biotin Rat Anti-Mouse CD45 Clone 30-F11	BD Biosciences	Cat#553077
Biotin Rat Anti-Mouse CD31 Clone MEC 13.3	BD Biosciences	Cat#553371
Biotin Rat Anti-Mouse TER-119/Erythroid Cells Clone TER-119	BD Biosciences	Cat#553672
Purified monoclonal anti-mouse P-selectin Clone RB40.34	gift	N/A
Purified monoclonal anti-mouse α4 integrin Clone PS/2	gift	N/A

Rat anti-mouse E-selectin Clone 9A9	B. Wolitzky	N/A
Human/Mouse CXCL12/SDF-1 Antibody	R&D Systems	Cat# MAB350
Human/Mouse CXCL12/SDF-1 Biotinylated Antibody	R&D Systems	Cat# BAF310
Rabbit polyclonal tyrosine hydroxylase antibody	Millipore	Cat# AB152
Chicken polyclonal Green Fluorescent (GFP) antibody	Aves	Cat# GFP-1020
Living Colors® Full-Length GFP Polyclonal Antibody	Clontech	Cat# 632592
Rabbit Anti-Choline Acetyltransferase antibody	Abcam	Cat# Ab178850
Rabbit Anti-Choline Acetyltransferase antibody	Phoenix Pharmaceuticals	Cat# H-V006
APC anti-mouse CD48 antibody Clone HM48-1	BioLegend	Cat# 103411
BV421 anti-mouse Sca1 antibody Clone D7	BioLegend	Cat# 108128
PE-Cy7 anti-mouse CD150 antibody Clone TC15-F12.2	BioLegend	Cat# 115914
APC-Cy7 anti-mouse ckit antibody Clone 2B8	BioLegend	Cat# 105856
BV510 Streptavidin	BioLegend	Cat# 405233

3.1.4 Biochemical reagents

Table 4 Biochemical reagents list

BIOCHEMICAL REAGENT	SOURCE	IDENTIFIER
Collagenase from Clostridium histolyticum	Sigma-Aldrich	Cat# C2674
BD IMag™ Streptavidin Particles Plus	BD Biosciences	Cat# 557812
Lympholyte®-M Cell Separation Media	Cedarlane	Cat# CL5031
Hydrocortisone	StemCell Technologies	Cat# 07904
MyeloCult™ M5300	StemCell Technologies	Cat# 05300
G-CSF (Filgrastim)	gift	N/A
5-fluoruracil	Sigma-Aldrich	Cat# F6627
6-Hydroxydopamine hydrochloride	Sigma-Aldrich	Cat# H4381
Detoxi-Gel™ Endotoxin Removing Columns	Pierce Biotechnology	N/A
Tetramethylrhodamine isothiocyanate–Dextran	Sigma-Aldrich	Cat# T1037
VECTASHIELD HardSet Antifade Mounting Medium	Vector Laboratories	Cat# H-1400
Alexa Fluor® 488 Phalloidin	Molecular Probes™	Cat# A12379
Peroxidase-Conjugated Streptavidin	DAKO	Cat# P 0397
TMB/E Single Reagent, Blue color, Horseradish Peroxidase Substrate	Millipore	Cat# ES001
Recombinant Human/Rhesus Macaque/Feline CXCL12/SDF-1 alpha	R&D Systems	Cat# 350-NS
Penicillin-Streptomycin	Invitrogen	Cat# 15140122
L-ascorbic acid 2-phosphate	Sigma-Aldrich	Cat# A8960
Giemsa Stain	Sigma-Aldrich	Cat# 32884
SIGMAFAST BCIP/NBT	Sigma-Aldrich	Cat# B5655
Proteinase K	Sigma-Aldrich	Cat# 3115801001
REDTaq Ready Mix PCR Reaction Mix	Sigma-Aldrich	Cat# R2523

3.1.5 Commercial assays kits

Table 5 Commercial assays kits list

COMMERCIAL ASSAYS KIT	SOURCE	IDENTIFIER
VECTASTAIN Elite ABC HRP Kit	Vector Laboratories	Cat# PK-6100
TSA Cyanine 3 Tyramide Reagent Pack	PerkinElmer	Cat# SAT704A001EA
Bi-CAT (Epinephrine & Norepinephrine) ELISA	ALPCO	Cat# 17-BCTHU-EO2.1
Acetylcholinesterase Activity Assay Kit	Sigma-Aldrich	Cat# MAK119
MouseTRAP (TRAcP 5b) ELISA	Immunodiagnosticsystems	Cat# SB-TR103
MicroVue DPD ELISA	Quidel	N/A

3.1.6 Sequence-based reagents

Table 6 Sequence-based reagents list

SEQUENCE-BASED REAGENT	SOURCE	IDENTIFIER
Primers for genotyping and quantitative real-time RT-PCR (Table 10 and 11).		
RNeasy Mini Kit	QIAGEN	Cat# 74104
Dynabeads® mRNA DIRECT™ Micro Purification Kit	Ambion™	Cat# 61021
Reverse Transcription System	Promega	Cat# A3500
SuperScript® II Reverse Transcriptase	ThermoFisher	Cat# 18064071
KAPA HiFi Hotstart ReadyMix	KAPA Biosystems	Cat# KK2601
Agencourt AMPure XP beads	Beckman Coulter	Cat# A63881
Quant-iT™ PicoGreen® dsDNA Assay Kit	ThermoFisher	Cat# P7589
KAPA qPCR quantification kit	KAPA Biosystems	Cat# KK4824

3.1.7 Software

Table 8 Software list

SOFTWARE	SOURCE	IDENTIFIER
FACSDiva Software	BD Biosciences	N/A
Poisson statistics. L-Calc™ software.	StemCell Technologies	N/A
ImageJ Software.	Java	N/A
GraphPad Prism	GraphPad	N/A
Microsoft Excel	Microsoft Office	N/A
GSNAP	N/A	Version 2015-09-29
Htweq-count	N/A	HTSeq version 0.5.3p3
Nucline software	Mediso, Budapest, Hungary.	N/A

3.2 Methods

3.2.1 Mouse strains

The following mouse strains were used in this study (see Table 1 for more details):

- *Gfra2*$^{-/-}$ (Rossi et al., 1999). This mouse model lacks the receptor for neurturin, a member of the glial cell-derived family of neurotrophic factors, and exhibits deficits in the enteric and parasympathetic nervous system.
- *Nes-gfp* (Mignone et al., 2004) (gift from G.E. Enikolopov). Mouse model expressing GFP under the promoter of the nestin gene. This strain was bred with *Gfra2*$^{-/-}$ mice to generate *Nes-gfp; Gfra2*$^{-/-}$ mice.
- *Adrb2tm1Bkk/J* (Chruscinski et al., 1999). This mouse strain lacks functional adrenergic receptor β2. This strain was bred with *Gfra2*$^{-/-}$ model to get double *Adrb2*$^{-/-}$*; Gfra2*$^{-/-}$ mice.
- *Adrb3tm1Lowl*. This mouse strain lacks adrenergic receptor β3. This strain was bred with *Gfra2*$^{-/-}$ model to get double *Adrb3*$^{-/-}$*; Gfra2*$^{-/-}$ mice.
- B6.129S7 *Chrna7tm1Bay*/J. This mouse model lacks the nicotinic cholinergic receptor α7.
- *Th-IRES-Cre* (Lindeberg et al., 2004) (gift from T. Ebendal). This mouse model expresses Cre recombinase under the tyrosine hydroxylase promoter and labels sympathetic fibres.
- *Dhh-IRES-Cre* (gift of D.N. Meijer). This mouse model expresses Cre recombinase under control of the mouse desert hedgehog (Dhh) promoter/regulatory regions.
- *ChAT-IRES-Cre*. This strain expresses Cre recombinase in cholinergic neurons, without disrupting endogenous *ChAT* expression.
- *B6.Cg-Gt(ROSA)26Sortm14(CAGtdTomato) Hze/J*. This reporter strain harbours a loxP-flanked STOP cassette preventing transcription of a CAG promoter-driven tdTomato red fluorescent protein from the Gt(ROSA)26Sor locus. This strain was bred with the different strains expressing Cre recombinase to label Cre-expressing cells.
- Congenic CD45.1 and CD45.2 C57BL/6J mice (Jackson Laboratories).

Mice were age- and sex-matched and housed in specific pathogen free facilities. All experiments using mice followed protocols approved by the Animal Welfare Ethical Committees and were compliant with EU recommendations.

3.2.2 Cell culture methods

3.2.2.1 Cell lines

Cell lines were purchased from ATCC (see Table 2 for more details).

MS-5 murine stromal cells were grown in a monolayer using α-MEM supplemented with 10% foetal bovine serum (FBS), 2mM l-glutamine and 2mM sodium pyruvate (Invitrogen).

The stromal cell line ST-2 was grown in RPMI1640 medium containing 10% FBS. MC3T3-E1 cells are osteoblastic precursors derived from mouse skull. They were grown in α-MEM medium supplemented with 10% FBS.

The osteocyte-like cell line MLO-Y4 was seeded in collagen I pre-coated-6 well dishes and grown with α-MEM medium supplemented with 5% FBS and 5% iron-supplemented calf serum (Invitrogen).

3.2.2.2 Cell maintenance

All cultures were maintained with 1% penicillin–streptomycin (P/S) (Invitrogen) at 37 °C in a water-jacketed incubator with 5% CO_2. Cells were split 1:5 with 0.05% trypsin/EDTA (Invitrogen) every three or four days when cells reached about 80% confluence. Routine tests confirmed the absence of mycoplasma contamination in the cultures.

3.2.2.3 Colony-forming-unit culture (CFU-C) assay

For measurement of HSPCs *in vitro* CFU-C assay was performed from blood and BM samples. 500µl of diluted blood samples were layered carefully over 2ml of Lympholite-M (Cedarlane). Tubes were centrifuged at room temperature (RT) for 25min, 1350 rpm with slow acceleration and without rotor brake. The mononuclear white blood cell fraction was collected and mixed with methylcellulose medium (recipe). Then 1ml cell suspension was seeded with an 18G syringe into non-adhesive 35mm culture dishes (Stem Cell Technologies). For BM samples, 10^4 BM nucleated cells were mixed with methylcellulose-based media and seeded into

35mm dishes as previously described (Frenette, Subbarao, Mazo, von Andrian, & Wagner, 1998). Colonies were scored after 7 days of culture.

For the fibroblastic colony-forming unit (CFU-F) assay, 10^6 BM nucleated cells were seeded into wells of 6-well plates and cultured at 37°C, 5% CO_2 in a water-jacketed incubator with α-MEM supplemented with 15% FBS, 1% (P/S) and 1mM l-ascorbic acid 2-phosphate (Sigma). After 10-12 days in culture, adherent cells were fixed with 100% methanol and stained 10min with Giemsa Stain (Sigma) at 37ºC to reveal fibroblastic colonies. Giemsa Stain is diluted 1:10 in phosphate buffer pH 6.8.

For the colony-forming unit-osteoblast (CFU-OB) assay, cells were allowed to grow in the same medium for 28 days, with half-medium changes twice a week. After this period, adherent cells were fixed with cold 4% paraformaldehyde (PFA) in PBS and alkaline phosphatase staining (Sigma Fast BCIP/NBT) was performed to reveal osteoblastic clusters. Alkaline phosphatase substrate was diluted in 10ml of dH_2O to prepare fresh staining solution. Cells were incubated with alkaline phosphatase solution for 10min protected from light.

For all the CFU-C assays, colonies with more than 50 cells were scored as positive.

3.2.2.4 BM primary cultures

BM myeloid cultures were obtained by seeding 3 x 10^6 BM cells into wells of 6-well plates with M5300 medium supplemented with 0.1µM hydrocortisone (StemCell Technologies), 1% P/S and 1% fungizone. Cells were maintained at 33°C and 5% CO_2 in a water-jacketed incubator. Half medium changes were performed weekly and cells were pharmacologically treated after two weeks in culture.

3.2.3 Biochemical methods

3.2.3.1 Blood, BM and spleen cell extraction

For BM haematopoietic cell isolation, bones were crushed in a mortar and filtered through a 40-µm strainer to obtain single cell suspensions. Adult and foetal livers as well as spleens were mechanically dispersed on a 40µm strainer. All cell suspensions were depleted of red blood cells by lysis in 0.15M NH_4Cl for 10min at 4ºC. Blood samples were directly lysed at RT.

To isolate HSPCs from bone-associated and non-associated marrow fractions, long bones were flushed gently with a 21G needle to obtain non-endosteal haematopoietic cells. The remaining bones were then crushed in a mortar to obtain haematopoietic cells of the endosteal compartment (Fig. 5).

To isolate nestin$^+$ cells, bones were cleaned from surrounding tissue, crushed in a mortar with a pestle, and digested with 0.25% collagenase/20% FBS/PBS (C2674, Sigma) in a water bath at 37ºC for 30min with agitation. Cells were filtered through a 40µm strainer and erythrocytes were lysed as described above. The resulting BM-enriched cell suspensions were pelleted, washed and resuspended in PBS containing 2% FBS for further analyses.

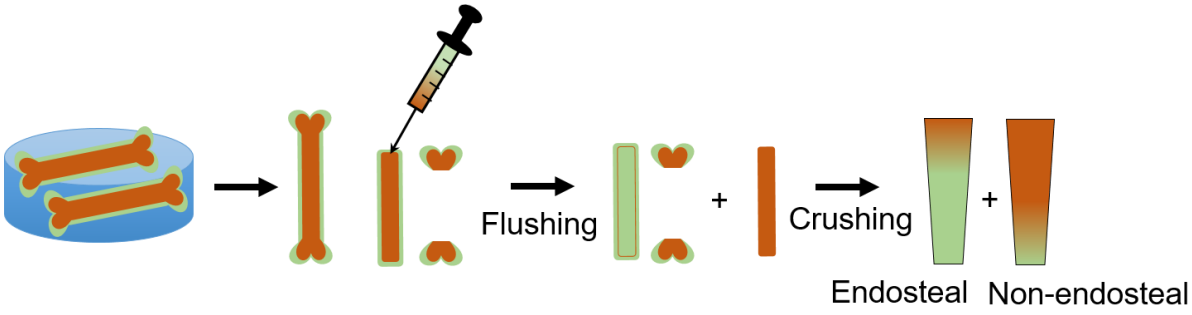

Figure 5. Scheme showing the protocol for enrichment of endosteal and non-endosteal BM fractions. *To separate endosteal and non-endosteal nestin$^+$ cells, long bones were gently flushed as described above. The flushed fraction and the remaining bone sample were digested with 0.25% collagenase/20% FBS/PBS (C2674, Sigma) in a water bath at 37ºC for 30min with agitation.*

3.2.3.2 Flow-cytometry and fluorescence-activated cell sorting (FACS)

Cells suspensions were incubated with the appropriate dilution (2-5 µg/ml) of fluorescent antibody conjugates in 2% FBS/PBS for 20min on ice. After washing with 2% FBS/PBS dead cells were excluded by 4',6-diamidino-2-phenylindole (DAPI) staining (1:3000). Cells were analysed on LSRFortessa flow cytometer (BD Biosciences, Franklin Lakes, NJ) equipped with FACSDiva Software (BD Biosciences), or sorted on Aria III cell sorter or BD Influx sorter (BD Bioscience).

The following antibodies were used to label haematopoietic cells (see Table 3 for more details): fluorescent CD45.1 (A20), CD45.2 (104), B220 (RA3-6B2), CD11b (M1/70), CD3e (145-2C11), LY-6G (1A8), CD90 (53-2.1), SCA1 (E13-161.7), CD34 (RAM34), CD135/flt3 (A2F10.1) and biotinylated lineage (LIN) antibodies (CD11b,

Gr-1, TER119, B220, CD3e) (BD Biosciences); cKIT (2B8) (eBioscience); CD150 (TC15-12F12.2), CD41 (MWReg30), CD48 (HM48-1) and SCA1 (D7) (BioLegend). Biotinylated antibodies were detected with fluorochrome-conjugated streptavidin (BD Biosciences). HSCs were immunophenotypically defined as $LIN^-CD41^-SCA1^+cKIT^+CD150^+$ cells.

BM stromal cells were defined as $CD45^-CD31^-Ter119^-$ and further purified according to Nes-GFP fluorescence (*Nestin-gfp*).

3.2.3.3 Cell cycle analysis

Cell cycle was analysed in sorted HSCs (defined as LIN^-CD41^- $SCA1^+cKIT+CD135^-$ cells) to study their quiescence/proliferative status. Hoechst 33342 (H42) and Pyronin Y (PY) staining to discriminate G0 ($H42^-PY^-$), G1 ($H42^-PY^+$) and G2/M/S ($H42^+PY^+$) cell cycle phases was performed as described in previously (Sanchez-Aguilera et al., 2014).

Briefly, sorted HSCs were collected in α-MEM medium supplemented with 2% FBS and 10mM HEPES. Cells were incubated with H42 (5µg/ml) 35min in α-MEM medium supplemented with 2% FBS, 10mM HEPES and 50µM verapamil at 37ºC. PY (1µg/ml) was added and the cells were incubated 20min at 37ºC. Finally, cells were resuspended in medium containing 50µM verapamil and analysed by flow cytometry.

3.2.3.4 Long-term competitive repopulation assay

HSC activity was assessed by long-term competitive repopulation assay using the congenic CD45.1 and CD45.2 isotypes of haematopoietic cells. Recipient female CD45.1 C57BL/6 mice (8 weeks old) were subjected to lethal irradiation (137Cs source, 11-12Gy whole body irradiation, split dose, 3h apart). To measure circulating HSCs, various blood volumes (75, 150 and 300µl) obtained from (CD45.2) 8-week-old male *Gfra2*$^{-/-}$ mice and control *Gfra2*$^{+/-}$ littermates were mixed with 2×10^5 BM nucleated cells from CD45.1 C57BL/6 mice in 200µl sterile PBS and intravenously (i.v) transplanted into the lethally-irradiated CD45.1 C57BL/6 mice. At various time points after transplantation (4, 8, 12 and 16 weeks), peripheral blood nucleated cells were collected from recipients. Cells were stained with fluorescent-conjugated antibodies against B220, MAC1 and CD90 antigens, and analysed by flow cytometry. The percentage of recipients in which reconstitution

failed was plotted against the number of transplanted cells and Poisson statistics (L-CalcTM software, StemCell Technologies) was applied to calculate the HSC concentration within the donor samples.

To measure BM HSC activity from endosteal and non-endosteal compartments, 10^6 BM nucleated cells from flushed BM or the remaining endosteal fraction of *Gfra2*$^{+/-}$ or *Gfra2*$^{-/-}$ (CD45.2) mice were used as donor cells. These cells were transplanted into lethally irradiated CD45.1 mice together with 10^6 CD45.1 competitor BM nucleated cells. Haematopoietic reconstitution was assessed in the peripheral blood of recipient mice after 24 weeks by measuring blood CD45.2 chimerism in the different mature haematopoietic lineages.

3.2.3.5 Homing of haematopoietic progenitors

To study BM HSPC homing in conditioned recipients, *Gfra2*$^{-/-}$ mice and control *Gfra2*$^{+/-}$ mice were lethally irradiated (137Cs source, 9.5Gy whole body irradiation, one dose). After 3h, 5 x 10^6 nucleated cells from congenic CD45.1 C57BL/6 donor mice were i.v. injected in 200µl PBS into each recipient mouse.

To study BM HSPC homing in unconditioned recipients, we enriched lineage negative donor cells by incubating BM nucleated cells obtained from CD45.1 C57BL/6 or *Gfra2*$^{-/-}$ mice. Cell suspensions were stained for 20min with biotinylated lineage antibodies (BD Biosciences) diluted in 2% FBS/PBS. After washing with 0.5% BSA/2mM EDTA in PBS, samples were incubated for 30min with streptavidin-conjugated magnetic beads (BD Bioscience) diluted in 0.5% BSA/2mM EDTA in PBS. Then, samples were placed in a magnetic particle concentrator (DynaMag, Invitrogen) for 8min to deplete LIN$^+$ cells. 5 x 10^6 haematopoietic lineage-depleted CD45.1 *WT* or *Gfra2*$^{-/-}$ nucleated cells were i.v. injected in 200µl PBS into *Gfra2*$^{-/-}$ mice and control CD45.1 *WT* or *Gfra2*$^{+/-}$ mice (CD45.2).

HSPC homing was assessed 16 hours after transplantation. BM and blood were harvested and used for CFU-C assay, as described below.

3.2.3.6 *In vivo* treatments

The following drugs were administered to mice according study plans approved by the local animal welfare committees for studying physiological responses *in vivo* (see Table 4 for more details):

- Granulocyte colony-stimulating factor (G-CSF; Filgrastim). HSPC mobilisation was induced with 8 consecutive injections of G-CSF (125µg/kg every 12h, sub-cutaneously (s.c.), dissolved in 5% dextrose in PBS). Five hours after the last injection mice were bled and CFU-C assay was performed.
- 5-fluoruracil (5-FU). A single dose of 5-FU (150 mg/kg, intra peritoneal (i.p.), diluted in PBS) was administered to assess haematopoietic recovery after myelosupressive stress. Mice were bled before the 5-FU injection and then every 3-4 days for haematological analysis.
- 6-hydroxydopamine (6-OHDA; Sigma). 6-OHDA is a neurotoxic synthetic compound used for chemical sympathetic denervation. Mice were s.c. injected with 6-OHDA (100 mg/kg, diluted in 0.2% ascorbic acid in 0.9% NaCl) on postnatal days P2, P4, P6, P8 and P9.
- Homing blocking antibodies. The following antibodies (1mg/kg) were injected i.v. for pharmacological blocking of HSPC homing. Rat monoclonal antibodies against P-selectin (RB40.34) and mouse α4 integrin (PS/2) were purified from hybridoma supernatants and subjected to potential endotoxin decontamination with a polymyxin B column (Detoxi-Gel; Pierce Biotechnology Inc.). Rat anti–mouse E-selectin Ab (9A9) was a gift from B. Wolitzky. Control rat IgG was obtained from Sigma.
- Nicotinic blocking drugs. For pharmacological nicotinic blockage experiments, mice were injected with 2 doses of methylatropine nitrate, mecamylamine (3mg/kg, diluted in PBS, i.p.) or vehicle on consecutive days. Peripheral blood was harvested five hours after the second dose.

3.2.4 Imaging & Immunoassays methods

3.2.4.1 Immunostaining

Immunofluorescence staining of 10µm cryo-sections was performed as previously described (Isern et al., 2014). Briefly, frozen tissues were allowed to thaw for 15min and slightly rinsed in PBS. Tissue sections were permeabilised with 0.1% Triton X-100 (Sigma) for 10min at RT and blocked with TNB buffer (0.1M Tris–HCl, pH 7.5, 0.15M NaCl, 0.5% blocking reagent, Perkin Elmer) for 1h at RT. Primary antibody incubations were conducted for 2h at RT. After 3 washing steps with 0.05%Triton-

X-100/PBS secondary antibody incubations were performed for 1h at RT. Stained tissue sections were counterstained for 5min with 5µM DAPI and rinsed with PBS. Slides were mounted in Vectashield Hardset mounting medium (Vector Labs) and sealed with nail polish. For whole mount staining of long bones and skull, all incubation times were extended.

We used the following primary antibodies (see Table 3 for more details): anti-tyrosine hydroxylase (1:1000, rabbit polyclonal antibody, Millipore), anti-GFP (1:200, chicken polyclonal, Aves), living colors full-length anti-GFP (1:500, rabbit polyclonal, Clontech) and anti-VAChT (1:100, rabbit polyclonal antibody, Abcam and Phoenix laboratories). Tyrosine hydroxylase staining included an amplification step using the Vectastain Elite ABC Kit (Vector Labs) and Cy3-Tyramide (PerkinElmer). Osteocyte projections were detected incubating for 48h with Alexa488-conjugated phalloidin (Sigma). Confocal images were acquired with a laser scanning confocal microscope (Zeiss LSM 700) or with a multiphoton confocal microscope (Zeiss LSM 780). At least 3 different sections per sample were blindly analysed using ImageJ software.

3.2.4.2 Intravital microscopy

Intravital microscopy is a very useful imaging tool that allows the study of physiological processes in living animals (Fig. 6). In this case we chose the skull BM for in vivo imaging of the vascular integrity. The skull cortical bone layer is sufficiently thin to allow for light penetration, avoiding to disrupt the BM microarchitecture. Anesthetized *Gfra2*$^{+/-}$ and *Gfra2*$^{-/-}$ mice were i.v. injected with 100µg Dextran-TRITC (1µg/µl in PBS 70 kDa, Sigma). Then mice were prepared for skull imaging. After depilating the skull area, an incision was made in the skin to expose the bone. Mice were placed in an animal holder to stabilize their position and maintain the body temperature. Imaging was performed through an “imaging window” created with a plastic ring fixed with hydrophobic glue and filled with PBS to keep the tissue hydrated. Acquisition was performed with a multiphoton confocal microscope (Zeiss LSM 780). The BM cavities closer to the parietal bones and distributed parasagitally along the sagittal suture were used for vasculature imaging. After imaging process mice were euthanized according to animal procedures legislation.

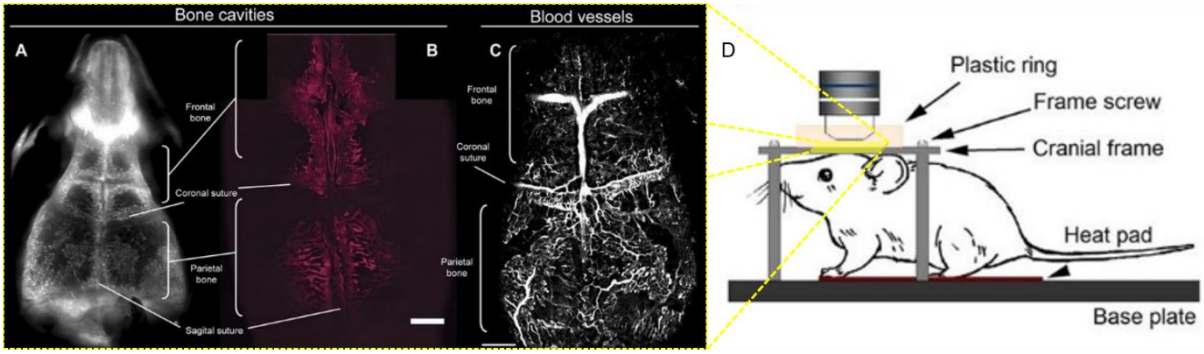

Modified from Pérez-Álvarez et al. 2013 & Lassailly et al. 2013

Figure 6. Illustration of the experimental setup for skull BM intravital microscopy. *Calvarium structures are shown using near-infrared spectroscopy (A) and confocal microscopy (B). C, 3D reconstruction of skull BM vasculature is shown. D, Scheme showing mouse position while intravital imaging.*

3.2.4.3 Sample preparation and staining for electron microscopy

Pre-anesthetised *Gfra2*$^{+/-}$ and *Gfra2*$^{-/-}$ mice were transcardially perfused with 2% formaldehyde (made from PFA) and 2% vacuum distilled glutaraldehyde, containing 2ml/l $CaCl_2$, in 0.05M sodium cacodylate buffer at 4 ºC and pH 7.4. Bones were removed and post-fixed by immersion in fixative solution for 24h at 4ºC. Bones were decalcified for one week with several changes of 0.25M EDTA in 20% fixative solution in dH_2O.Specimens were sliced into 2-4mm sections and fixed for an additional 4-6 hours at 4ºC. Samples were rinsed 5x 3min with cold cacodylate buffer containing 2mM $CaCl_2$. Subsequently, specimens were incubated with 1% osmium ferricyanide for 18h, at 4ºC and rinsed 5x in deionized water. This was followed by a 30min incubation in 1% thiocarbohydrazide at RT followed by 5 rinses in dH_2O. Tissues were than incubated in 1% uranyl acetate in 0.05 maleate buffer at pH 5.5 and at 4°C overnight. After 5 washing steps for 3min with dH_2O at RT, specimens were dehydrated via a graded series of alcohol (50%, 70%, 90%, and 100%, ethanol) followed by incubation in dry ethanol, dry acetone and dry acetonitrile. Finally, samples were infiltrated with a Quetol 651 epoxy resin over a period of 5 days. The resin was cured for 48h at 65 ºC. Thin sections were prepared with a Leica Ultracut S mounted on 200 mesh copper grids and viewed with a Tecnia G2 operated at 200kV.

3.2.4.4 Micro computer tomography (µCT)

Ex vivo µCT imaging of femurs and skulls was performed using a nanoPET/CT small animal imaging system (Bioscan, Washington DC) equipped with a micro-focus X-ray source and a high-resolution radiation-imaging device featuring a 1024x3596 pixel photodiode array with a 48µm pixel pitch. For CT measurements, scan parameters were 360 projections/rotations, 45kV (peak) 145µA current, and a detector pixel size of 71µm. Acquisition and reconstruction were performed with proprietary Nucline software (Mediso, Budapest, Hungary).

3.2.4.5 Enzyme-Linked Immunosorbent Assay (ELISA)

Cxcl12 protein levels were measured by conventional ELISA from BM extracellular fluid or BM stromal cell line supernatants (Fig. 7). Briefly, 96-well plates were coated overnight at 4ºC with 2µg/ml of monoclonal Cxcl1212/Sdf-1 antibody (MAB350, R&D Systems). After blocking with 3% sucrose/1% BSA/PBS, BM extracellular fluids were incubated in the Cxcl12 antibody-coated dishes for 2h at RT. 3 washing steps with 0.05% Tween20/PBS were accomplished and were followed by 2h incubation with a biotinylated anti-human/mouse Cxcl12/Sdf-1 antibody (BAF310, R&D). Streptavidin-conjugated horseradish peroxidase (HRP) (RPN1231V, Dako) was used to detect the antibody-binding to Cxcl12 by converting its substrate TMB (Tetramethylbenzidine, ES001-500ML, Chemicon, Millipore) into a colourful blue precipitate. Enzymatic reaction was stopped with hydrochloric acid (HCl) 1N. Absorbance at 450nm was measured photometrically to determine the Cxcl12 content in the samples relative to a standard curve with recombinant Cxcl12 (350-NS, R&D).

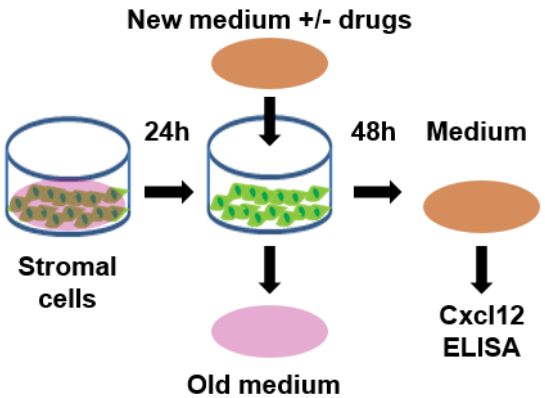

Figure 7. Experimental design used for cell culture and Cxcl12 ELISA.

ELISA for detecting noradrenaline (Bi-CAT ELiSA, 17-BCTHU-EO2.1, ALPCO), acetylcholinesterase activity (MAK119, Sigma), TRAP (SB-TR103, IDS) and DPD (Quidel) were performed according to the manufacturer's recommendations (see Table 5).

3.2.5 Molecular biological methods

3.2.5.1 Genotyping polymerase chain reaction (PCR)

Mice genotype was determined from tail/ear biopsies obtained when weaning. Tissue digestion was performed with proteinase K (Sigma) diluted (1/40) in 500µl lysis buffer (50mM NaCl + 50mM Tris-KCl pH8 + 5mM EDTA + 0.2% SDS). Samples were allowed to digest in the thermomixer at 55ºC and 750 rpm overnight.

The following day DNA extraction was performed. Samples were spin 5min at 13000 rpm and non-digested debris was discarded transferring the supernatant to new tubes. For DNA precipitation 500µl isopropanol was added and mixed gently with the supernatant. Samples were spin again 5min at 13000 rpm to get DNA pellet. Supernatant was discarded carefully and 500µl ethanol 70% added to wash DNA pellet. After a last spinning for 5min at 13000 rpm. DNA pellet was resuspended in 500µl TE buffer (1M Tris-HCl + 0.5M EDTA in distilled water). After 5min incubation at 55ºC and 750 rpm in the thermomixer, samples were ready for polymerase chain reaction (PCR). Extracted DNA was mixed with REDTaq ReadyMix PCR Reaction Mix (Sigma), 100µm oligonucleotides and nuclease-free water to run PCR. The PCR reaction mix and primer sequences used for genotyping PCR are shown in Table 9 and Table 10, respectively.

Table 9 Genotyping PCR reaction mix

REAGENT	**VOLUME PER SAMPLE (µl)**
REDTaq ReadyMix PCR Reaction Mix	12.5
dH_2O	8.5
Oligonucleotides mix	2
Extracted DNA	2

Table 10 Genotyping primer sequences

PRIMER NAME	SEQUENCE (5‘-3‘)
Gfra2. P1	CACATACACACAAAACTGTGGG
Gfra2. P2:	ATTCGCAGCGCATCGCCTTC
Gfra2. P3:	ATGTTGGAAGTCTCCTTCTC
GFP. P1	ATCATGGCCGACAAGCAGAAGAAC
GFP. P2	GTACAGCTCGTCCATGCCGAGAGT
Adrb2. P1	AGGGGCACGTAGAAAGACAC
Adrb2. P2	ACCAAGAATAAGGCCCGAGT
Adrb2. P3	GAGACTAGTGAGACGTGCTACT
Adrb3. P1	CGCATCGCCTTCTATCGCCTTCTTG
Adrb3. P2	GTTGCGAACTGTGGACGTCAGTGG
Adrb3. P3	ATTGCCGTTGGCGCTTAGCCAC
Chrna7. P1	TTCCTGGTCCTGCTGTGTTA
Chrna7. P2	ATCAGATGTTGCTGGCATGA
Chrna7. P3	CCCTTTATAGATTCGCCCTTG
Cre. P1	AATGCTTCTGTCCGTTTGCCGGT
Cre. P2	CCAGGCTAAGTGCCTTCTCTACA
tdTomato. P1	AGCAAGGGCGAGGAGGTCATC
tdTomato. P2	CCTTGGAGCCGTACATGAACTGG

3.2.5.2 RNA isolation, reverse transcription and Real time (RT) quantitative polymerase chain reaction (qPCR)

Total RNA extraction was performed mixing resuspended cells with 500µl of TRIzol (Invitrogen) and 100µl of chloroform. After 10min samples were spin at 4ºC for 15min (12.000 RCF). The nucleic acid fraction (top aqueous layer) was recovered and RNA precipitation was performed adding 250µl of isopropanol and letting samples to stand for 10min at room temperature. Samples were spin at 4ºC for 15min (12.000 RCF) and RNA pellet was later washed with 1000µl 80% ethanol. Later samples were spin again at 4ºC for 15min (7500 RCF) to remove the supernatant and leave the washed RNA pellet in the bottom of the tube. To eliminate

contaminating genomic DNA, DNase treatment with RNase-free DNase Set (Qiagen) was included in the protocol. RNA pellet was incubated with 87.5µl nuclease free water and 10µl RDD buffer (Qiagen). After 10min, 2.5µl DNAse were added and mixed up with RNA suspension. DNAse was allowed to work for 10min at room temperature. RNA was further purified with RNeasy Mini Kit (Qiagen) following the manufacturer's recommendations.

For low cell numbers (<100.000), RNA was isolated using the Dynabeads® mRNA DIRECT™ Micro Kit (Invitrogen) according to manufacturer's instructions.

Table 11 RT-qPCR primer sequences

PRIMER	SEQUENCE FORWARD (5'-3')	SEQUENCE REVERSE (5'-3')
Cxcl12	CGCCAAGGTCGTCGCCG	TTGGCTCTGGCGATGTGGC
Kitl	CCCTGAAGACTCGGGCCTA	CAATTACAAGCGAAATGAGAGCC
Chrna3	ACTCCAAAAGCTGCAAGGAA	CAGAGCAGACAGGGACAACA
Chrna4	GCAGGGTCTCACAGGAAGAG	ACAGGATTTGGCTCCATCAC
Chrna5	CGCTCTTCTTCCACACACAA	TCTCGTGATGTAGCGAATGC
Chrna7	TTGTGCTGCGATATCACCAC	TTCATGCGCAGAAACCATGC
Chrnb2	GGGAAGATTATCGCCTCACA	GTGCAGTTCTGCTGGTCAAA
Chrnb4	GCTGAAGCTACGTCCACCTC	GAAGCTGACGCCCTCTAATG
Chrm1	CAGAAGTGGTGATCAAGATGCCTAT	GAGCTTTTGGGAGGCTGCTT
Chrm2	TGGAGCACAACAAGATCCAGAAT	CCCCTGAACGCAGTTTTCA
Chrm3	CCGCTCTACCTCTGTCCTTCA	GGTGATCTGACTTCTGGTCTTGAG
Chrm4	GTGACTGCCATCGAGATCGTAC	CAAACTTTCGGGCCACATTG
Chrm5	GGCCCAGAGAGAACGGAAC	TTCCCGTTGTTGAGGTGCTT
Gapdh	TGTGTCCGTCGTGGATCTGA	CCTGCTTCACCACCTTCTTGA

RNA concentration was determined with NanoDrop Spectrophotometer (Thermo Scientific). A maximum of 2µg RNA was used for the reverse transcription using the Reverse Transcription System (Applied Biosystems), following the manufacturer's recommendations. Absolut gene expression levels were determined by RT qPCR (Applied Biosystems). The cDNA was mixed with 100µm oligonucleotides and SYBR Green master mix (Applied Biosystems) containing buffer, dNTPs,

thermostable hot-start DNA polymerase and SYBR Green dye. The expression level of each gene was determined by the relative standard curve method, using a standard curve prepared from serial dilutions of a mouse or human reference total RNA (Clontech).

The expression level of each gene was calculated by interpolation from the standard curve. All values were normalised to *Gapdh* as the endogenous control. The primer sequences used for RT-qPCR are shown in Table 11.

3.2.5.3 RNA sequencing

Whole transcriptome sequencing was performed to compare gene expression profiles in *Gfra2*$^{+/-}$ and *Gfra2*$^{-/-}$ HSCs isolated from endosteal and non-endosteal compartments. Pools of 30 viable LSK CD48^{-}CD150^{+} cells were sorted (BD Influx™ cell sorter) into 4µl lysis buffer (0.5U/µl SUPERase In RNase Inhibitor in 0.2% (v/v) Triton-X-100) containing 12.5mM DTT and 2.5mM dNTP.

RNAseq was performed following the Smart-seq2 protocol (Picelli et al., 2014). Briefly, RNA was primed with oligo-dT primers and reverse transcribed using Superscript II Reverse Transcriptase (200U/µl, ThermoFisher 18064071). KAPA HiFi Hotstart ReadyMix (KAPA Biosystems, KK2601) and IS PCR primers were used to amplify the cDNA, later purified with Agencourt AMPure XP beads (Beckman Coulter, A63881). cDNA quality was checked with Agilent Bioanalyser 2100 using Agilent High Sensitivity DNA chip and quantity was measured with Quant-iT™ Picogreen double stranded DNA assay kit (Thermo Fisher P7589).

Pooled libraries of 4 replicates per sample were prepared using the Illumina Nextera XT DNA preparation kit. Amplified libraries were purified using Agencourt AMPure XP beads, quality-checked using Agilent high-sensitivity DNA chip on Agilent Bioanalyser 2100 and quantified using KAPA qPCR quantification kit (KAPA Biosystems, KK4824). Sequencing was performed on the Illumina Hi-Seq 4000 (single end, 50bp read length) by the CRUK Cambridge Institute Genomics Core facility.

RNA-seq reads were aligned to the Mus musculus genome (Ensembl version 38.81) using GSNAP (version 2015-09-29) with parameters (-B 5 –t 24 –n 1 –Q –N 1). Reads in features were counted with htweqcount (HTSeq version 0.5.3p3) with the parameter (-s no). Quality control was performed with the following cut-offs: more

than one and a half million uniquely mappable reads, less than 20% of reads mapping to mitochondrial genes over mitochondrial + nuclear genes and more than 8500 high coverage genes identified. Counts were normalized using size factors calculated by DESeq2 protocol using a 10% FDR. Values were then represented in log10 scale. Highly variable genes were selected using the method described by Brennecke *et al.* PCA was then performed in *R* using the *prcomp* function (Brennecke et al., 2013).

Gene set enrichment analyses (*http://www.broadinstitute.org/gsea/index.jsp*) were performed using a weighted statistic, ranking by signal to noise ratio, 1000 gene-set permutations, and a custom gene set database gene lists manually compiled from the literature, as previously described (Sanchez-Aguilera et al., 2014).

3.2.6 Statistical analysis

For calculation of sample sizes, the total cellularity and composition of the different cell populations was determined in peripheral blood and BM using a hematologic analyser (Abacus Junior Vet, Beckman Coultier) and a cell counter (CASYton, CASY systems).

The compared groups were set similarly in all procedures. For each scenario we established the number of conditions (including at least one control condition) to test the hypothesis. Results were scored blindly. Data shown in figures are means ± SEM; n and p values are indicated in each single figure.

For statistical analysis, One Way ANOVA and Bonferroni comparison were used for multiple group comparisons, and unpaired two-tailed t tests for two-group comparisons. The data met the assumptions of the tests. Significant statistical differences between groups were indicated as: * $p < 0.05$; ** $p < 0.01$; *** $p < 0.001$. Statistical analyses and graphics were carried out with GraphPad Prism 5 software and Microsoft Excel.

“Con la responsabilidad gestionamos lo que depende de nosotros, la persecución de los objetivos que nos hemos marcado. Con la capacidad de aguante, gestionamos lo que no depende de nosotros, es decir, la adversidad”

Toni Nadal

4 Results

4.1 GDNF Family Receptor Alpha 2 Knock-out (KO) mouse (*Gfra2*$^{-/-}$) as a model of peripheral parasympathetic deficiency

Gfrα2 is a glycosylphosphatidylinositol-linked cell surface co-receptor which belongs to the GDNF receptor family together with Gfrα1, Gfrα3 and Gfrα4. Although all co-receptors are anchored to and activate RET tyrosine kinase receptor, each co-receptor preferentially binds to a different neurotrophic factor (GDNF/Gfrα1, Nrtn/Gfrα2, Artn/Gfrα3 and Pspn/Gfrα4). Nrtn/Gfrα2 signalling has been shown to be essential for development and maintenance of the enteric and parasympathetic nervous system (Heuckeroth et al., 1999; Rossi et al., 1999). Thus, we used a *Gfra2*$^{-/-}$ mouse model to study a possible parasympathetic regulation of BM HSC niches. Measurement of acetylcholinesterase (AchE) activity in urine of *Gfra2*$^{-/-}$ and control mice indirectly confirmed the reduction of parasympathetic tone in *Gfra2*$^{-/-}$ mice (Fig. 8A). However, the reduced parasympathetic activity did not affect the haematopoietic system as the numbers of BM nucleated cells and BM as well as spleen HSCs were not altered (Fig. 8B and 8C).

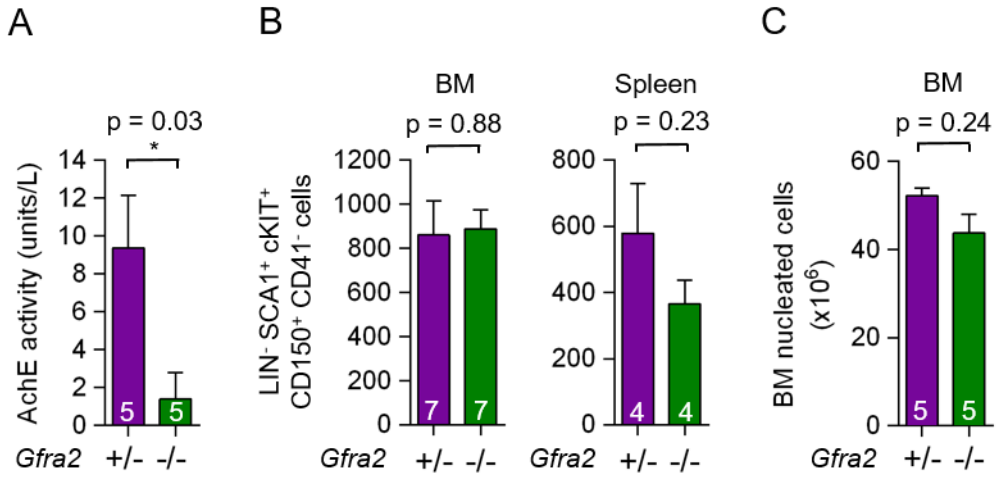

Figure 8. *Gfra2*$^{-/-}$ mice exhibit decreased parasympathetic activity while haematopoietic numbers remain unaltered. *A, AChE activity in urine samples collected at night from Gfra2*$^{-/-}$ *mice and control Gfra2*$^{+/-}$ *mice. B, Number of* LIN^{-} *SCA1*$^{+}$*cKIT*$^{+}$*CD150*$^{+}$*CD41*$^{-}$ *HSCs in BM and spleen. C, BM nucleated cells in Gfra2*$^{-/-}$ *mice and control Gfra2*$^{+/-}$ *mice (2 femurs).* Data are means ± SEM; n and p values are indicated. * $p < 0.05$.

4.2 Circadian autonomic cholinergic regulation of HSC trafficking

The autonomic nervous system controls the circadian circulation of HSPCs between the BM and other peripheral organs like the blood. Following exposure to light, sympathetic signals are transmitted to efferent nerve terminals in the BM where they induce the release of noradrenaline. Adrenergic stimulation of BMSCs decreases Cxcl12 levels and leads to HSPC egress during the day, reaching a peak at Zeitgeber time (ZT, hours after light onset) 5 (Mendez-Ferrer et al., 2008). Since the PNS antagonises sympathetic signals in many peripheral systems (Beauregard & Smith, 1994; Benthem, Mundinger, & Taborsky, 2001; Miyashita et al., 1999; Pendry & Maclagan, 1991), we decided to study the circadian HSPC trafficking in *Gfra2*$^{-/-}$ mice. Measurement of circulating HSPCs over 24h revealed normal circadian oscillations in control mice and in *Gfra2*$^{-/-}$ mice during the day period. However, circulating leukocytes and HSPCs were 2-3-fold increased at night (ZT13) (Fig. 9A). To analyse circulating HSCs *in vivo*, we performed long-term repopulation assays using limiting dilutions of blood harvested at ZT13 from *Gfra2*$^{-/-}$ and control mice. The number of HSCs in the bloodstream was similarly elevated 3-5 times in *Gfra2*$^{-/-}$ mice at night (Fig. 9B). These results suggest a role for PNS in circadian regulation of HSC trafficking, specifically during the night time when HSPC homing to the BM is predominant (Fig. 9C).

4.3 HSPC accumulation in peripheral blood in *Gfra2*$^{-/-}$ mice at night is not due to reduced HSPC BM homing

Murine leukocytes and HSPCs preferentially home to the BM at night (Scheiermann et al., 2012). Thus, we investigated whether the observed accumulation of HSPCs in the blood of *Gfra2*$^{-/-}$ mice at night is caused by defective HSPC BM homing. We performed reciprocal BM transplantations using *Gfra2*$^{-/-}$ or control *Gfra2*$^{+/-}$ mice as donors as well as recipients as indicated in Fig. 10A. HSPC BM homing was similar in lethally-myeloablated mice in all conditions tested (Fig. 10B). Lethal irradiation increases BM homing efficiency but also induces damage of BM niches in recipient mice and thus might interfere with niche-dependent homing mechanisms (Green & Rubin, 2014). For this reason, we transplanted HSPC-enriched cells into non-irradiated recipient mice (Fig. 10C). Surprisingly, HSPC BM homing was not reduced, but even increased in unconditioned *Gfra2*$^{-/-}$ mice (Fig. 10D). BM homing

was not affected when transplanting *Gfra2*$^{-/-}$ donor HSPCs into control *Gfra2*$^{+/-}$ recipients, suggesting that increased HSPC homing detected in *Gfra2*$^{-/-}$ mice is a non-cell autonomous defect. HSPC homing takes place in the BM sinusoids and HSC adhesion to sinusoids via integrins and selectins is an essential step in the BM homing process (Lapidot, Dar, & Kollet, 2005).

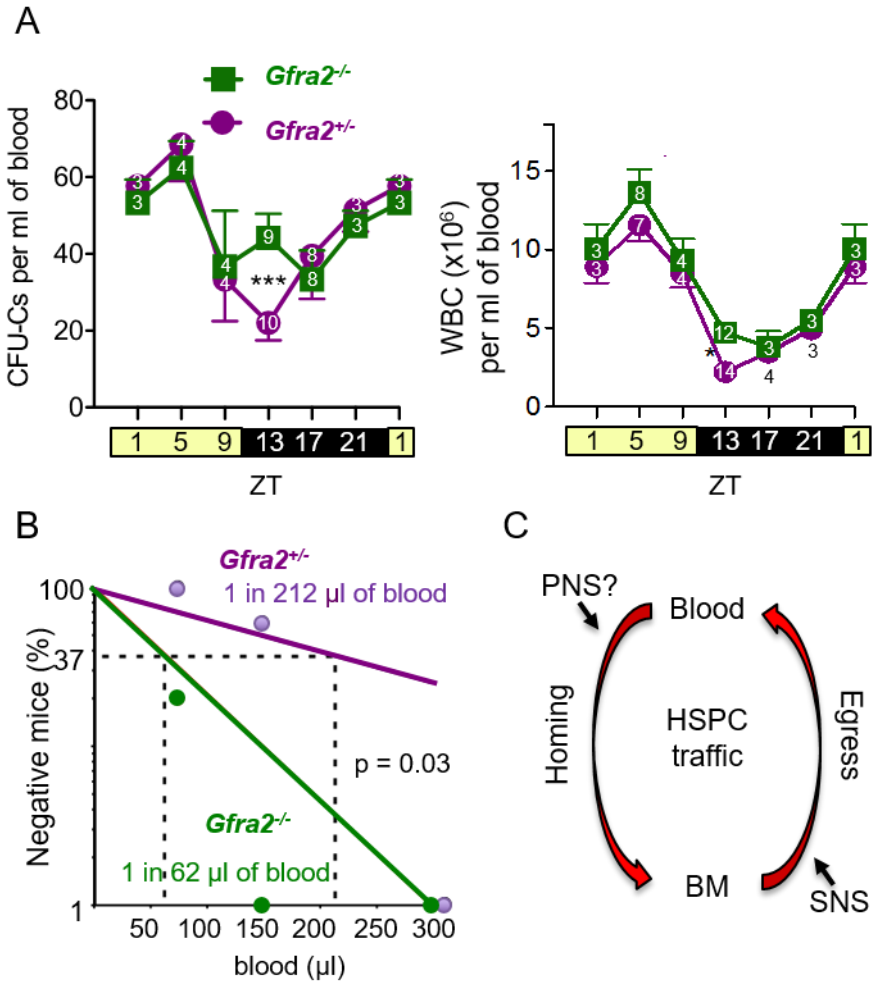

Figure 9. HSPCs accumulate in peripheral blood of *Gfra2*$^{-/-}$ mice at ZT13. *A, HSPCs, measured as CFU-Cs, and white blood cells (WBCs) in the peripheral blood of Gfra2*$^{-/-}$ *mice (green) and control Gfra2*$^{+/-}$ *mice (purple) harvested at the specified ZT. B, HSCs, measured by long-term competitive repopulation assay, in peripheral blood harvested at ZT13 from Gfra2*$^{-/-}$ *mice (green) and control Gfra2*$^{+/-}$ *mice (purple). The frequency of mice with failed reconstitution is plotted against the transplanted blood volume. Blood HSC concentrations are indicated (n = 5). C) Scheme illustrating our hypothesis about the role of PNS in HSPC traffic regulation. Data are means ± SEM; n and p values are indicated. * p < 0.05; *** p < 0.001.*

In order to study whether the increased accumulation of HSPC in the BM of *Gfra2*$^{-/-}$ mice was due to an increase in active BM homing, we treated the mice with

antibodies against integrin α4 (Papayannopoulou, Priestley, Nakamoto, Zafiropoulos, & Scott, 2001), E-selectin and P-selectin (Katayama et al., 2003) at night (Fig. 10E). Homing blockade abrogated nocturnal differences in circulating HSPCs between *Gfra2*$^{-/-}$ and control *Gfra2*$^{+/-}$ mice (Fig. 10F). In summary, HSPC homing to the BM is increased in *Gfra2*$^{-/-}$ mice, but does not contribute to HSPC accumulation in the bloodstream at night.

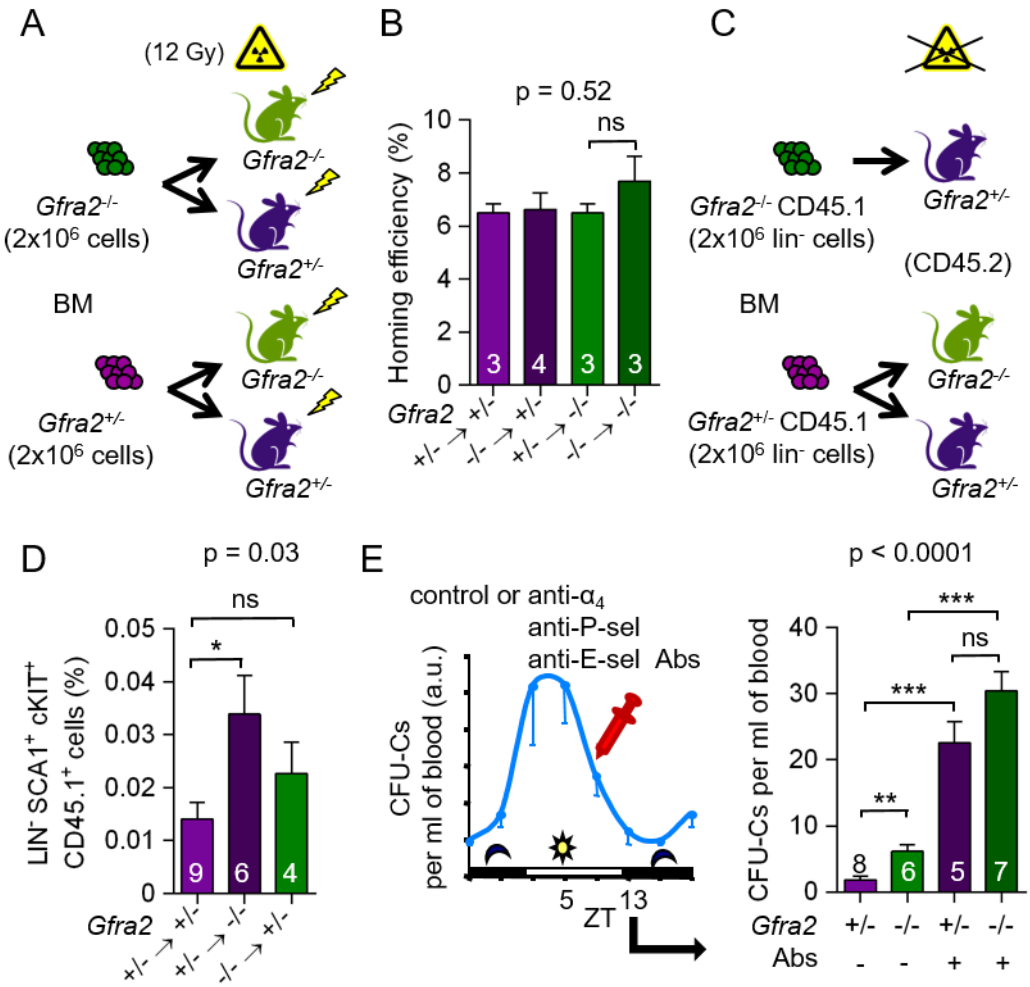

Figure 10. Increased HSPC BM homing in *Gfra2*$^{-/-}$ mice. *A, Scheme showing the protocol used for the HSPC BM homing assay with lethal irradiation. B, Frequencies of HSPCs (CFU-Cs) that homed to the BM 16h after reciprocal transplantation of Gfra2*$^{-/-}$ *or control Gfra2*$^{+/-}$ *BM cells into lethally irradiated Gfra2*$^{-/-}$ *or control Gfra2*$^{+/-}$ *mice. C) Scheme showing the protocol used for HSPC BM homing assay without irradiation. D, Frequencies of CD45.1*$^{+}$ *Gfra2*$^{+/-}$ *or CD45.1*$^{+}$ *Gfra2*$^{-/-}$ *HSPCs that homed to BM 16h after transplantation into non-irradiated CD45.1 or CD45.2 mice. E, Scheme showing the protocol used for homing blockade. F, HSPCs circulating at ZT13 5h after injection of blocking antibodies against* integrin α4, P- and E-selectin (Abs) or control IgG. *Data are means ± SEM; n and p values are indicated. * p < 0.05; ** p < 0.01; *** p < 0.001.*

4.4 PNS signals regulate HSC trafficking indirectly

Despite the increased BM homing in *Gfra2*$^{-/-}$ mice, HSPCs intriguingly accumulated in the peripheral blood at night. Increased numbers of circulating HSPC suggested us that HSPC mobilisation might be similarly increased in our parasympathetic-deficient mouse model at night. Since the SNS contributes to physiological HSC egress from the BM (Mendez-Ferrer et al., 2008; Spiegel et al., 2007) and enforced mobilisation by G-CSF (Katayama et al., 2006), we next studied sympathetic signalling in *Gfra2*$^{-/-}$ mice.

For this purpose we quantified BM sympathetic fibres and measured the concentration of the sympathetic neurotransmitter noradrenaline in the urine of *Gfra2*$^{-/-}$ and control mice during the day and the night. Interestingly, TH^{+} fibres as well as nocturnal but not diurnal noradrenaline levels were increased in *Gfra2*$^{-/-}$ mice compared to control *Gfra2*$^{+/-}$ mice (Fig. 11A-D). Hence, the sympathetic tone is specifically increased during the night in parasympathetic-deficient *Gfra2*$^{-/-}$ mice. As it has been shown that PNS can modulate sympathetic activity in other systems (Gavioli et al., 2014), we hypothesized that increased parasympathetic activity might have an important inhibitory role during the night by dampening sympathetic tone and contributing to reduced HSPC egress in a setting when BM homing is the predominant process.

To address this hypothesis and locate this possible inhibitory regulation, we treated wild-type mice during the night with acetylcholine antagonists that are blood-brain barrier permeable (mecamylamine) or non-permeable (atropine methyl nitrate). While mice treated with the non-permeable antagonist showed normal numbers of circulating HSPCs, those treated with blood-brain barrier-permeable drug exhibited a 3-fold increase of HSPCs in the blood (Fig. 11E). Thus, central cholinergic signals contribute to BM HSPC-trafficking during the night.

To confirm the indirect cholinergic regulation of circadian HSPC trafficking via SNS modulation, we bred *Gfra2*$^{-/-}$ mice with mice lacking the main β-adrenergic receptors that cooperate during enforced mobilisation: β2- and the β3-adrenergic receptor (Mendez-Ferrer, Battista, & Frenette, 2010). Nocturnal circulating HSPCs and leukocytes were similarly increased in *Gfra2*$^{-/-}$ mice and *Gfra2*$^{-/-}$;*Adrb2*$^{-/-}$ (Fig. 11F). In contrast, *Gfra2*$^{-/-}$;*Adrb3*$^{-/-}$ mice recovered normal circulating HSPC numbers at night (ZT13) (Fig. 11G). In conclusion, central and nocturnal PNS signals interfere

with SNS innervating the BM and this results in HSPC trafficking regulation by inhibition of sympathetic activity transmitted by β3-adrenergic receptor.

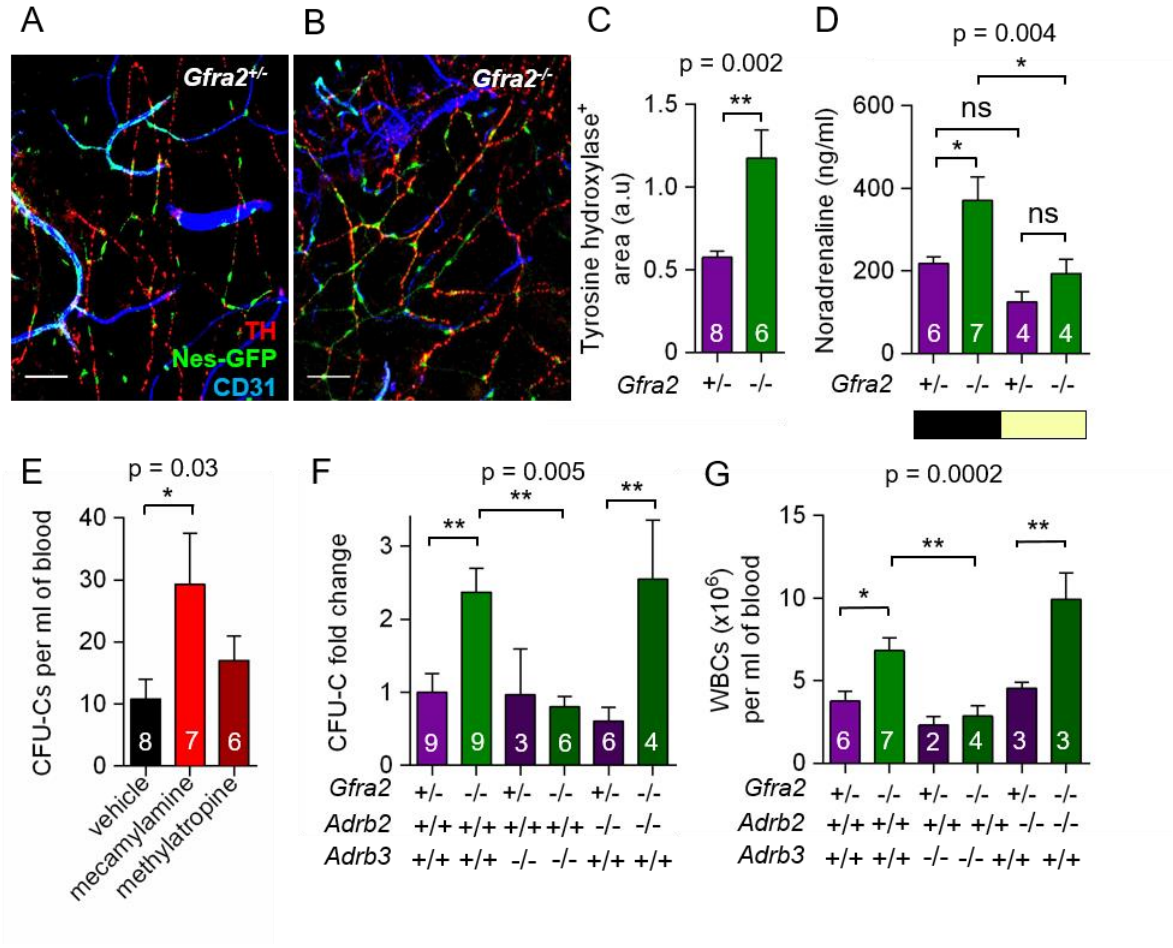

Figure 11. The PNS controls HSPC trafficking indirectly through central SNS regulation. *A-B, IF staining of CD31⁺ endothelial cells (blue), tyrosine hydroxylase (TH)⁺ sympathetic nerve fibres (red) and Nes-GFP⁺ cells (green) in the skull BM of Nes-gfp;Gfra2$^{-/-}$ and control Nes-gfp;Gfra2$^{+/-}$ mice. Scale bar, 100µm. C, Quantification of BM sympathetic noradrenergic nerve fibres. D, Noradrenaline concentration in the urine of Gfra2$^{-/-}$ and control Gfra2$^{+/-}$ mice collected at night (black box) and day (yellow box). E, HSPCs circulating in the blood of C57BL/6 mice treated with mecamylamine, atropine methyl nitrate or vehicle (3mg/kg). F, HSPCs circulating at ZT13 in Gfra2$^{-/-}$ mice or compound mice deficient for Gfra2 and β2- or β3-adrenergic receptors. G, WBCs circulating at ZT13 in Gfra2$^{-/-}$ mice or compound mice deficient for Gfrα2 and β2- or β3-adrenergic receptors. C-F, Data are means ± SEM; n and p values are indicated. C, Unpaired two-tailed t test. D-G, One-way ANOVA and Bonferroni comparisons. * p < 0.05; ** p < 0.01.*

4.5 Deregulated HSPC-trafficking in parasympathetic fibre deficient-mice is a non-cell autonomous effect

In contrast to β2-adrenergic receptors which are broadly expressed by haematopoietic cells, β3-adrenergic receptor is mostly expressed in non-haematopoietic cells (adipocytes, BMSCs and endothelial cells), indicating that the exacerbated sympathetic tone in *Gfra2*$^{-/-}$ mice most likely affects stromal cells in the BM microenvironment. However, RET, which mediates the downstream signalling upon Gfrα co-receptors binding to it respective ligand, has been shown to be expressed by HSCs. RET-signalling in HSCs promotes HSC survival, expansion and improves *in vivo* transplantation efficiency (Fonseca-Pereira et al., 2014). Thus, in addition to central SNS deregulation, defective RET signalling in HSPCs might contribute to increased HSPC egress in *Gfra2*$^{-/-}$.

To dissect the contribution of direct vs stromal cell mediated neural signals in regulating HSPC trafficking in *Gfra2*$^{-/-}$ mice, we generated chimeric mice through long-term reciprocal BM transplantations. Lethally-irradiated *Gfra2*$^{-/-}$ or control *Gfra2*$^{+/-}$ recipient mice were reciprocally transplanted with *Gfra2*$^{-/-}$ or control *Gfra2*$^{+/-}$ donor BM cells. This results in the generation of mice with *Gfra2*$^{-/-}$ haematopoietic cells and control BMSCs and vice versa. Control mice carrying *Gfra2*$^{-/-}$ haematopoietic cells had normal blood counts. In contrast, *Gfra2*$^{-/-}$ recipients transplanted with control haematopoietic cells exhibited nocturnal accumulation of circulating HSPCs and leukocytes in the blood (Fig. 12). These experiments strongly suggest that circadian HSPC trafficking defects in parasympathetic-fibre deficient *Gfra2*$^{-/-}$ mice are mediated by the BM stromal compartment rather than HSPCs directly.

The chemokine Cxcl12 is the master regulator of HSC function in BM niches. Multiple studies have shown its role in controlling HSC quiescence as well as HSPC migration/retention (Greenbaum et al., 2013; Nagasawa et al., 1996). Interestingly, circadian oscillations of circulating HSPCs correlate with anti-phase fluctuations in BM *Cxcl12* expression (Mendez-Ferrer et al., 2008; Schajnovitz et al., 2011). Based on this knowledge we reasoned that Cxcl12 might be affected in parasympathetic fibre-deficient *Gfra2*$^{-/-}$ mice. We measured *Cxcl12* gene expression levels over 24h and detected a significant decrease at ZT13 (Fig. 13A). Importantly, this reduction of Cxcl12 at transcriptomic level was accompanied by a decrease at protein level

(Fig. 13B). Thus, we found that nocturnally increased numbers of circulating HSPCs and leukocytes correlate with a Cxcl12 reduction at the same circadian time in *Gfra2*$^{-/-}$ mice.

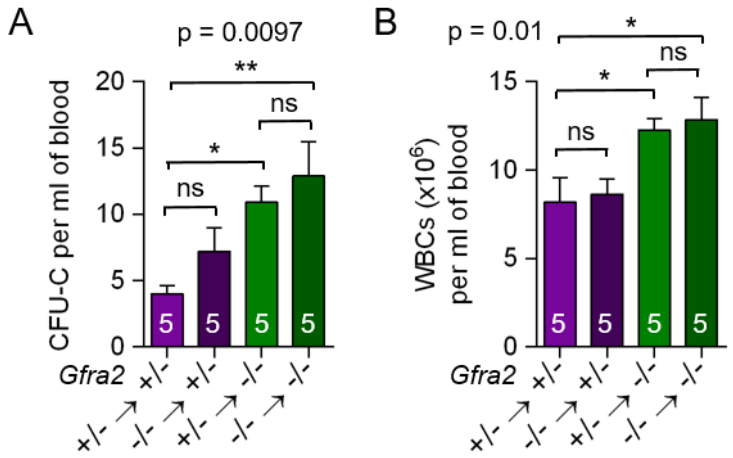

Figure 12. HSPC-trafficking defect in *Gfra2*$^{-/-}$ mice results from neural deregulation of the BM microenvironment. *A-B, HSPCs, measured as CFU-Cs (A) and WBCs (B) circulating in the blood at ZT13, 16 weeks after reciprocal BM transplantations in lethally-irradiated mice. Gfra2*$^{-/-}$ *mice and control Gfra2*$^{+/-}$ *mice were used as donor or recipients. Data are means ± SEM; n and p values are indicated. One-way ANOVA and Bonferroni comparisons. * p < 0.05; ** p < 0.01.*

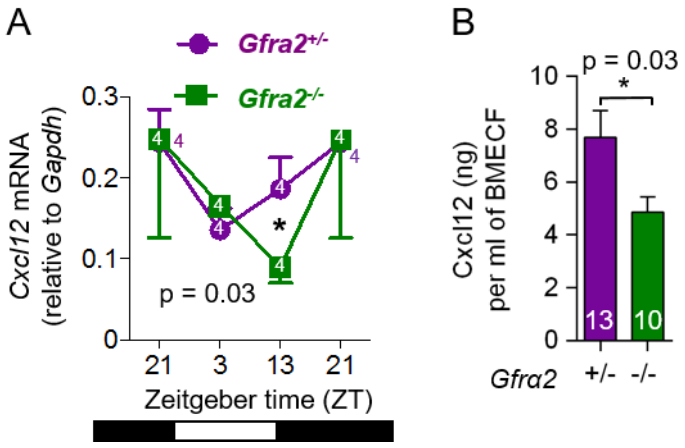

Figure 13. Reduced Cxcl12 level in *Gfra2*$^{-/-}$ mice at ZT13. *A, Cxcl12 mRNA expression in the BM of Gfra2*$^{-/-}$ *and control Gfra2*$^{+/-}$ *mice at the specified ZT. B, Cxcl12 protein concentration in BM extracellular fluid (BMECF). Data are means ± SEM; n and p values are indicated. A, Multiple two-tailed t test. B, Unpaired two-tailed t test. * p < 0.05.*

Cxcl12 is highly expressed and released in BM niches by multiple cell types including osteoblasts and different BMSCs (NG2^{+} perivascular cells, Lepr^{+} cells, CAR cells and nestin^{+} cells) (Fig. 3). Interestingly, BM sinusoids, which are the most

permeable vessels through which HSPCs traffic in and out of the BM (Itkin et al., 2016), are surrounded by Nes-GFP^{lo}Lepr^{+} BMSCs. This perisinusoidal BMSC population controls HSC maintenance by secreting Cxcl12, but specially Scf (Ding et al., 2012). In contrast, Nes-GFP^{hi}NG2^{+} BMSCs are associated with less permeable arteriolar-like vessels (Kunisaki et al., 2013) as well as TZ vessels in endosteal areas (Kusumbe et al., 2014) and secrete mainly Cxcl12. This together with the fact that nestin^{+} BMSCs can respond to sympathetic signals via β3-adrenergic receptor signalling encouraged us to study the role of nestin^{+} cells as BMSCs mediating the *Gfra2*$^{-/-}$ phenotype.

The global number of Nes-GFP^{+} cells with in the BM was not changed in *Gfra2*$^{-/-}$ mice compared to control mice (Fig. 14A). To have a closer look at different subpopulations of nestin^{+} cells including sinusoidal Nes-GFP^{lo} cells and non-sinusoidal Nes-GFP^{hi} cells in *Nes-gfp*;*Gfra2*$^{-/-}$ mice, we mechanically separated BM fractions as previously shown (Grassinger & Nilsson, 2011) (see Fig. 5). This technique, allows the efficient separation of an endosteal fraction from a non-endosteal and sinusoidal cell-enriched fraction.

The Nes-GFP^{hi} population was more abundant in the endosteal compartment in which nestin^{+} cells have been described to be closely associated with TZ vessels (Kusumbe et al., 2016), validating our method for separating endosteal and non-endosteal fractions. In fact, Nes-GFP^{hi} cells associated with arteriolar vessels remained attached to endosteal structures after BM flushing (Fig. 14B,D). Nes-GFP^{lo} cells were more abundant in non-endosteal compartment. Whereas the Nes-GFP^{hi} cell number was comparable between *Gfra2*$^{-/-}$ and control mice, Nes-GFP^{lo} cells were reduced by 40% in non-endosteal fraction of *Gfra2*$^{-/-}$ mice (Fig. 14C). Since sinusoidal Nes-GFP^{lo} cells constitute the vast majority of nestin^{+} in the BM, the decrease of Nes-GFP^{lo} cells may explain the reduced Cxcl12 level in *Gfra2*$^{-/-}$ mice (Fig. 13). Nes-GFP^{lo} cell number reduction might also result from the increased sympathetic activity in parasympathetic deficiency, since noradrenaline has been shown to inhibit Nes-GFP^{+} cell proliferation (Mendez-Ferrer, Michurina, et al., 2010).

This suggests that impaired cholinergic signalling in parasympathetic fibre-deficient *Gfra2*$^{-/-}$ mice leads to increased sympathetic activity, which reduces sinusoidal HSPC maintenance by decreasing Nes-GFP^{lo} cell numbers and Cxcl12 level. As consequence HSPC trafficking through sinusoids is over-activated in *Gfra2*$^{-/-}$ mice.

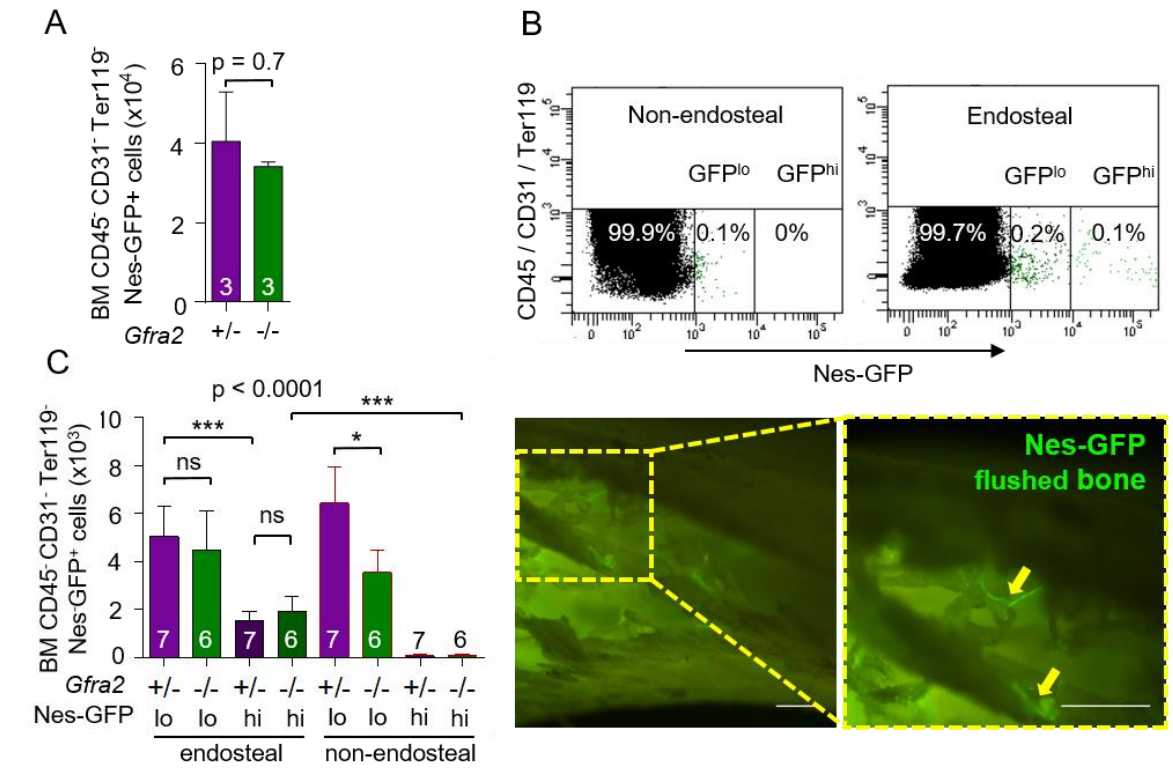

Figure 14. Nes-GFP^{lo} cell numbers are reduced in the non-endosteal compartment of *Gfra2*$^{-/-}$ mice. *A, Nes-GFP^{+} BMSC numbers in Gfra2$^{-/-}$ and control mice. B, Representative flow cytometry profiles of non-endosteal GFP^{+}CD45^{-}CD31^{-} Ter119^{-} BMSCs obtained by flushing out the BM of long bones and of endosteal GFP^{+} BMSCs in the remaining in long bones of adult Nes-gfp mice. Both cell fractions were digested with collagenase. C, Stromal Nes-GFP$^{lo/hi}$ cells in endosteal and non-endosteal BM of Gfra2$^{-/-}$ and control mice. D, Images illustrating the high enrichment of Nes-GFP^{hi} cells in the bone-associated fraction of flushed Nes-GFP^{+} bones. Scale bar, 200 µm. A, Unpaired two-tailed t test. C, One-way ANOVA and Bonferroni comparisons. A, C, Data are means ± SEM; n and p values are indicated. * p < 0.05; *** p < 0.001.*

4.6 PNS independently regulates HSPC trafficking and bone formation

Whereas the evidence for parasympathetic regulation of the BM is scarce, several studies have reported the involvement of the PNS in the bone formation process. In this context, cholinergic fibres have been reported to directly transmit bone anabolic signals from the brain (Bajayo et al., 2012). However, the PNS has also been proposed to regulate bone formation indirectly by modulating the sympathetic tone centrally (Shi et al., 2010). Based on these initial studies, we investigated whether bone remodelling is affected in parasympathetic-deficient *Gfra2*$^{-/-}$ mice and whether

this interferes with the HSPC trafficking defect. Considering that PNS activity was shown to promote bone formation, we checked the number of osteoprogenitor cells in *Gfra2*$^{-/-}$ mice.

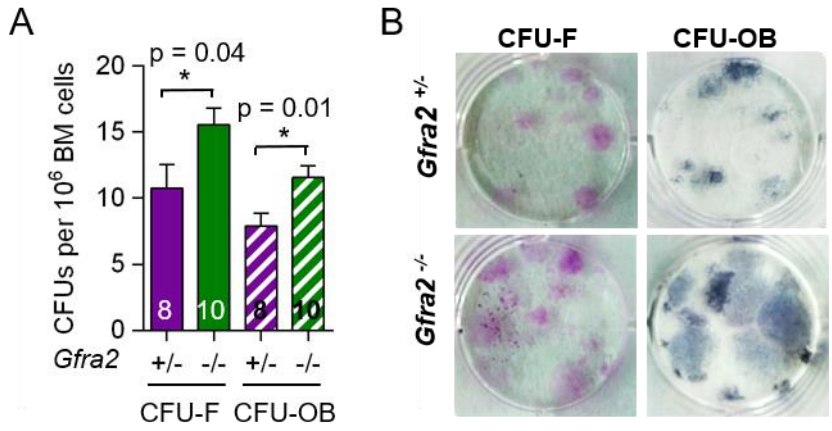

Figure 15. Deregulated osteoprogenitor activity in *Gfra2*$^{-/-}$ mice. *A, Quantification of BM CFU-fibroblast (CFU-F) and –osteoblast (CFU-OB) from Gfra2*$^{-/-}$ *and control Gfra2*$^{+/-}$ *mice. B, Representative images of CFU-F and CFU-OB colonies. A, Data are means ± SEM; n and p values are indicated. One-way ANOVA and Bonferroni comparisons. * p < 0.05.*

In vitro CFU-C assays showed that both fibroblastic (CFU-F) and osteoblastic (CFU-OB) progenitors were significantly increased in BM from *Gfra2*$^{-/-}$ compared to control mice (Fig. 15). Increased osteoprogenitor activity most likely represents a compensatory response to previously described impaired bone growth in *Gfra2*$^{-/-}$ mice (Rossi et al., 1999). Further characterization of bones from *Gfra2*$^{-/-}$ mice by micro computed tomography (µCT) and bone immunofluorescence revealed enlarged cranial sutures and decreased trabecules in *Gfra2*$^{-/-}$ mice (Fig. 16A-D). However, markers of bone resorption such as *tartrate-resistant acid phosphatase (TRAP)* and *deoxypyridinoline (DPD) cross-linking* levels in urine were not altered in *Gfra2*$^{-/-}$ mice suggesting that bone defects observed were not caused by increased osteoclastic activity (Fig. 16E,F)

Importantly, intercellular contact between bone-embedded osteocytes has been suggested to be required for sympathetic fibre-mediated HSPC mobilisation in response to granulocyte colony-stimulating factor (G-CSF) administration (Asada et al., 2013). To investigate whether altered sympathetic activity and bone remodelling in *Gfra2*$^{-/-}$ mice could be related to defective osteocyte cell contact formation, we labelled F-actin elements in the cytoskeleton of osteocytes by phalloidin staining.

Phalloidin staining revealed that osteocyte projections were markedly reduced in *Gfra2*$^{-/-}$ mice compared to control mice, indicating that bone remodelling is defective in these mice (Fig. 17A-B). In consequence, we dissected whether the HSPC trafficking defect observed in *Gfra2*$^{-/-}$ mice was rather a direct consequence of the bone phenotype or an independent alteration caused by parasympathetic deficiency. Intravital microscopy analysis showed that vascular integrity was intact in *Gfra2*$^{-/-}$ mice (Fig. 17C). *Gfra2*$^{-/-}$ mice and control mice were treated with the mobilising agent G-CSF and circulating HSPCs were measured. Mobilisation was similar in both groups, suggesting that HSPC trafficking alteration and bone defects are independent phenotypes present in parasympathetic-deficient *Gfra2*$^{-/-}$ mice (Fig. 17D).

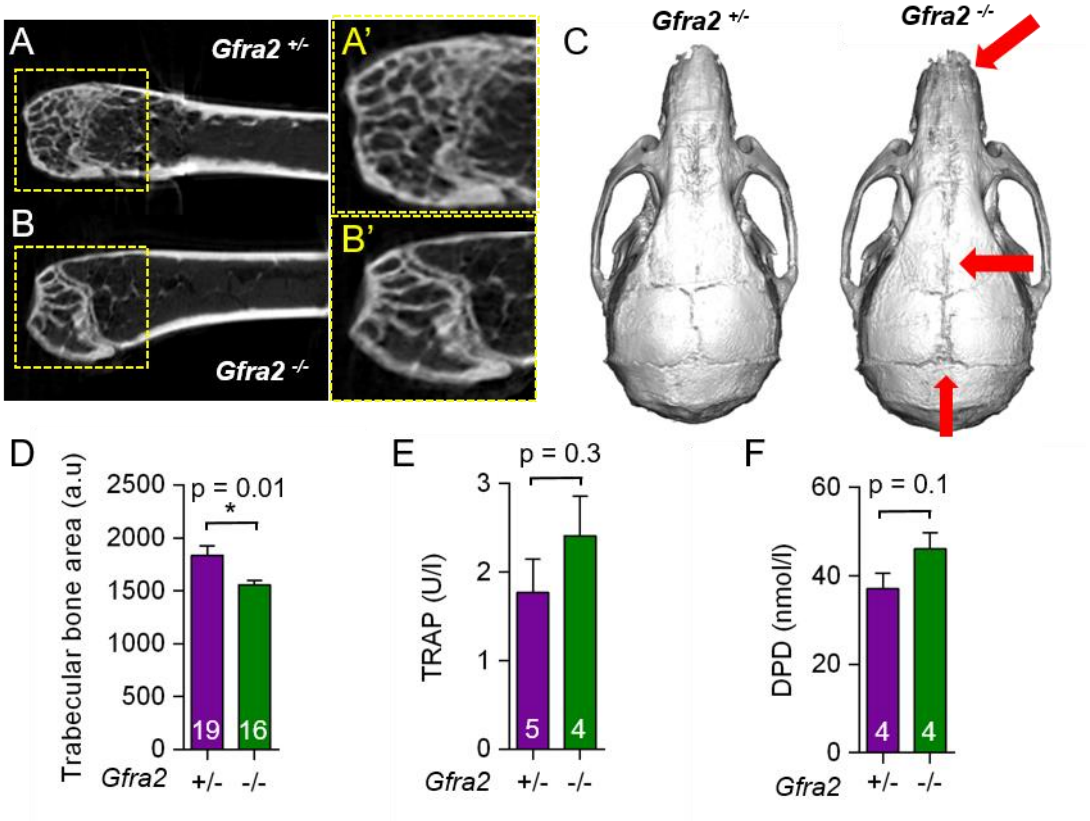

Figure 16. Bone defects in *Gfra2*$^{-/-}$ model are not caused by increased bone resorption. *A-C, µCT of femoral trabecular bone area (A-B) and skull (C) from Gfra2*$^{-/-}$ *and control Gfra2*$^{+/-}$ *mice. Arrows indicate enlarged cranial sutures and ossification defects. D, Quantification of trabecular bone area. E-F, Osteoclast activity measured in Gfra2*$^{-/-}$ *and control Gfra2*$^{+/-}$ *mice in the night by determining urine concentration of tartrate-resistant acid phosphatase (TRAP) (E) and by performing deoxypyridinoline (DPD) cross-link test (F). D-F, Data are means ± SEM; n and p values are indicated. Unpaired two-tailed t test. * p < 0.05.*

In conclusion, although cholinergic signals contribute to modulate both HSPC trafficking and bone remodelling processes, this regulation seem to be mediated by different mechanisms in *Gfra2*$^{-/-}$ mice.

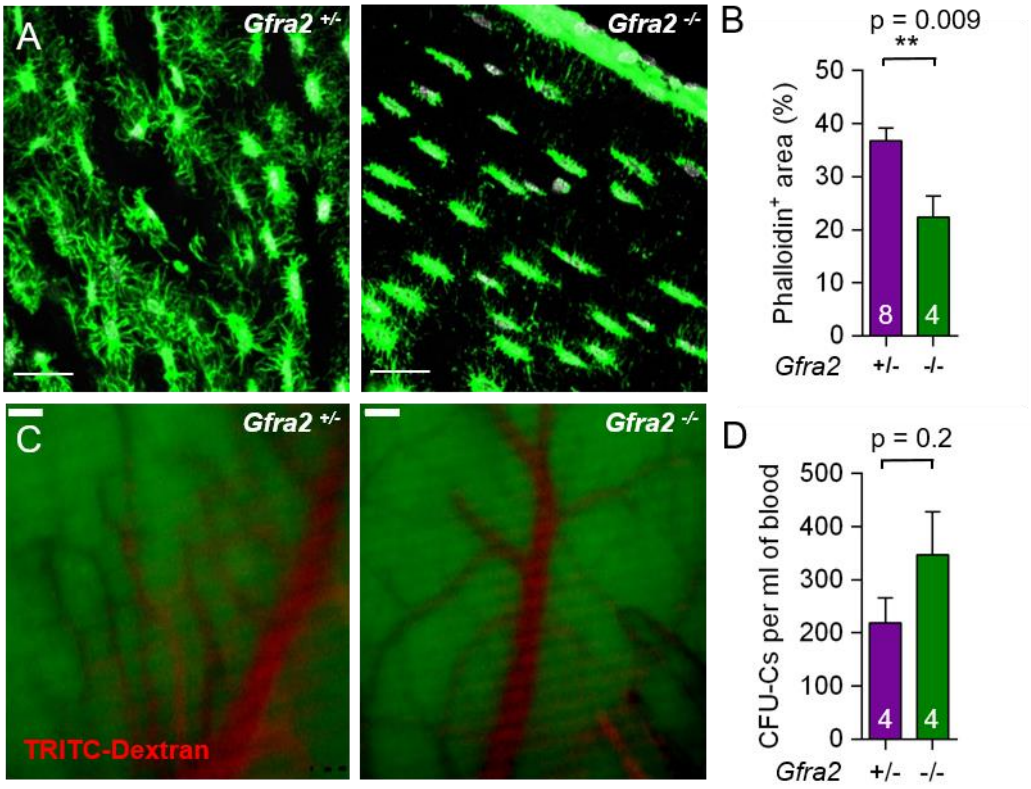

Figure 17. Decreased osteocyte projections is not associated with HSPC traffic defect in parasympathetic-deficient *Gfra2*$^{-/-}$ mice. *A-B, Phalloidin staining of osteocyte actin skeleton (green) (A) and quantification of phalloidin*$^{+}$ *area (B). Scale, 25 µm. C, Intravital microscopy of the skull BM 5min after intravenous injection of TRITC-Dextran (red). Scale, 100 µm. D, HSPCs circulating at ZT13, 5h after the last injection of G-CSF (8 doses of 125 µg/kg every 12h). B-C, Data are means ± SEM; n and p values are indicated. Unpaired two-tailed t test. ** p < 0.01.*

4.7 Cholinergic nerve fibres innervate bone and endosteal BM

The first part of this thesis has shown the importance of central cholinergic signalling in regulating circadian HSPC trafficking through modulation of SNS activity. The PNS has been similarly suggested to promote bone formation by antagonising central sympathetic signals (Shi et al., 2010). Similarly, our data supports a parasympathetic regulation of HSPC trafficking at the central level. Experiments with blood-brain barrier permeable and non-permeable acetylcholine antagonists placed the inhibitory modulation of sympathetic activity by parasympathetic fibres inside of

the CNS (Fig. 10E). However, these experiments cannot rule out the possibility that cholinergic fibres might also directly innervate the BM and regulate BM niches locally.

Despite some immunohistochemistry studies suggesting the presence of cholinergic fibres in the BM (Artico et al., 2002), the existence of these fibres have not been validated and thus remains unclear. In contrast of the scarce neuroanatomical evidence, parasympathetic innervation in the BM has been reported to transmit bone anabolic signals from the brain (Bajayo et al., 2012). In this work authors used vesicular acetylcholine transporter (VAChT) as a marker to label skeletal PNS fibres in the bone. VAChT is a membrane transporter which loads acetylcholine into secretory organelles and has been used as specific maker of synaptic vesicles in PNS terminals (Weihe, Tao-Cheng, Schafer, Erickson, & Eiden, 1996).

To study the possible innervation of the BM by cholinergic fibres, we immunostained *WT* whole-mount bone samples for VAChT. As previously reported, VAChT$^+$ fibres were found at the outer surface of the bone (periosteum) (Asmus et al., 2000). We also detected some cholinergic fibres in the bone proper and at the inner surface of the bone (endosteum), which is in close contact with the BM (Fig. 18). VAChT is not the only marker used to identify cholinergic fibres and the enzyme choline acetyltransferase (ChAT) has also been used to mark cholinergic fibres in the rat BM (Artico et al., 2002). To confirm the presence of cholinergic nerve fibres in the murine endosteal BM we used *ChAT-IRES-cre* mice (Rossi et al., 1999) intercrossed with *Ai35D* reporter mice (Madisen et al., 2012). In this mouse model, Cre-mediated recombination in cholinergic neurons renders them GFP$^+$. *ChAT-IRES-cre;Ai35D* mice revealed the presence of ChAT$^+$ fibres in the skull BM and in long bones of *WT* mice. Similar to VAChT staining, ChAT-labelled structures were always associated with the endosteal compartment in the BM (Fig. 19). In contrast to *WT* mice, endosteal VAChT$^+$ cholinergic fibres were undetectable in parasympathetic-deficient *Gfra2*$^{-/-}$ mice (Fig. 20A-C). Given the small size and the fact that this is the first time this innervation has been reported in the BM, we performed transmission electron microscopy to further characterize it. In this detailed analysis, unmyelinated axons (compatible with the cholinergic phenotype) were present in the endosteal bone of WT mice, while reduced in *Gfra2*$^{-/-}$ mice (Fig. 20D-E).

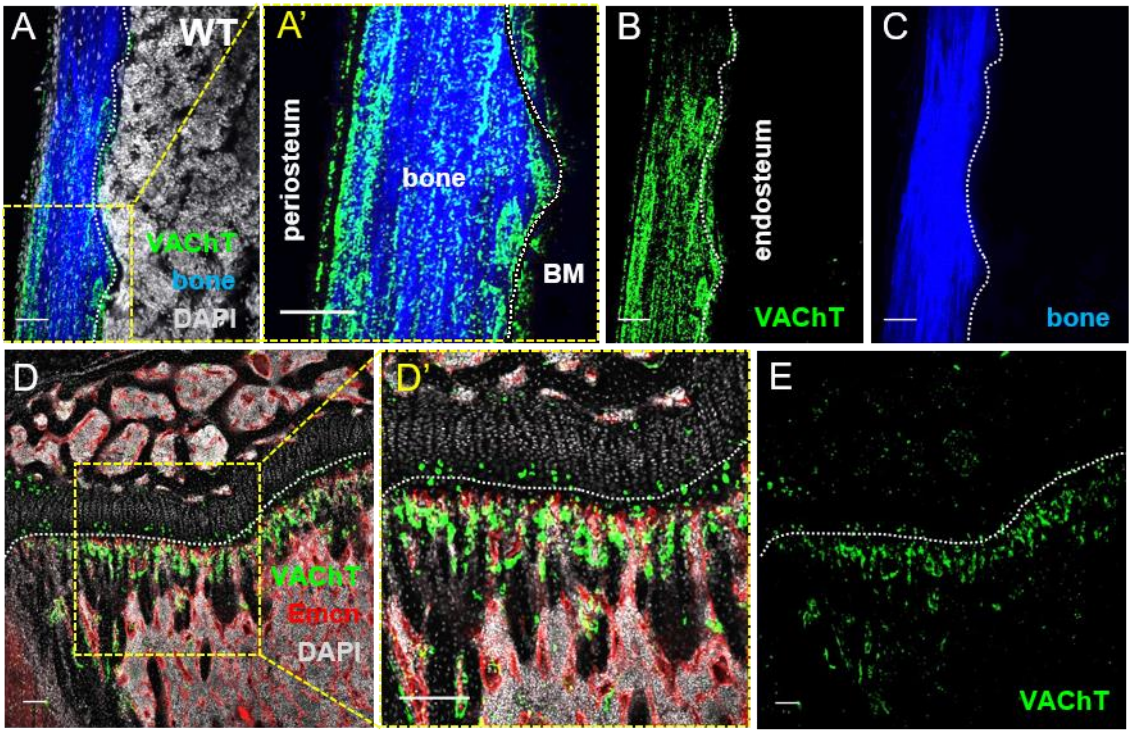

Figure 18. Vesicular acetylcholine transporter (VAChT) labels cholinergic fibres in the bone and endosteal BM. *Immunofluorescent staining for VAChT to label cholinergic nerve fibres (green) in adult diaphyseal BM (A-C) or epiphyseal BM (D-E) sections of C57Bl/6 mice. Bone (blue) was visualised by second harmonic collagen signals. Endomucin (red) helped to visualize the vasculature in epiphyseal BM. Nuclei were counterstained with DAPI (grey). Endosteal surface is depicted by a dashed line. Close-ups of A and D are shown in A' and D' respectively. Scale bar, 100 µm.*

In conclusion, using several different approaches we confirmed the presence of autonomic cholinergic innervation in bone proper and, more interestingly, in the endosteal BM which was drastically reduced in *Gfra2*$^{-/-}$ mice.

4.8 A sympathetic origin for cholinergic fibres in the BM

Although noradrenaline is the primary postsynaptic neurotransmitter of the SNS, some exceptions to this rule have been reported. During development, some peripheral sympathetic neurons releasing noradrenaline start producing acetylcholine, thereby becoming sympathetic cholinergic neurons (Francis & Landis, 1999). This phenomenon was named "cholinergic switch" (Wolinsky & Patterson, 1983) and has been described in at least three different structures, including sweat glands, vasculature in skeletal muscle and periosteum. Importantly, sympathetic cholinergic neurons require Gfrα2 signalling for survival, being completely absent in the periosteum of *Gfra2*$^{-/-}$ mice (Hiltunen & Airaksinen, 2004).

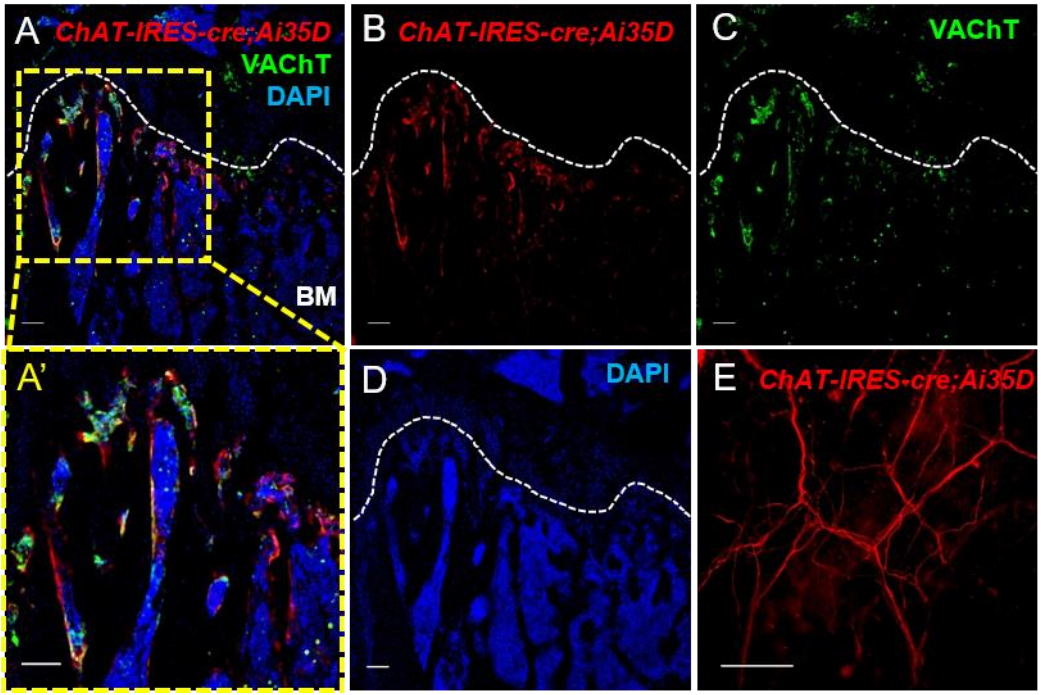

Figure 19. Choline acetyltransferase (ChAT)-traced and VAChT-stained neural fibres innervate bone and endosteal BM. *Immunofluorescence of VAChT to label cholinergic nerve fibres (green) and anti-GFP (red) in adult femoral BM sections (A-D) or skull BM (E) of ChAT-IRES-cre;Ai35D mice with GFP expression in genetically-traced cholinergic neurons. Endosteal surface is depicted by a dashed line. Nuclei were counterstained with DAPI (blue). A' shows a close-up of A. Scale bar, 100 µm.*

The cholinergic switch occurs early postnatally around week 1-3 (Asmus et al., 2000). We performed chemical sympathectomy with 6-OHDA during the first postnatal days because this treatment targets sympathetic fibres that would later become cholinergic (at the time when they are still adrenergic). We followed this approach to determine if endosteal VAChT$^+$ fibres are sympathetic, like those previously reported in the periosteum, or parasympathetic. For this purpose, neonatal mice were treated with 6-OHDA during the first postnatal week and the BM innervation was analysed in the same mice at adulthood (Fig. 21A). Postnatal 6-OHDA treatment ablated not only adult sympathetic noradrenergic fibres ("normal sympathetic fibres"), but also the majority of adult VAChT$^+$ fibres. This result indicates that endosteal and periosteal VAChT$^+$ fibres correspond to sympathetic cholinergic neurons (Fig. 21B-C).

In order to confirm the sympathetic origin of endosteal VAChT$^+$ fibres and to analyse their relationship with sympathetic noradrenergic fibres, we took advantage of the *Th-cre;Ai14D* mouse model. Since the Cre-recombinase is activated when the TH

enzyme is expressed in the neuron, this mouse model has genetically-labelled Tomato$^+$ neurons that synthesize or have synthesized noradrenaline at some point. Thus, fibres with sympathetic origin, including sympathetic cholinergic fibres, are labelled in this model. Immunostaining of whole mount femur samples of *Th-cre;Ai14D mice* revealed the presence of VAChT$^+$Tomato$^+$ double positive fibres, confirming the sympathetic origin of VAChT$^+$ fibres (Fig. 22A-D).

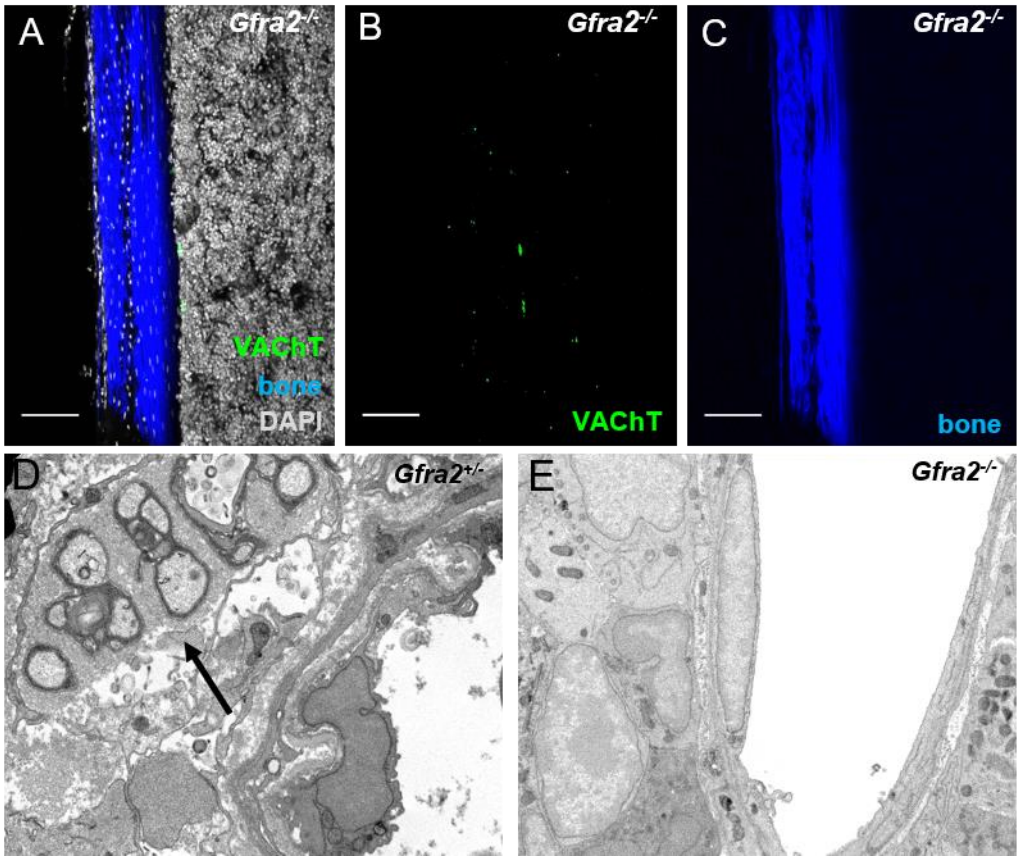

Figure 20. VAChT$^+$ cholinergic fibres are dramatically reduced in *Gfra2*$^{-/-}$ mice. *A-C, Immunofluorescent staining of VAChT to label cholinergic fibres (green) in adult femur sections of Gfra2$^{-/-}$ mice. Bone (blue) is visualised by second harmonic collagen signals and nuclei are counterstained with DAPI (gray). Endosteal surface is depicted by a dashed line. D-E, Transmission electron microscopy images of control Gfra2$^{+/-}$ (D) and Gfra2$^{-/-}$ (E) bones. The arrow depicts a non-myelinated fibre. Scale bar, 100 µm.*

Analysis of the relative position of sympathetic cholinergic fibres with respect to other fibres revealed close association of sympathetic cholinergic fibres with TH$^+$vAChT$^-$ sympathetic noradrenergic fibres as well as Schwann cells (genetically-labelled using a *Dhh-cre;Ai14D* mouse model) (Fig. 22E-J). Therefore, postganglionic regulatory feedback loops might be in place at the peripheral level to control the final neural output regulating the BM HSPC niche.

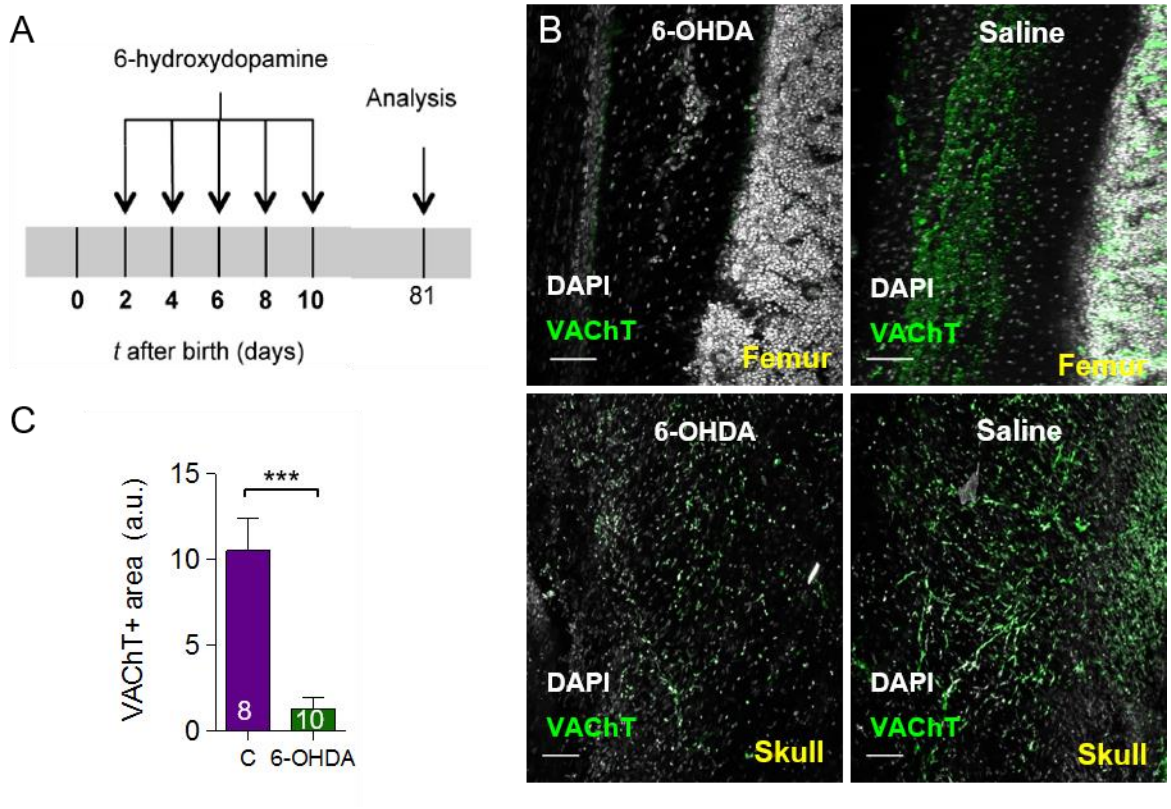

Figure 21. Cholinergic fibres innervating bone and endosteal BM have a sympathetic origin. *A, Scheme showing the protocol used for neonatal sympathectomy using 6-OHDA (100 mg/kg diluted in 0.2% ascorbic acid in 0.9% NaCl, s.c. on alternate days). B, Immunofluorescent staining for VAChT$^+$ cholinergic nerve fibres (green) in femoral BM (upper panels) or skull BM (lower panels) from adult C57Bl/6 mice, which were previously treated with 6-OHDA or saline at neonatal stages. Bone (blue) was visualised by second harmonic collagen signals. Nuclei were counterstained with DAPI (gray). Scale bar, 100 µm. C, Quantification of VAChT$^+$ fibres in C57Bl/6 mice treated with saline or 6-OHDA. Data are means ± SEM; n and p values are indicated. Unpaired two-tailed t test. *** p < 0.001.*

4.9 Sympathetic cholinergic innervation might contribute to maturation of the perinatal BM niche

Although BM niche colonisation by HSCs starts at late stages of embryonic development, HSC migration from the liver to the BM persists early postnatally (Wolber et al., 2002). During this period the BM stroma still undergoes maturation and becomes vascularised as well as innervated (Gajda et al., 2000). Because the cholinergic switch takes place during these first postnatal days, we analysed whether the absence of sympathetic cholinergic fibres in *Gfra2*$^{-/-}$ mice had any relevance in BM HSC colonisation.

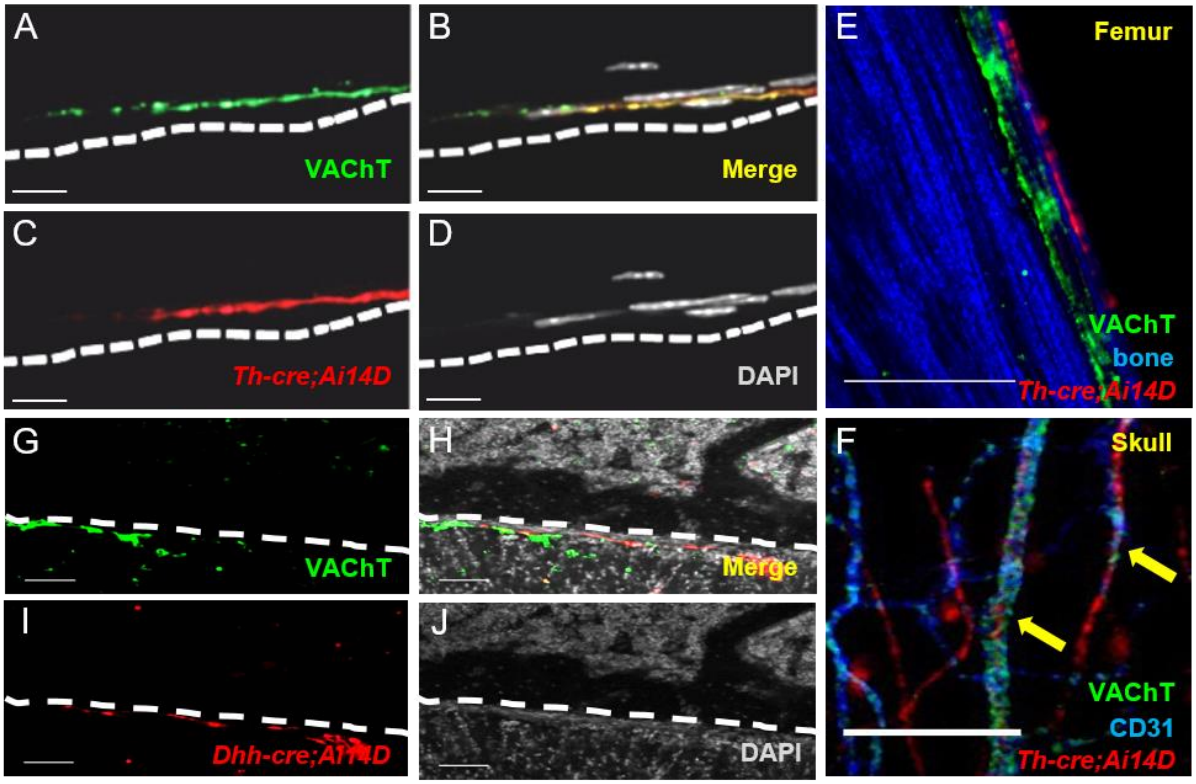

Figure 22. Sympathetic noradrenergic and sympathetic cholinergic fibres run closely in periosteal locations. *A-F, Immunofluorescent staining of VAChT$^+$ fibres (green) in adult femur BM (A-E) and skull BM (F) of Th-cre;Ai14D mice with genetically-labelled TH$^+$ sympathetic neurons (red). Bone (blue) was visualized by secondary harmonic signals from collagen (E). Blood vessels were stained with CD31 (F). G-J, Immunofluorescent staining of VAChT$^+$ fibres (green) in adult femur of Dhh-cre;Ai14D mice with genetically-labelled Schwann cells (red). Endosteal surface is depicted by a dashed line. Nuclei were counterstained with DAPI (gray). Scale bar, 100 µm.*

While HSC numbers were normal in the FL of *Gfra2*$^{-/-}$ embryos before birth, we detected a severe reduction of HSCs in the BM one week after birth (Fig. 23 A-C). This was accompanied by a 3-fold-decrease in BM *Cxcl12* gene expression, whereas *Scf* expression remained unchanged (Fig. 23D). Considering that Cxcl12 is key to HSC attraction from the FL and colonisation of the BM (Isern et al., 2014), these results suggest that sympathetic cholinergic fibres contribute to developmental BM HSC niche maturation in early postnatal life.

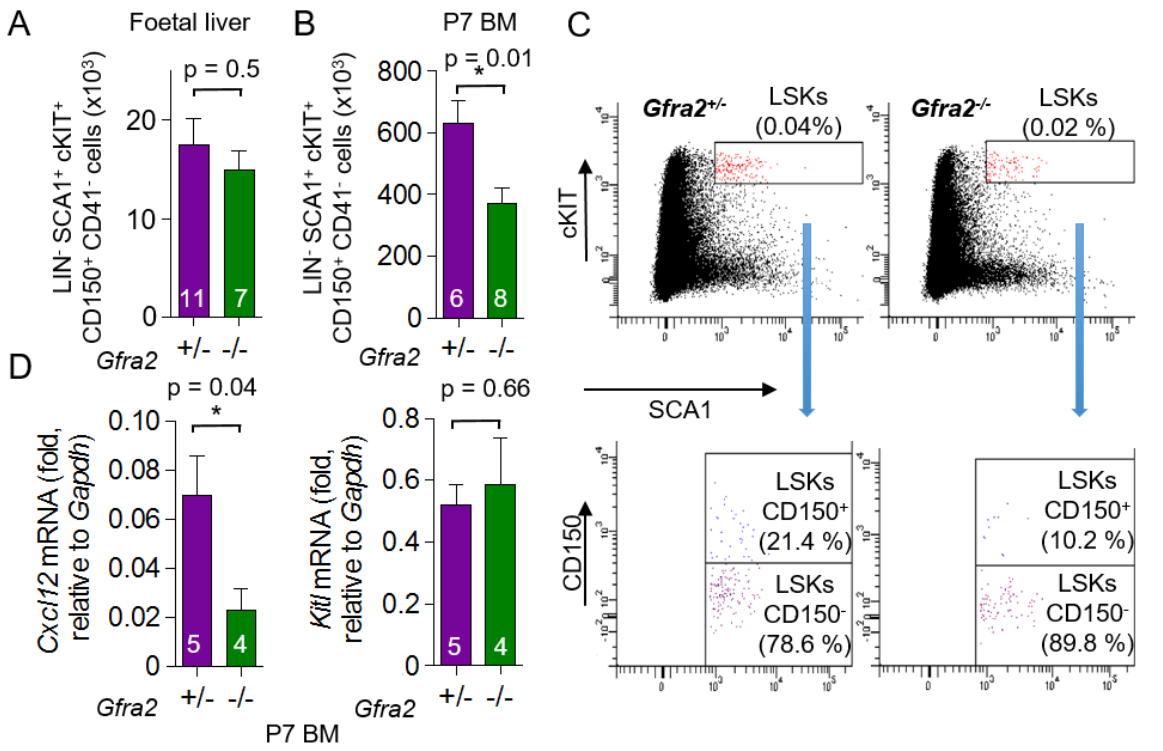

Figure 23. Developmental switch of neurotransmitter might contribute to BM HSC niche maturation. *A, Foetal liver (FL) HSC numbers of Gfra2$^{-/-}$ and control Gfra2$^{+/-}$ mice at E17.5. B, BM HSC numbers in 1-week old (P7) Gfra2$^{-/-}$ and control Gfra2$^{+/-}$ mice. C, Representative flow cytometry diagrams of BM LIN^{-}SCA1^{+}cKIT^{+} (LSK) HSPCs from 1-week-old Gfra2$^{-/-}$ and control Gfra2$^{+/-}$ mice. D, Cxcl12 and Kitl mRNA expression (qPCR) in BM of P7 Gfra2$^{-/-}$ and control mice. Data are means ± SEM; n and p values are indicated. Unpaired two-tailed t test. * p < 0.05.*

4.10 Sympathetic cholinergic nerve fibres target Nes-GFP^{hi} BMSCs in endosteal BM niches

The postnatal HSC reduction in the BM of *Gfra2$^{-/-}$* mice is restored during adulthood (Fig. 8B). Restoration of HSC numbers might result from an increase in HSC proliferation to balance the low postnatal HSC numbers, or it might even suggest that cholinergic fibres negatively regulate HSC proliferation (coinciding with the endosteal location where HSC quiescence in enforced). Physiological postnatal BM colonisation involves a drastic reduction of HSC proliferation in a Cxcl12-dependent manner (Bowie et al., 2006; Williams, Xu, & Cancelas, 2006). Intriguingly, this dramatic change of HSC proliferation coincides in time with the cholinergic switch maturation. Taking into account the unbalanced HSC numbers and Cxcl12 levels in *Gfra2$^{-/-}$* mice, we hypothesized that sympathetic cholinergic fibres could promote HSC quiescence signals and that their absence might increase HSC proliferation.

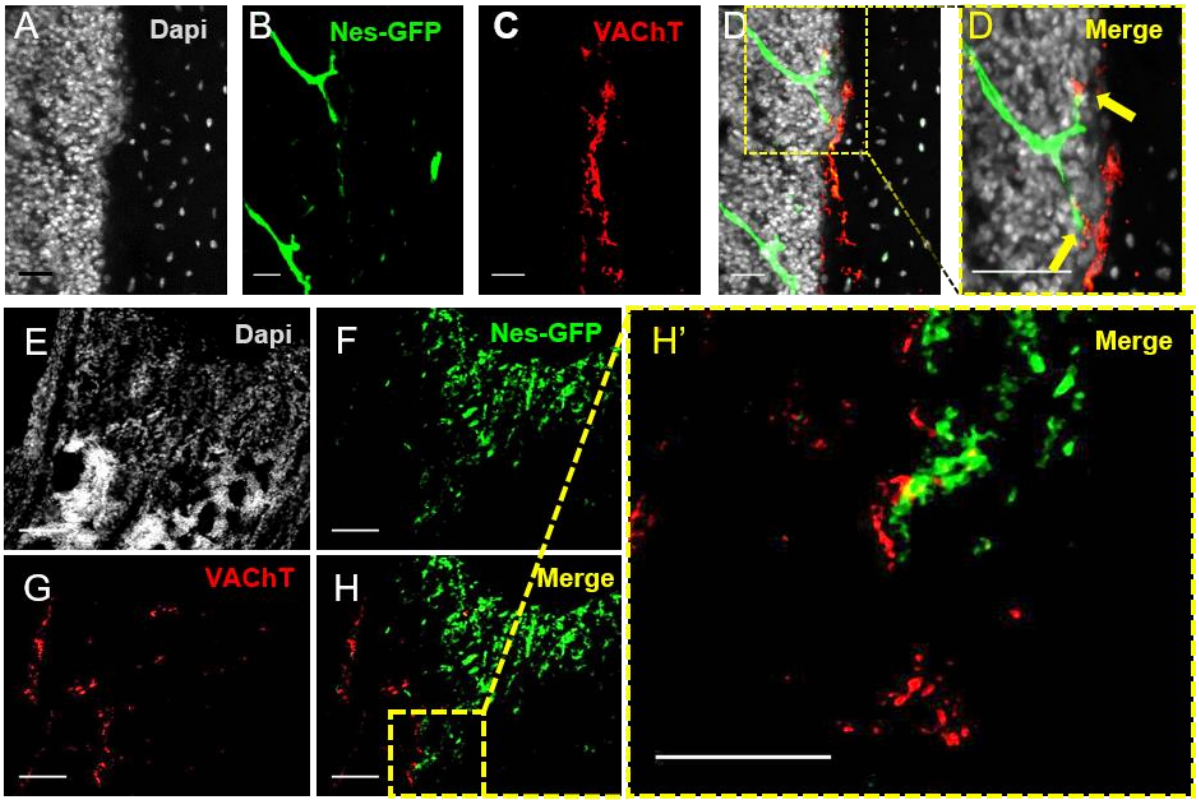

Figure 24. VAChT^{+} fibres innervate Nes-GFP^{hi} cells in endosteal BM niches. *A-H, Endogenous GFP signal (green) and immunofluorescence for VAChT to mark cholinergic nerve fibres (red) in femoral BM section from representative adult Nes-gfp mice. Nuclei were counterstained with DAPI (gray). Scale bar, 100 µm.*

In adult mice, sympathetic cholinergic fibres were found in close association with bone surfaces (Fig. 18 and 19). The inner bone surface-endosteum plays an active role in HSC quiescence and maintenance through multiple cells including osteoblasts and endosteal macrophages. Endosteal niches have been found to be enriched for quiescent/dormant HSCs (Arai et al., 2004; Nilsson et al., 2005; Winkler et al., 2010). Endosteal vessels and their associated perivascular cells are also important components of these quiescent BM niches. Particularly, the recently described TZ-vessels have been restricted to endosteal/growth plate areas, in which we detected the sympathetic cholinergic innervation. In addition, TZ vessels and arterioles are surrounded by Nes-GFP^{hi} perivascular BMSCs, which have been reported to regulate HSC quiescence (Kunisaki et al., 2013). All these evidences led us to study whether Nes-GFP^{hi} BMSCs are a target population of modulated by sympathetic cholinergic fibres.

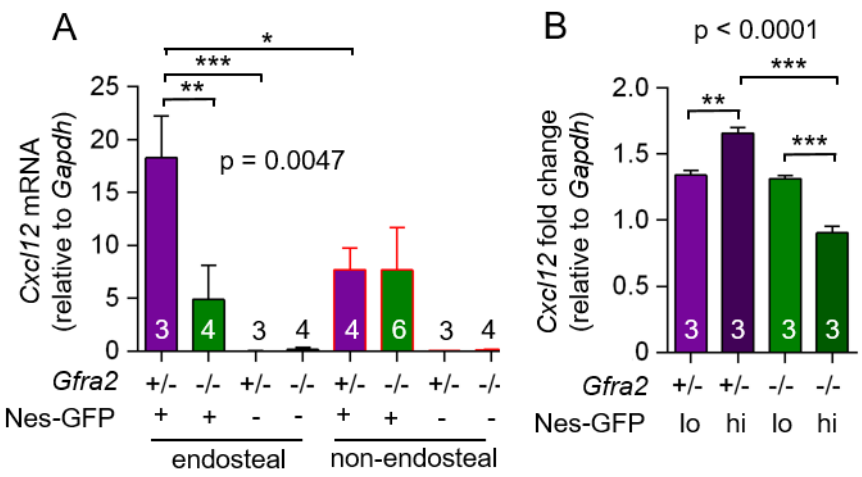

Figure 25. Cxcl12 expression is decreased in endosteal Nes-GFP^{hi} cells in *Gfra2*$^{-/-}$ mice. *A, Cxcl12 mRNA expression (qPCR) in endosteal and non-endosteal BM Nes-GFP$^{+/-}$ BMSCs from Nes-gfp;Gfra2$^{-/-}$ and control Nes-gfp;Gfra2$^{+/-}$ mice. B, Cxcl12 mRNA expression (qPCR) in Nes-GFP$^{hi/lo}$ BMSCs from Nes-gfp;Gfra2$^{-/-}$ and control Nes-gfp;Gfra2$^{+/-}$ mice. Data are means ± SEM; n and p values are indicated. One-way ANOVA and Bonferroni comparisons. * p < 0.05; ** p < 0.01; *** p < 0.001.*

We found that Nes-GFP^{hi} cells were closely associated with the bone and innervated by VAChT^{+} cholinergic fibres (Fig. 14 and Fig. 24). We also detected a 2.5 fold increase in *Cxcl12* mRNA expression in bone associated Nes-GFP^{+} cells of *Gfra2*$^{-/-}$ mice compared to Nes-GFP^{+} cells isolated from the flushed marrow. Interestingly, *Cxcl12* mRNA expression was decreased in endosteal Nes-GFP^{+} cells in *Gfra2*$^{-/-}$ mice. The decrease in *Cxcl12* expression was shown to be specific for Nes-GFP^{hi} BMSCs (Fig. 25).

To resolve the mechanism underlying the innervation of BMSCs by cholinergic sympathetic fibres in more detail, we first analysed the expression of acetylcholine receptors in different BM stromal populations. Broad expression of several acetylcholine receptors was detected in different BM stromal cell lines (Fig. 26A). To study whether cholinergic signals can directly trigger a Cxcl12 response, we treated different murine stromal cell lines with cholinergic agonists *in vitro* (Fig. 7). The stromal cell line MS-5 produced the highest Cxcl12 level compared to osteoblastic cell line MC3T3-E1 and osteocytic cell line MLO-Y4 (Fig. 26B-D). Both acetylcholine (ach) and nicotine strongly increased Cxcl12 release by MS-5 cells, while the muscarinic receptor antagonist atropine had no effects on Cxcl12 level (Fig. 26B). Thus, cholinergic fibre-dependent Cxcl12 induction seems to be mediated by direct nicotinic receptor signalling. Along the same lines, *Chrna7* mRNA

expression was upregulated in Nes-GFP^{+} BMSCs ((Mendez-Ferrer, Michurina, et al., 2010) and Fig. 26D).

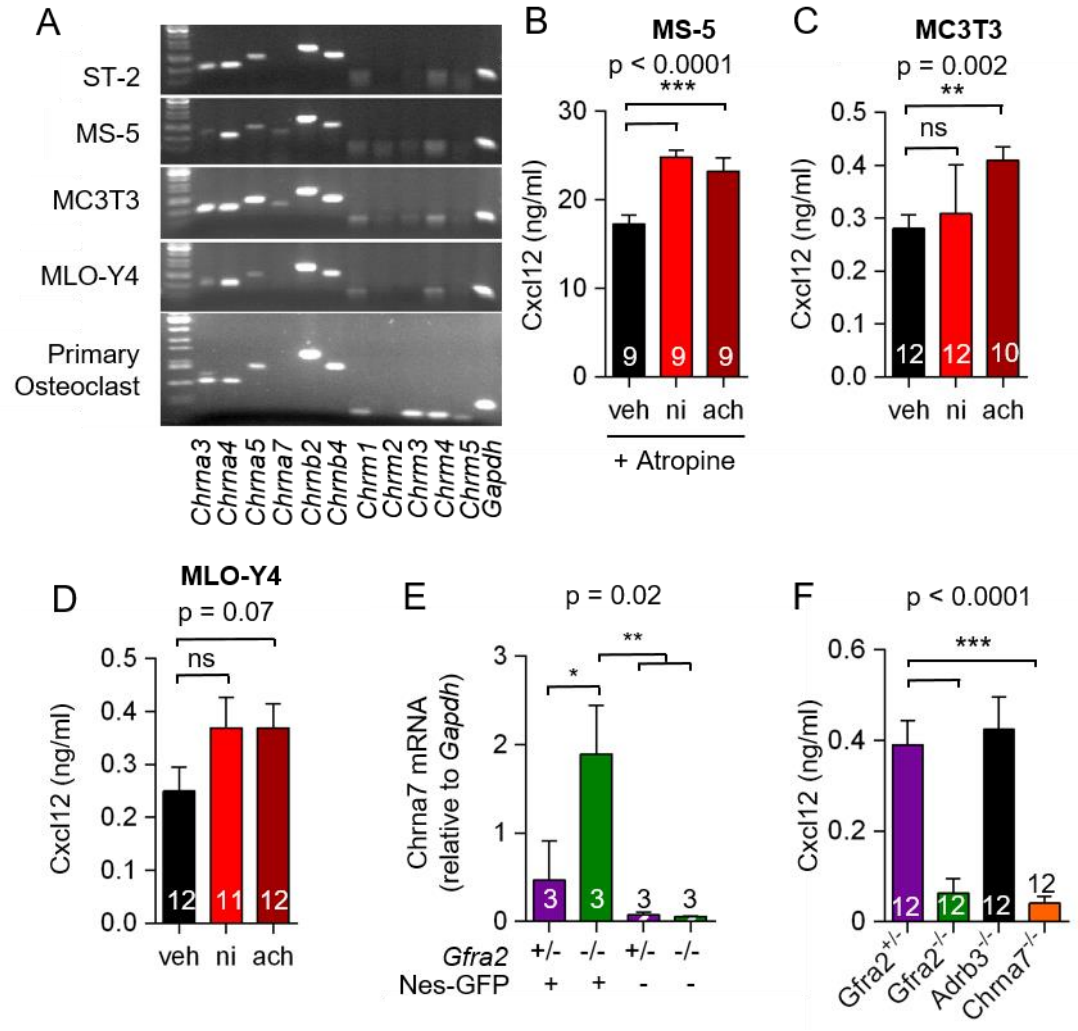

Figure 26. Cholinergic signals induce Cxcl12 production. *A, Expression (mRNA) of cholinergic nicotinic and muscarinic receptors in ST-2, MS-5, MC3T3, MLO-Y4 murine stromal cell lines and primary murine osteoclasts. B-D, Cxcl12 secretion by MS-5 (B), MC3T3 (C) and MLO-Y4 (D) BMSCs treated for 24h with nicotine, acetylcholine (ach) (10 µM) or vehicle. MS-5 cells were also pre-treated with the muscarinic antagonist atropine (10µM). E, Chrna7 mRNA expression (qPCR) in sorted Nes-GFP$^{+/-}$ BMSCs. F, Cxcl12 secretion in primary BM cultures derived from mice with the indicated genotype. B-F, Data are means ± SEM; n and p values are indicated. One-way ANOVA and Bonferroni comparisons. * p < 0.05; ** p < 0.01; *** p < 0.001.*

Additionally, we used BM myeloid primary cultures to confirm the direct link between cholinergic stimulation and Cxcl12 production. While Cxcl12 secretion was normal in BM of *WT* and *Adrb3*$^{-/-}$ mice, cholinergic fibre-deficient *Gfra2*$^{-/-}$ mice and mice lacking the α7 cholinergic receptor (*Chrna7*$^{-/-}$) showed a 5-fold reduction of BM

Cxcl12 levels (Fig. 26E). In conclusion, these results demonstrate that cholinergic fibres can directly induce *Cxcl12* expression by activating Chrnα7 receptor in endosteal Nes-GFP^{hi} BMSCs.

4.11 Sympathetic cholinergic nerve fibres regulate HSC quiescence in endosteal BM niches

Although the vast majority of HSCs are located around perisinusoidal niches in the central bone marrow (Acar et al., 2015), a small subset of quiescent HSCs have been found enriched in endosteal niches. According to this, we found that the frequency of quiescent HSPCs (arrested in G0) was significantly higher in endosteal BM compared to non-endosteal flushed BM (Fig. 27A). However, this normal distribution was disrupted in *Gfra2*$^{-/-}$ mice. Specifically, the percentage of quiescent HSPCs was dramatically reduced in the endosteal compartment while unaltered in the non-endosteal environment, suggesting that HSPC quiescence could be compromised in *Gfra2*$^{-/-}$ BM endosteal niches. Unlike the HSPC trafficking defect (Fig. 11F), the reduced frequency of quiescent endosteal HSPCs in *Gfra2*$^{-/-}$ mice was not corrected by abrogating β3-adrenergic signalling (Fig. 27A-B). Interestingly, when cell cycle analysis was performed in *Chrna7*$^{-/-}$ mice a similar disruption was observed in normal distribution of quiescent HSPCs, indicating that endosteal HSC quiescence is controlled by α7 cholinergic receptor signalling (Fig. 27C). These results highlight sympathetic cholinergic fibres, rather than sympathetic noradrenergic fibres, as putative regulators of HSC quiescence in endosteal niches. Then, different HSC functions, such as migration and quiescence, are differentially regulated by noradrenergic and cholinergic signals in separate BM niches.

Although endosteal quiescent HSCs only represent a minority of the whole HSC population, their biological relevance for haematopoiesis seems high under stress/regenerative paradigms. Quiescent or dormant HSCs have been proposed to remain protected in endosteal compartments until activation in stress situations (i.e irradiation) to contribute to the replenishment of the haematopoietic system (Trumpp et al., 2010)**.** To study the role of cholinergic HSC quiescence signals in contributing to stress-induced haematopoiesis we investigated the HSC response to myelosupressive stress induced by 5-fluoruracil (5-FU) treatment. 5-FU is a pyrimidine analog which blocks DNA synthesis and thus depletes actively cycling HSPCs (in G2/S/M phase). Consistent with the increased fraction of endosteal

HSCs in the G1 phase of the cell cycle, *Gfra2*$^{-/-}$ mice exhibited an accelerated haematopoietic recovery from myelotoxic injury triggered by 5-FU. A similarly improved recovery from myelotoxic stress was observed in *Chrna7*$^{-/-}$ mice (Fig. 27D).

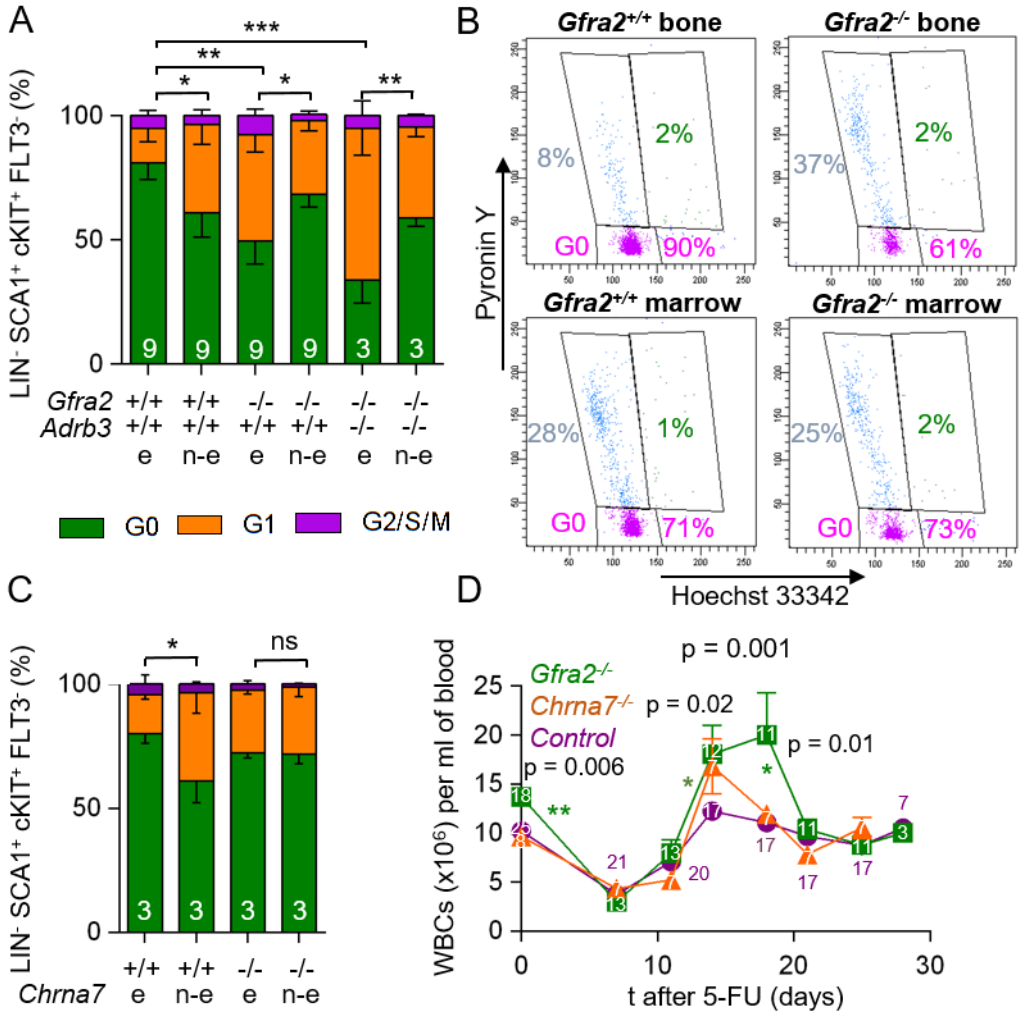

Figure 27. Endosteal quiescent HSCs are activated in *Gfra2*$^{-/-}$ mice. *A, Distribution of G0 (green), G1 (orange) and G2/S/M (purple) cell cycle phases in HSCs isolated from endosteal (e) and non-endosteal (n-e) BM from C57Bl/6J mice, Gfra2*$^{-/-}$ *mice and Gfra2*$^{-/-}$*;Adrb3*$^{-/-}$*. B, Representative plots of cell cycle analysis in HSPCs. Cell cycle distribution, determined by PY/H42 staining, of LIN*$^{-}$ *SCA1*$^{+}$*cKIT*$^{+}$*FLT3*$^{-}$ *HSCs isolated from endosteal (bone) and non-endosteal (marrow) BM fractions of Gfra2*$^{-/-}$ *and Gfra2*$^{+/+}$ *mice. The frequencies of the gated populations are indicated. C, Distribution of cell cycle phases in HSCs isolated from Chrna7*$^{-/-}$ *mice. D, Haematopoietic recovery after myeloablation with 5-FU (150 mg/kg). Circulating WBCs before and 30 days after 5-FU treatment of Gfra2*$^{-/-}$*, Chrna7*$^{-/-}$ *and control mice. A, C-D, Data are means ± SEM; n and p values are indicated. A,C, One-way ANOVA and Bonferroni comparisons. D, Multiple two-tailed test. * p < 0.05; ** p < 0.01; *** p < 0.001.*

Gene sets (signatures)	*Gfra2*$^{-/-}$ vs. *Gfra2*$^{+/+}$ (endosteal)	*Gfra2*$^{-/-}$ vs. *Gfra2*$^{+/+}$ (non-endosteal)	end vs. non-end (*Gfra2*$^{+/+}$)	end vs. non-end (*Gfra2*$^{-/-}$)
LT-HSC specific genes (Forsberg et al., 2010)	1.0	1.0	1.2	2.2
HSC fingerprint (Chambers et al., 2007)	-1.3	1.0	1.1	1.5
High-expression signature in self-renewing HSCs (Krivtsov et al., 2006)	-1.9	1.0	1.5	1.0
Low-expression signature in self-renewing HSCs (Krivtsov et al., 2006)	1.5	1.0	-1.9	-1.7
High expression signature in mobilized HSCs (Forsberg et al., 2010)	1.4	1.7	-1.4	-1.9

Figure 28. Cholinergic fibre deficiency deregulates endosteal HSCs. *Gene set enrichment analysis (GSEA) of gene sets previously linked to self-renewing or mobilised HSCs in LIN$^-$SCA1$^+$cKIT$^+$CD150$^+$CD48$^-$CD41$^-$ cells isolated from endosteal (end) or non-endosteal (non-end) BM from control Gfra2$^{+/+}$ or Gfra2$^{-/-}$ mice. FDR, False discovery rate. Significantly changed gene sets (FDR<0.25) are labelled in red (up-regulated) and green (down-regulated). Normalized enrichment scores (NES) are indicated.*

Decrease self-renewal capacity can be a possible physiological consequence of abnormal HSC proliferation in *Gfra2*$^{-/-}$ mice. To study potential alterations in the HSC self-renewal program we analysed the transcriptomic profile HSCs isolated from endosteal and non-endosteal BM of *Gfra2*$^{-/-}$ and control mice by RNASeq.

Taking advantage of the gene set enrichment analysis (GSEA) tool, we compared our differentially expressed genes with published gene sets which have been reported to be enriched in self-renewing or mobilised HSCs. In line with the increased quiescence of endosteal HSCs, GSEA revealed an up-regulation of long-term HSC specific genes (Forsberg et al., 2010), the HSC “fingerprint” (Chambers et al., 2007) and genes highly expressed in self-renewing HSCs (Krivtsov et al., 2006) in endosteal HSCs (compared with non-endosteal HSCs). Similarly, genes expressed at a low level in self-renewing HSCs (Krivtsov et al., 2006) and highly enriched in mobilised HSCs (Forsberg et al., 2010) were found to be down-regulated in endosteal HSCs (Fig. 28)

In general these gene sets were unchanged when comparing non-endosteal HSCs from control and *Gfra2*$^{-/-}$ mice. However, important differences were revealed between endosteal HSCs from control and *Gfra2*$^{-/-}$ mice. Long-term HSC-specific genes, the HSC “fingerprint” and genes highly expressed in self-renewing HSCs were down-regulated in endosteal HSCs isolated from *Gfra2*$^{-/-}$ mice (Fig. 28).

Overall, the RNAseq data analysis supports the concept of a cholinergic signalling-dependent regulation of HSPC quiescence in the endosteal BM compartment. Lack

of cholinergic innervation in the *Gfra2*$^{-/-}$ model results in abnormal activation of quiescent HSCs in endosteal niches.

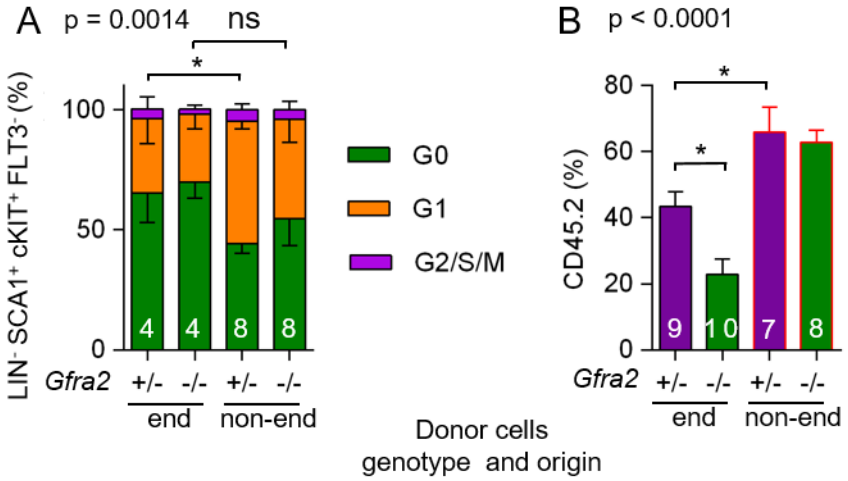

Figure 29. Cholinergic innervation contributes to long-term HSC maintenance and function in endosteal BM niches. *A, Distribution of G0 (green), G1 (orange) and G2/S/M (purple) cell cycle phases in CD45.2*$^{+}$ *HSCs isolated from lethally-irradiated CD45.1 C57Bl/6J mice transplanted with endosteal or non-endosteal BM from Gfra2*$^{+/-}$ *or Gfra2*$^{-/-}$ *mice. B, Circulating CD45.2*$^{+}$ *donor-derived haematopoietic cells 24 weeks after transplantation. Donor cells were mixed with 10*^{6} *CD45.1*$^{+}$ *competitor BM cells. Data are means ± SEM; n and p values are indicated. One-way ANOVA and Bonferroni comparisons. * p < 0.05.*

To study the functional relevance of decreased HSC quiescence and self-renewal in endosteal *Gfra2*$^{-/-}$ BM, we performed competitive long-term repopulation assays using endosteal and non-endosteal BM cells from *Gfra2*$^{-/-}$ and control *Gfra2*$^{+/-}$ mice.

In these experiments donor cells were mixed with supporting CD45.1 haematopoietic cells to assess long-term HSC maintenance in *WT* recipients. The analysis of recipient mice was performed 24 weeks after transplantation. Surprisingly, the frequency of quiescent HSCs was still higher in those mice transplanted with endosteal BM (Fig. 29A), although mice transplanted with non-endosteal BM showed a better haematopoietic reconstitution (Fig. 29B). These results could suggest that even 6 months after transplantation endosteal HSCs could keep quiescent, while non-endosteal HSCs would be responsible for the replenishment of the haematopoietic system. Further transplants are under current investigation to clarify this. In any case, those recipient mice transplanted with endosteal BM from *Gfra2*$^{-/-}$ mice showed significantly reduced haematopoietic reconstitution 24 weeks after transplantation (Fig. 29B).

Since HSC quiescence is required for long-term HSC self-renewal, these results suggest that sympathetic cholinergic fibres promote HSC quiescence and long-term maintenance in endosteal niches.

“Yin and yang, male and female, strong and weak,
rigid and tender, heaven an earth, light and darkness,
thunder and lightning, cold and warmth, good and evil…
The interplay of opposite principles constitutes the universe”
Confucius

5 Discussion

The complexity of BM niches appreciated over the past few years challenges our complete dissection of the functional relationships between BMSCs and HSCs. Despite intense debate and a tendency to exacerbate new markers and relatively small differences across studies, these efforts have allowed for significant conceptual refinements. Now, the existence of distinct BM niches harbouring different HSCs/HSC states is becoming the predominant idea. Current investigations in this field are trying to understand how such different spatially-separated BM niches can be regulated in a coordinated manner to ensure physiological haematopoiesis (Morrison & Scadden, 2014).

At the same time, the ANS is a master regulator of peripheral organ function controlling the fine-tuning of multiple physiological processes. In this context several studies in the last decade have shown how sympathetic innervation in the BM contributes to HSC niche regulation. On one hand, sympathetic fibres and their associated Schwann cells directly regulate HSC quiescence/proliferation via β2-adrenergic receptor and Tgf-β signalling, respectively (Maestroni et al., 1997; Spiegel et al., 2007; S. Yamazaki et al., 2011). On the other hand, the SNS targets osteoblasts and BMSCs to modulate HSC functions indirectly via β2- and β3-adrenergic receptors (Katayama et al., 2006; Mendez-Ferrer, Battista, et al., 2010).

Among these processes, sympathetic control of HSPC circadian trafficking has been intensively studied (Mendez-Ferrer et al., 2008; Scheiermann et al., 2012), since the stimulation of this physiological trafficking allows for life-saving HSC transplantation procedures. These studies also suggested apparently paradoxical messages, such as the induction of opposite processes (HSPC egress vs homing) via similar sympathetic mechanisms only separated on a temporal scale (day vs night).

In this study we show for the first time how the ANS uses a postsynaptic neurotransmitter different from noradrenaline – acetylcholine – to regulate BM HSC niches in a spatiotemporal manner. We have uncovered a dual autonomic cholinergic regulation of HSC niches. Firstly, the PNS modulates circadian HSPC trafficking through sinusoids antagonising sympathetic noradrenergic signals at the end of the night phase. Secondly, sympathetic cholinergic fibres identified in the

bone and endosteal niches innervate nestin^{+} cells to promote HSC quiescence and long-term maintenance (Fig. 30).

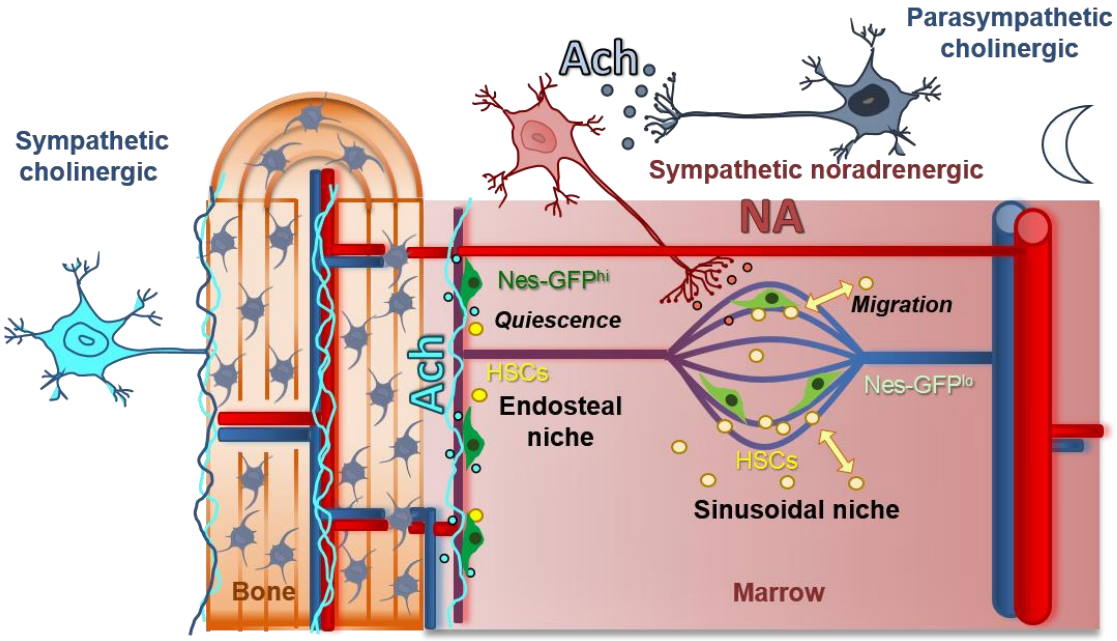

Figure 30. Model of dual autonomic cholinergic regulation of HSC niches. *Cholinergic autonomic signals antagonize sympathetic noradrenergic signals at the end of the resting period contributing to circadian HSPC and leukocyte trafficking through sinusoidal niches. Sympathetic cholinergic fibres activate bone associated nestin^{+} BMSCs, thereby locally regulating HSC quiescence and maintenance in endosteal niches.*

5.1 The PNS indirectly regulates circadian HSPC trafficking in perisinusoidal niches

Gfra2$^{-/-}$ mice were initially used in this study as model of peripheral parasympathetic deficiency. The absence of Nrtn/Gfrα2 signalling in these mice, which is critical for the survival of postganglionic parasympathetic neurons, results in dramatic reduction of cholinergic innervation in several ganglia and glands of *Gfra2*$^{-/-}$ mice while leaving sympathetic innervation intact (Rossi et al., 1999). Our data confirmed a 7-fold reduction in acetylcholinesterase activity (indirectly measurement of parasympathetic tone) in *Gfra2*$^{-/-}$ mice (Fig. 8A), making this model suitable to address the study of parasympathetic regulation of BM HSC niches.

Although HSPC and haematopoietic cell numbers are normal in the BM of *Gfra2*$^{-/-}$ mice (Fig. 8B-C), an abnormal accumulation of HSPCs and leukocytes was observed in the peripheral blood at the beginning of the night phase (Fig. 9). This

result suggests that normal circadian traffic of blood cells is disrupted in parasympathetic fibre-deficient mice. The other branch of the autonomic nervous system, the SNS, is involved in the regulation circadian HSPC trafficking at two different time points. Two daily peaks of sympathetic activity have been detected in mice: one during the night associated with increased nocturnal activity in mice (De Boer & Van der Gugten, 1987; Maestroni et al., 1998), and another following light exposure to induce sympathetic efferent activity and suppress parasympathetic tone (Niijima, Nagai, Nagai, & Nakagawa, 1992; Terazono et al., 2003). These two daily peaks of sympathetic activity are associated with opposite functions of the SNS in regulating HSPC trafficking in and out of the BM.

HSPCs are mainly released into the bloodstream during the day in response to light stimuli (Mendez-Ferrer et al., 2008). Postganglionic sympathetic terminals innervating the BM release noradrenaline and modulate *Cxcl12* expression in nestin^{+} BMSCs via β3-adrenergic receptor signalling. During the night phase, when HSPCs and leukocyte preferentially home to the BM, sympathetic signalling contributes to their BM recruitment (Scheiermann et al., 2012). In this context, specific nocturnal accumulation of circulating HSPCs in the peripheral blood of parasympathetic fibre-deficient *Gfra2*$^{-/-}$ mice suggests that HSPC egress and/or homing could be deregulated in this mouse model. However, nocturnal HSPC accumulation in the peripheral blood was not related to a decrease in BM homing but rather correlated with increased recruitment of HSPCs to the BM of *Gfra2*$^{-/-}$ mice at the same time (Fig. 10). This together with the increased nocturnal noradrenaline concentration (Fig. 11A-D) indicates that increased HSPC homing to the BM in *Gfra2*$^{-/-}$ mice could be promoted by an abnormal nocturnal sympathetic tone. In fact, considering that the predominant phenotype is HSPC accumulation in peripheral blood, we can discard that increased BM homing in *Gfra2*$^{-/-}$ mice also actually contributes to expand the pool of “mobilisable” HSPCs.

The simultaneous increase of HSPC BM homing and HSPC accumulation in the blood of *Gfra2*$^{-/-}$ mice suggests that HSPC mobilisation is enhanced in this mouse model. HSPC circadian egress and mobilisation in response to G-CSF are triggered by sympathetic β2- and β3-adrenergic receptor signalling in the BM (Mendez-Ferrer, Battista, et al., 2010). Combined genetic deletion of *Gfra2* and *Adrb2* or *Adrb3* revealed the importance of parasympathetic fibres in specifically dampening

sympathetic β3-adrenergic signalling in the BM. Only *Gfra2*$^{-/-}$ mice also lacking β3- but not β2-adrenergic signalling recovered normal numbers of circulating HSPCs during the nocturnal phase (Fig. 11F-G). While β2-adrenergic-dependent HSPC mobilisation has been associated with osteoblastic cells in endosteal niches (Katayama et al., 2006), β3-adrenergic receptor-dependent HSPC egress is mediated by perisinusoidal nestin^{+} BMSCs (Mendez-Ferrer et al., 2008). Exacerbated sympathetic tone and increased HSPC mobilisation in *Gfra2*$^{-/-}$ mice correlate with reduced BM Cxcl12 level at the same circadian time (Fig. 13), highlighting the importance of the PNS in controlling BMSC Cxcl12 production by blocking the sympathetic β3-adrenergic axis.

Overall these results suggest that the PNS contributes to orchestrate physiological day/night oscillations of circulating HSPCs and leukocytes by dampening sympathetic tone specifically during the night period. Although normal sympathetic activity induces HSPC homing to the BM during the nocturnal period (Scheiermann et al., 2012), the abnormally high sympathetic signalling in *Gfra2*$^{-/-}$ mice also induces enforced HSPC egress (mobilisation) during this period. Thus, unrepressed SNS triggers HSC egress to the bloodstream after light exposure during the day, but parasympathetic activation at the beginning of the night period decreases sympathetic tone. The low sympathetic tone that remains during the night period stimulates nocturnal BM homing.

How different levels of sympathetic activity cooperate to stimulate opposite processes at different circadian times requires further analysis. The expression of different types of adrenergic receptors is variable among both haematopoietic cells and BMSCs. Furthermore, exposure of β-adrenergic receptors to high levels of their ligands could cause rapid desensitization of the adenylyl-cyclase response triggered by the receptor. β2-adrenergic receptor has been reported to be quite sensitive to receptor desensitization (Lohse, Benovic, Codina, Caron, & Lefkowitz, 1990). A mild nocturnal sympathetic tone could induce HSPC homing via β2-adrenergic receptors during the night. The strong diurnal sympathetic tone could partially desensitize β2-adrenergic receptors and promote HSPC egress through more resistant β3-adrenergic receptors.

Recently, cholinergic signals originated at central level have been reported to control G-CSF-mediated mobilisation in the BM through the glucocorticoid system (Pierce

et al., 2017), suggesting that the PNS could also have an impact on enforced HSPC trafficking on a central level. Similarly, treatment of mice with blood-brain barrier permeable and non-permeable cholinergic antagonists suggested that parasympathetic-mediated inhibition of sympathetic activity takes place at the central level (Fig. 11E). Central cholinergic signalling might particularly contribute to HSPC trafficking during stress situations.

5.2 Non-cell autonomous HSPC trafficking alteration

Reciprocal transplantation experiments in *Gfra2*$^{-/-}$ and control mice exclude any cell-autonomous role for Gfra2 signalling in HSCs in contributing to the HSPC trafficking phenotype (Fig. 12). Although neither Nrtn either Gfrα2 seem to be expressed in adult BM haematopoietic cells (Nakayama et al., 1999), FL HSPCs express high levels of RET and Gfrα1-3 co-receptors. On the other hand, although GDNF and Nrtn bind preferentially to Gfrα1 and Gfrα2 respectively, both co-receptors share structural and functional similarities (Baloh et al., 1997; Hoane et al., 1999) so it is possible some overlapping between Gfrα1 and Gfrα2 signalling. In any case, RET has been shown to be expressed in haematopoietic cells, HSCs, while the neurotrophic factors GDNF and Nrtn are enriched in BMSCs (Fonseca-Pereira et al., 2014; Nakayama et al., 1999). This is particularly relevant because it is known that RET can be activated in *cis* but also in *trans* by its co-receptors and ligands (Fleming et al., 2015); and this *trans* signalling could play a role in myeloid differentiation (Nakayama et al., 1999). Interestingly, osteoblasts seem to be one of the most important source of Nrtn in adult BM. Therefore, Nrtn/Gfrα2 signalling between osteoblasts and sympathetic cholinergic fibres in endosteal niches should be further analysed.

5.3 The PNS independently controls HSPC trafficking and anabolic bone signalling

Gfra2$^{-/-}$ mice have been described to be growth-retarded after weaning. This phenotype has initially been attributed to malnutrition due to reduced enteric innervation in these mice. Bone remodelling and bone formation more specifically are very active processes during early stages of life. As cholinergic signalling has been described to promote bone anabolic signals (Bajayo et al., 2012; Shi et al., 2010), parasympathetic deficiency in *Gfra2*$^{-/-}$ mice could have a relevant impact on

skeletogenesis and bone remodelling. Thus, delayed growth of *Gfra2*$^{-/-}$ mice might be caused complementary defects in bone formation as well as malnutrition.

Along this line, bone µCT showed that *Gfra2*$^{-/-}$ mice had enlarged cranial sutures and decreased trabecular bone. These defects could not be explained by increased bone resorption (Fig. 16) and also the number of osteoprogenitor cells was rather increased (CFU-F and CFU-OB) than decreased. These results have been interpreted has a compensatory response to impaired bone growth in *Gfra2*$^{-/-}$ mice and point out a role of the PNS as positive regulator of bone formation. Indeed, osteoprogenitor cell accumulation could suggest a bias towards cell proliferation, instead of osteoblastic differentiation. Therefore, it would be important to check if the numbers of mature osteoblasts are reduced in *Gfra2*$^{-/-}$ mice. On the other hand, sympathetic denervation in rats has been associated with decreased osteoblastic activity and increased resorption activity (Herskovits & Singh, 1984), but this intervention would affect all types of innervation, including noradrenergic and cholinergic nerve fibres. Along this line, it is known that sympathetic signals control both aspects of bone remodelling (decrease bone formation and increase bone resorption) downstream of leptin signalling (Elefteriou et al., 2005; Takeda et al., 2002).

Neural regulation of bone metabolism is a recent concept and, the expansion of this regulation to the BM compartment over the last few years, has given rise to the theory of the “brain-bone-blood triad” (Lapidot & Kollet, 2010; Takeda & Karsenty, 2008). This concept is based on the idea that the interactions between these three systems are essential for the regulation of HSPC trafficking. In line with this brain-bone-blood model, intercellular connections between osteocytes have been described as essential for sympathetic fibre-mediated HSPC mobilisation in response to G-CSF (Asada et al., 2013). However, in our study G-CSF treatment similarly promoted HSPC mobilisation in *Gfra2*$^{-/-}$ despite the dramatic reduction in osteocyte projections (Fig. 17A-B), suggesting that circadian HSPC trafficking regulation and bone remodelling are independently regulated in our model. Along these lines, acute inhibition of cholinergic signalling in *WT* mice, which show normal bone remodelling, by treatment with cholinergic antagonists stimulated HSPC mobilisation, confirming that HSPC mobilisation occurs independently of bone remodelling (Fig. 11E).

5.4 Local sympathetic cholinergic fibres innervate BM endosteal niches

Whereas the SNS is a key regulator of HSC functions in BM niches, the local contribution of possible cholinergic fibres to BM niche regulation has remained unexplored. It was previously believed that parasympathetic efferent terminals innervating the BM can originate from cranial (projections from the vagus nerve) or sacral areas of the spinal cord. So far, only few immunohistochemistry studies have reported the presence of scarce fibres close to the bone (Artico et al., 2002; Bajayo et al., 2012). Nevertheless, these studies have mostly used immunohistochemistry techniques in thin sections. The processing of paraffin sections could expose the samples to fixatives and organics dissolvent that could mask or reduce some antigens. As consequence, a physiological role for cholinergic signals in BM niche regulation has been remained elusive.

Taking advantage of *ChAT-IRES-cre* mouse model and optimized VAChT immunofluorescence imaging in whole-mount thick BM sections, we have found cholinergic fibres in murine bone proper and endosteal BM (Fig. 18 and 19). Interestingly, those fibres were almost absent in *Gfra2*$^{-/-}$ mice (Fig. 20).

The two branches of the autonomic nervous system, SNS and PNS, primarily use noradrenaline and acetylcholine as postsynaptic neurotransmitters respectively. However, exceptions to this general rule have been described. Some embryonic sympathetic neurons (i.e. in stellate ganglion) have been identified to exhibit cholinergic features, but their frequency gradually diminishes to only ~4% at birth (Huang et al., 2013). Likewise, postnatal sympathetic neurons innervating the sweat glands and the periosteum can change their neurotransmitter properties and start producing acetylcholine (Schutz et al., 2015). Based on their origin and neurotransmitter properties, these are sympathetic cholinergic fibres.

Interestingly, Gfrα2 has been shown to be required for the survival of sympathetic cholinergic fibres in the periosteum (Hiltunen & Airaksinen, 2004), which prompted us to analyse the origin of the new cholinergic fibres we identified in the bone proper and endosteal regions.

The ‘cholinergic switch’ (Wolinsky & Patterson, 1983) was first characterised *in vivo* in rodents during the first postnatal weeks in sympathetic neurons innervating sweat

glands (Guidry & Landis, 1998) and periosteum (Asmus et al., 2000). Neurotransmitter change in bone and sweat glands (Habecker & Landis, 1994) requires initial noradrenergic activity, ensuing secretion of undefined cholinergic differentiation factors, acetylcholine release and maturation of both the target organ and its cholinergic innervation. Furthermore, a very recent study has revealed that all sacral and pelvic autonomic neurons, which innervate the lower limbs, are sympathetic instead of parasympathetic as originally thought (Espinosa-Medina et al., 2016).

Sympathectomy of mice with 6-OHDA during the first postnatal week resulted in dramatic reduction of $VAChT^+$ fibres during adulthood, suggesting that endosteal and periosteal cholinergic fibres are of sympathetic origin. Along these lines, lineage tracing of sympathetic fibres in *Th-cre;Ai4D* mice, confirmed the sympathetic origin if $VAChT^+$ fibres in adult mice (Fig. 22). To sum up, while parasympathetic signals indirectly regulate HSPC circadian trafficking by modulating sympathetic activity at the central level, cholinergic terminals that innervate the BM locally are of sympathetic origin and restricted to endosteal areas.

5.5 Sympathetic cholinergic fibres contribute to postnatal BM HSC niche maturation

As stated before, the full conversion of neurons from noradrenergic to cholinergic phenotype in the periosteum takes around 3-4 postnatal weeks in rats (Asmus et al., 2000). During this period HSCs are still migrating from the FL to colonize the immature BM (Wolber et al., 2002; Zanjani, Ascensao, & Tavassoli, 1993) and diminish their proliferative features to acquire a more quiescent phenotype. Both processes have been shown to be Cxcl12-dependent (Nagasawa et al., 1996). The temporal coordination of the cholinergic switch and HSC quiescence induction prompted us to study whether the neurotransmitter switch directly affects Cxcl12-induced HSC quiescence. Although HSC numbers were not affected in the FL before the birth, they were significantly reduced in BM one week after birth. Moreover, *Cxcl12* gene expression was reduced at P7, pointing toward the lack of the main HSC chemoattractant as the cause of reduced BM colonisation by HSCs. These results suggest that the appearance of sympathetic cholinergic fibres in

endosteal areas and the subsequent up-regulation of Cxcl12 might control two important end-stage changes – BM colonisation and induction of HSC quiescence - in developmental haematopoiesis. Neural crest-derived nestin^{+} BMSCs play an important role as mediators of Cxcl12-dependent HSC migration to the BM (Isern et al., 2014). Endosteal sympathetic cholinergic fibres could therefore target these nestin^{+} BMSCs thereby helping to establish HSC niches by secreting Cxcl12. In conclusion, endosteal sympathetic cholinergic fibres might be important control element of developmental haematopoiesis.

Although it is known that the cholinergic switch in sympathetic neurons is retrogradely specified by periosteum-derived secreted factors, it remains controversial the identity of these factors (Asmus et al., 2000). The leukemic inhibitory factor (LIF) and CNTF were initially proposed, but mice lacking CNTF, LIF or both exhibit normal sympathetic cholinergic fibres (Francis, Asmus, & Landis, 1997; Landis, 1996). Interestingly, triple knock-out mice of CNTF. LIF and another neurotrophic factor called cardiotrophin-1 (CT-1) show significant motoneuron (cholinergic fibre) cell loss and functional deficits very early during postnatal, pointing out CT-1 as another possible mediator of cholinergic switch. Then, it would be interesting to check if this triple knock-out model shows similar HSPC and Cxcl12 reductions than to *Gfra2*$^{-/-}$ mice early postnatally

5.6 The master HSC regulator Cxcl12 controls different HSC functions in separated BM niches

We found endosteal sympathetic cholinergic fibres in close contact with nestin-GFP^{hi} cells in adult endosteal BM and Nes-GFP^{hi} periarteriolar BMSCs have been described to regulate HSC quiescence (Kunisaki et al., 2013). These observation identify Nes-GFP^{hi} cells as interesting candidates to mediate sympathetic cholinergic signals. Indeed, we report here that Nes-GFP^{hi} cells are enriched in the endosteal compartment (Fig. 14B-C) and express higher level of *Cxcl12* compared to sinusoidal Nes-GFP^{lo} cells (Fig. 25). Interestingly, the reduction in quiescent HSCs in both *Gfra2*$^{-/-}$ and *Chrna7*$^{-/-}$ mice was accompanied with endosteal-specific *Cxcl12* down-regulation in Nes-GFP^{hi} BMSCs (Fig. 25). In addition, nicotine treatment induces Cxcl12 secretion in *in vitro* BM stromal cell lines and primary myeloid cell cultures and *Gfra2*$^{-/-}$ and *Chrna7*$^{-/-}$ mice (but not *Adrb3*$^{-/-}$ mice) release

less Cxcl12 compared to control mice (Fig. 26). This data strongly suggests that sympathetic cholinergic fibres innervate endosteal Nes-GFP^{hi} cells to up-regulate *Cxcl12* expression and thus induce HSPC quiescence. Thus, HSC trafficking and quiescence are differentially regulated by sympathetic noradrenergic and sympathetic cholinergic nerve fibres in separate compartments.

Although our data indicates that different HSC functions like migration/retention and quiescence might be regulated by different nerve fibres in spatially-separated BM niches, both types of regulations seem to converge in Cxcl12 level modulation. Since its discovery (Nagasawa et al. 1996), Cxcl12 deregulation in the BM has been associated with multiple types of BM niche disorders. However, it is still unclear how Cxcl12 and other HSC maintenance factors like Scf differentially regulate HSC functions. In our study, we have found a dual cholinergic signalling which controls HSPC trafficking and quiescence in separate BM compartments by modulating Cxcl12 level.

Current opinions in the field highlight the importance of different cellular sources of HSC chemoattractant cytokines for determining their effects on HSC regulation. Recently, Cxcl12 deletion in periarteriolar NG2^{+}Nes-GFP^{hi} BMSCs has been proposed to reduce HSC numbers and delocalize HSC in the BM. NG2^{+}Nes-GFP^{hi} BMSCs have therefore been suggested as major Cxcl12 source responsible for HSC localization in different BM niches (Kunisaki et al., 2013). In contrast, Lepr^{+}Nes-GFP^{lo} BMSCs-derived Scf is especially important to maintain BM HSC numbers (Ding et al., 2012). In any case, both Cxcl12 as well as Scf are required in the different BM niches since their deletion in all Nes-GFP^{+} BMSCs depleted BM HSCs in a similar manner (Asada et al., 2017).

In our study we have provided evidence suggesting that parasympathetic indirect regulation of HSPC trafficking is mediated by perisinusoidal Nes-GFP^{lo} BMSCs. In contrast, endosteal sympathetic cholinergic innervation targets endosteal Nes-GFP^{hi} BMSCs to HSC quiescence. In addition, we show that both nestin^{+} populations exhibited different properties: while Nes-GFP^{lo} cells are more abundant and express lower Cxcl12 level, Nes-GFP^{hi} are rare (mostly restricted to arterioles and TZ vessels in endosteal niches) and express higher Cxcl12 level.

The Cxcl12 decrease associated with increased HSPC trafficking in *Gfra2*$^{-/-}$ mice most likely results from a reduction in Nes-GFP^{lo} BMSCs in perisinusoidal niches (Fig. 14C). Indeed, *Cxcl12* expression in non-endosteal nestin^{+} cells and Nes-GFP^{lo} cells were not affected *Gfra2*$^{-/-}$ mice, supporting a HSPC trafficking phenotype that is caused by reduction of central Nes-GFP^{lo} cell numbers. On the contrary, sympathetic cholinergic fibres directly target *Cxcl12* expression in endosteal Nes-GFP^{hi} BMSCs rather than affecting their numbers in endosteal niches (Fig. 25).

In summary, this work constitutes a significant example of how different HSC functions can be controlled by the same HSC chemoattractant factor in different spatiotemporal contexts.

5.7 Dynamic interactions between noradrenergic and cholinergic signalling

Although our data strongly argues for a spatial segregation of noradrenergic and cholinergic neuro-immune junctions in separate BM compartments, we cannot exclude the possibility that some nerve fibres might have mixed and/or highly dynamic properties.

The sympathetic superior cervical ganglion contains neurons with combined noradrenergic and cholinergic properties (Furshpan, Landis, Matsumoto, & Potter, 1986; Landis, 1976) and different neurotrophic factors can rapidly affect neurotransmitter synthesis, storage, release and uptake (Luther & Birren, 2009; Yang, Slonimsky, & Birren, 2002). Therefore, although our data suggest that parasympathetic-sympathetic interactions that coordinate circadian HSPC trafficking take place at CNS, we cannot exclude the possibility of a peripheral regulation. Using both *Th-cre;Ai4D* and *Dhh-cre;Ai4D* models, we have found that sympathetic cholinergic VAChT^{+} fibres and sympathetic noradrenergic TH^{+} fibres were closely associated in periosteal regions, suggesting that feedback loops could take place between these two types of innervation near the BM (Fig. 22). In fact, potential postsynaptic inhibitory feedback loops between the two branches of the ANS have been commonly observed in other systems. For instance, it has been shown that the PNS attenuates sympathetic activation of the pancreas in dogs (Benthem et al., 2001). Similarly, prejunctional cholinergic fibres in rat periorbital smooth muscle depress noradrenaline release through muscarinic receptors

expressed in sympathetic nerve fibres (Beauregard & Smith, 1994). Likewise, acetylcholine endogenously released from pulmonary parasympathetic nerves in guinea pigs can block neural transmission in the adjacent sympathetic nerves via activation of prejunctional muscarinic heteroreceptors (Pendry & Maclagan, 1991). Modulation of sympathetic activity by parasympathetic signalling has been studied in depth in the heart. In this system, parasympathetic activation decreases the heart rate by directly targeting sympathetic signalling under normal and pathological conditions (Azevedo & Parker, 1999; Buchholz et al., 2015; Gavioli et al., 2014; Miyashita et al., 1999). On the contrary, parasympathetic activity can also be repressed by sympathetic fibres (Smith-White, Wallace, & Potter, 1999). Moreover, synthesis of nerve growth factor, which is essential for the survival of sympathetic noradrenergic terminals, by neurons of the parasympathetic cardiac ganglion is regulated by β-adrenergic signals (Hasan & Smith, 2014). These observations demonstrate the importance of feed-back loops between both branches of the autonomic nervous system to control survival of PNS and SNS fibres, but also reveal a potential mechanism by which two important HSC functions like trafficking and quiescence could be precisely coordinated. Thus, local postsynaptic inhibitory feedback loops might be also placed in endosteal niches to fine-tune the neural regulation of haematopoiesis in relation to demands of the organism.

5.8 Target populations of sympathetic cholinergic fibres in endosteal BM niches

In line with previous studies (Acar et al., 2015), we show that more than 85% of HSCs are located in the central part of the BM (non-endosteal compartment) occupying perisinusoidal niches. This finding is not surprising as the central marrow represents over 90% of the inner volume of the long bones. However, in this study describe that sympathetic cholinergic fibres present exclusively in endosteal BM regulate a small subset of quiescent HSCs. This novel finding is consistent with previous studies suggesting that the endosteal environment promotes HSC quiescence and self-renewal (Arai et al., 2004; Calvi et al., 2003; Itkin et al., 2016; Kunisaki et al., 2013; Nilsson et al., 2005; Stier et al., 2005; Zhang et al., 2003).

In this context, we have identified Nes-GFP^{hi} BMSCs as putative target cells of cholinergic signalling in the endosteal compartment. This population has been

recently associated to endosteal arterioles named TZ vessels (Itkin et al., 2016; Kusumbe et al., 2014). Because their location in endosteal niches, TZ vessels might be functionally different from other arterioles which are located in the central part of the marrow and also surrounded by Nes-GFP^{hi} BMSCs (Kunisaki et al., 2013). Indeed, it has been proposed that these low-permeable endosteal arterioles form an osteo-vascular niche where low active HSCs are influenced by both endosteal and vascular elements supporting HSC maintenance (Itkin et al., 2016). Thus, we hypothesize that TZ vessels might play a relevant role in relaying local cholinergic signalling in the BM. According to this, we report that Nes-GFP^{+} cells express higher level of *Chrna7* gene expression compared to other stromal cells. Interestingly, expression of this receptor is even more up-regulated in *Gfra2*$^{-/-}$ Nes-GFP^{+} cells, suggesting a potential compensatory mechanism by which these BMSCs up-regulate cholinergic receptors in absence of cholinergic signals (Fig. 26C). These results support the emerging concept of distinct BM vessels in differentially regulating haematopoiesis (Itkin et al., 2016).

Although we identified endosteal Nes-GFP^{hi} cells as target population of cholinergic signalling, we cannot exclude the possibility that endosteal cholinergic signalling might target other BMSC or stromal populations. G-CSF-induced sympathetic noradrenergic signalling induces osteoblast suppression and HSPC activation through down-regulation of *Cxcl12* (Katayama et al., 2006). G-CSF treatment also depletes a population of trophic endosteal macrophages that support osteoblast function (osteomacs), suggesting that these macrophages could also be supressed by noradrenergic signalling. The influence of sympathetic cholinergic signalling on these other endosteal populations remains to be investigated. Alternatively, although less likely, a direct effect of cholinergic signalling on HSPCs cannot be excluded. Some studies have proposed the expression of cholinergic nicotinic receptors in HSPCs (Chang et al., 2010). Specifically, Chrnα7 identifies a HSPC population with an important role during regulation of inflammation (Gahring et al., 2013). Future experiments should aim at comparatively studying cholinergic receptor expression in endosteal versus non-endosteal HSPCs.

In summary, in this study we have presented evidence suggesting that endosteal BM niches are modulated by cholinergic signalling, identifying Nes-GFP^{hi} BMSCs

as one possible target population. Further studies will clarify which other populations can also be regulated and how this affects to HSC function.

5.9 Sympathetic cholinergic fibres regulate HSC self-renewal and long-term maintenance in endosteal BM niches

Transcriptomic analysis of HSPC from endosteal and non-endosteal HSPCs confirmed intrinsic differences between these populations. Comparing their transcriptomic profile with previously published gene sets shows increased self-renewal and anti-mobilising capacity of endosteal compared to non-endosteal HSCs (Fig. 28).

Importantly, the lack of sympathetic cholinergic innervations has a huge impact on the gene expression profile of endosteal HSCs from *Gfra2*$^{-/-}$ mice. Long-term HSC specific genes and self-renewal-associated genes are down-regulated in cholinergic fibre-deficient mice, while genes associated to HSC mobilisation are up-regulated (Fig. 28). These results suggest an abnormal over-activation of dormant HSCs in the endosteal compartment of *Gfra2*$^{-/-}$ mice, which independently confirms the increased activation of these cells as measured by PY/H42 assay.

Some authors have proposed that endosteal quiescent HSCs provide a HSC backup to restore normal haematopoiesis in emergency (Wilson et al., 2008)**.** Along these lines, *Gfra2*$^{-/-}$ mice exhibit an accelerated short-term haematopoietic recovery after myelosupressive therapy (Fig. 27D), while long-term repopulation capacity after transplantation was significantly reduced (Fig. 29).

But quiescence is not only important to ensure the self-renewal and long-term repopulation activity of HSCs (Cheng et al., 2000), cell cycle regulation is also critical to determine HSC fate (Pelayo et al., 2006; Walkley et al., 2007). In fact, there is evidence suggesting that disruption of endosteal niches induces HSC proliferation and mobilisation to perisinusoidal niches as intermediate step preceding egress to extramedullary sites (Visnjic et al., 2004). These observations imply that disruption of cholinergic signalling in endosteal BM niches might not only cause an increase in HSC proliferation but also a transition to sinusoidal areas. Furthermore, some studies have suggested that differentiation into certain haematopoietic lineages can be associated to certain sub-localizations in the BM (Cordeiro Gomes et al., 2016). Endosteal niches have been reported to harbour and regulate differentiation of early

lymphoid progenitors (Ding & Morrison, 2013; Morrison & Scadden, 2014). Future experiments should explore a possible involvement of cholinergic signalling as modulator of lymphoid differentiation.

5.10 Sympathetic noradrenergic vs sympathetic cholinergic: antagonistic regulation HSC functions in the BM

This study shows that a stress-response system, such as the SNS, can trigger sinusoidal transmigration of activated HSCs, but at the same time protect the HSC pool from exhaustion by inducing quiescence of a smaller subset of HSCs. This paradoxical situation is possible using different neurotransmitters. While HSPC transmigration in perisinusoidal niches is governed by noradrenergic signalling, acetylcholine released by sympathetic cholinergic fibres contribute to maintain HSC quiescence in endosteal niches.

This complex regulation might allow for fine-tuned HSC regulation and efficient response to stress, since the SNS does not only activate and mobilise stem cells in one compartment, but it also prevents stem cell attrition by inducing quiescence in a comparatively smaller compartment. This dual cholinergic regulation could be particularly important in the inflammatory/disease context. The SNS is key triggering pro-inflammatory effects in the early phases, but also in the later stages to inducing anti-inflammatory mechanisms to resolve the inflammatory process (Pongratz & Straub, 2014). At early stages, sympathetic cholinergic innervation could contribute to protect endosteal dormant HSCs from exhaustion while most HSCs get activated and mobilised. Later at later stages, parasympathetic signalling might coordinate sympathetic activity to shut down HSC mobilisation. Further studies should clarify the importance of cholinergic regulation of BM HSC niches in pathological conditions.

In summary, this is one of the first examples of how both branches of the autonomic nervous system cooperate to carry out a coordinated regulation of antagonistic HSC functions through noradrenergic sympathetic and cholinergic sympathetic signalling in spatially separated BM niches. And by extent, reveals how different signals from the autonomic nervous system regulate adult stem cells to meet distinct spatiotemporal physiological demands.

$$\text{É} = m\ x\ c^2$$

El éxito es igual a la motivación por la constancia al cuadrado

6 Conclusions

The results presented in this study lead to the following conclusions:

- The parasympathetic nervous system indirectly contributes to the circadian regulation of HSC trafficking between the BM and peripheral blood.

- The activity of the parasympathetic nervous system is triggered at the end of the resting phase (end of the day in the murine model before the start of the active nocturnal phase) and counterbalances sympathetic-induced HSC egress at night (in mice), when BM homing becomes predominant.

- The parasympathetic nervous system modulates sympathetic activity at the central level, which results in downregulation of β3-adrenergic receptor signalling in BMSCs, leading to increased *Cxcl12* expression.

- The cholinergic regulation of the BM might not only affect haematopoiesis but it might also impact bone remodelling.

- The BM endosteal compartment (close to the bone) is innervated by some sympathetic fibres, which switch their neurotransmitter properties postnatally and release acetylcholine, instead of noradrenaline (becoming sympathetic cholinergic fibres).

- Sympathetic cholinergic fibres induce *Cxcl12* expression and promote postnatal BM colonisation by HSCs, and possibly HSC quiescence. Therefore, the cholinergic switch seems to contribute to the BM HSC niche maturation during postnatal development.

- In adulthood, sympathetic cholinergic fibres target nestin$^+$ BMSCs in endosteal compartments and induce *Cxcl12* expression in these cells via nicotinic cholinergic signalling.

- Local cholinergic signalling in endosteal BM niches promotes HSC quiescence and long-term maintenance in a small subset of dormant HSCs allocated to this compartment.

- Both branches of the autonomic nervous system (parasympathetic and sympathetic) cooperate to regulate different HSC functions in spatially separated BM compartments. On the one hand, central cholinergic signalling modulates sympathetic noradrenergic tone to regulate HSC trafficking in the central part of the marrow. On the other hand, a sympathetic cholinergic innervation restricted to endosteal areas promote HSC maintenance and quiescence in a minor population of dormant HSC.

- This is one of the first examples of a stress-response system (the sympathetic nervous system) that can simultaneously promote two opposing processes (stem cell activation-migration and quiescence-maintenance) in two different niches. This might allow stem cells to efficiently respond to stress but simultaneously prevent stem cell attrition.

7 Conclusiones

Los resultados de este estudio permiten extraer las siguientes conclusiones:

- El sistema nervioso parasimpático contribuye a la regulación circadiana del tráfico de células madre hematopoyéticas entre la médula ósea y el torrente sanguíneo.

- La actuación del sistema nervioso parasimpático al final de la fase de reposo (fase diurna en el modelo murino, en contraposición a la fase de actividad nocturna) permite la inhibición del sistema nervioso simpático durante la noche y disminuye la salida de las células madre hematopoyéticas a la sangre cuando el proceso de “homing” hacia la médula ósea es predominante.

- El sistema nervioso parasimpático modula la actividad simpática a nivel central y, al igual que la contribución simpática durante la fase diurna, es transmitida a las células estromales del microambiente de la médula ósea a través de los receptores adrenérgicos β3 y la disminución de los niveles de Cxcl12.

- La regulación colinérgica de la médula ósea podría no limitarse a la hematopoyesis, sino también ejercer una función en el remodelado óseo.

- El compartimento endosteal de la médula ósea (próximo al hueso) está inervado por fibras simpáticas que cambian sus propiedades neurosecretoras en estadios postnatales, cuando cambian la noradrenalina por acetilcolina como neurotransmisor postsináptico (convirtiéndose así en fibras simpáticas colinérgicas).

- Las fibras simpáticas colinérgicas estimulan la producción de Cxcl12 y la colonización de la médula ósea postnatal por parte de las células madre hematopoyéticas (cuya proliferación podrían inhibir mediante mecanismos similares). De este modo el cambio colnérgico parece estar implicado en la

maduración del nicho de células madre en la médula durante el desarrollo postnatal.

- En el estadío adulto, las fibras simpáticas colinérgicas inervan las células estromales nestina^{+} presentes en el compartimento endostial e inducen la expresión de *Cxcl12* a través de la señalización colinérgica nicotínica en estas células.

- La señalización colinérgica local en en endostio promueve la quiescencia y mantenimiento a largo plazo de un pequeño grupo de células madre hematopoyéticas localizadas en este nicho.

- Las dos ramas del sistema nervioso autónomo (simpático y parasimpático) cooperan entre sí para regular distintas funciones de las células madre hematopoyéticas en distintos compartimentos de la médula ósea. Por un lado, la señalización colinérgica central modula el tono simpático noradrenergico para controlar el tráfico circadiano de células madre hematopoyéticas activas a través de los sinusoides. Por otro lado, la inervación simpática colinérgica restringida al compartimento endostial promueve el mantenimiento y la quiescencia de un grupo de células madres hematopoyéticas inactivas. Este es uno de los primeros ejemplos de un sistema de respuesta a estrés (el sistema nervioso simpático) capaz de promover dos procesos opuestos de manera simultánea: estimular la activación y migración de las células madre en un nicho, y simultáneamente promover la quiescencia y el mantenimiento del mismo tipo de células madres en otro nicho. Esto podría permitir a las células troncales responder a situaciones de estrés de modo eficiente, mientras se impide que se agote la reserva de células madre.

References

Aardal, N. P., & Laerum, O. D. (1983). Circadian variations in mouse bone marrow. *Exp Hematol, 11*(9), 792-801.

Abkowitz, J. L., Robinson, A. E., Kale, S., Long, M. W., & Chen, J. (2003). Mobilization of hematopoietic stem cells during homeostasis and after cytokine exposure. *Blood, 102*(4), 1249-1253. doi: 10.1182/blood-2003-01-0318

Acar, M., Kocherlakota, K. S., Murphy, M. M., Peyer, J. G., Oguro, H., Inra, C. N., . . . Morrison, S. J. (2015). Deep imaging of bone marrow shows non-dividing stem cells are mainly perisinusoidal. *Nature, 526*(7571), 126-130. doi: 10.1038/nature15250

Adams, G. B., Alley, I. R., Chung, U. I., Chabner, K. T., Jeanson, N. T., Lo Celso, C., . . . Scadden, D. T. (2009). Haematopoietic stem cells depend on Galpha(s)-mediated signalling to engraft bone marrow. *Nature, 459*(7243), 103-107. doi: 10.1038/nature07859

Ahmed, M., Bjurholm, A., Kreicbergs, A., & Schultzberg, M. (1993). Neuropeptide Y, tyrosine hydroxylase and vasoactive intestinal polypeptide-immunoreactive nerve fibers in the vertebral bodies, discs, dura mater, and spinal ligaments of the rat lumbar spine. *Spine (Phila Pa 1976), 18*(2), 268-273.

Ahmed, T., Wuest, D., & Ciavarella, D. (1992). Peripheral blood stem cell mobilization by cytokines. *J Clin Apher, 7*(3), 129-131.

Airaksinen, M. S., & Saarma, M. (2002). The GDNF family: signalling, biological functions and therapeutic value. *Nat Rev Neurosci, 3*(5), 383-394. doi: 10.1038/nrn812

Anderson, C., McKinley, M., Martelli, D., & McAllen, R. (2015). Letter to the editor: Parasympathetic innervation of the rodent spleen? *Am J Physiol Heart Circ Physiol, 309*(12), H2158. doi: 10.1152/ajpheart.00766.2015

Arai, F., Hirao, A., Ohmura, M., Sato, H., Matsuoka, S., Takubo, K., . . . Suda, T. (2004). Tie2/angiopoietin-1 signaling regulates hematopoietic stem cell quiescence in the bone marrow niche. *Cell, 118*(2), 149-161. doi: 10.1016/j.cell.2004.07.004

Artico, M., Bosco, S., Cavallotti, C., Agostinelli, E., Giuliani-Piccari, G., Sciorio, S., . . . Vitale, M. (2002). Noradrenergic and cholinergic innervation of the bone marrow. *Int J Mol Med, 10*(1), 77-80.

Asada, N., Katayama, Y., Sato, M., Minagawa, K., Wakahashi, K., Kawano, H., . . . Tanimoto, M. (2013). Matrix-embedded osteocytes regulate mobilization of hematopoietic stem/progenitor cells. *Cell Stem Cell, 12*(6), 737-747. doi: 10.1016/j.stem.2013.05.001

Asada, N., Kunisaki, Y., Pierce, H., Wang, Z., Fernandez, N. F., Birbrair, A., . . . Frenette, P. S. (2017). Differential cytokine contributions of perivascular haematopoietic stem cell niches. *Nat Cell Biol, 19*(3), 214-223. doi: 10.1038/ncb3475

Asmus, S. E., Parsons, S., & Landis, S. C. (2000). Developmental changes in the transmitter properties of sympathetic neurons that innervate the periosteum. *J Neurosci, 20*(4), 1495-1504.

Asmus, S. E., Tian, H., & Landis, S. C. (2001). Induction of cholinergic function in cultured sympathetic neurons by periosteal cells: cellular mechanisms. *Dev Biol, 235*(1), 1-11. doi: 10.1006/dbio.2001.0282

Azevedo, E. R., & Parker, J. D. (1999). Parasympathetic control of cardiac sympathetic activity: normal ventricular function versus congestive heart failure. *Circulation, 100*(3), 274-279.

Bajayo, A., Bar, A., Denes, A., Bachar, M., Kram, V., Attar-Namdar, M., . . . Bab, I. (2012). Skeletal parasympathetic innervation communicates central IL-1 signals regulating bone mass accrual. *Proc Natl Acad Sci U S A, 109*(38), 15455-15460. doi: 10.1073/pnas.1206061109

Baloh, R. H., Enomoto, H., Johnson, E. M., Jr., & Milbrandt, J. (2000). The GDNF family ligands and receptors - implications for neural development. *Curr Opin Neurobiol, 10*(1), 103-110.

Baloh, R. H., Tansey, M. G., Golden, J. P., Creedon, D. J., Heuckeroth, R. O., Keck, C. L., . . . Milbrandt, J. (1997). TrnR2, a novel receptor that mediates neurturin and GDNF signaling through Ret. *Neuron, 18*(5), 793-802.

Beauregard, C. L., & Smith, P. G. (1994). Parasympathetic innervation of rat peri-orbital smooth muscle: prejunctional cholinergic inhibition of sympathetic neurotransmission without direct postjunctional actions. *J Pharmacol Exp Ther, 268*(3), 1284-1288.

Bellinger, D. L., Felten, S. Y., Lorton, D., & Felten, D. L. (1989). Origin of noradrenergic innervation of the spleen in rats. *Brain Behav Immun, 3*(4), 291-311.

Bellinger, D. L., Lorton, D., Hamill, R. W., Felten, S. Y., & Felten, D. L. (1993). Acetylcholinesterase staining and choline acetyltransferase activity in the young adult rat spleen: lack of evidence for cholinergic innervation. *Brain Behav Immun, 7*(3), 191-204. doi: 10.1006/brbi.1993.1021

Bellinger, D. L., Lorton, D., Horn, L., Brouxhon, S., Felten, S. Y., & Felten, D. L. (1997). Vasoactive intestinal polypeptide (VIP) innervation of rat spleen, thymus, and lymph nodes. *Peptides, 18*(8), 1139-1149.

Benthem, L., Mundinger, T. O., & Taborsky, G. J., Jr. (2001). Parasympathetic inhibition of sympathetic neural activity to the pancreas. *Am J Physiol Endocrinol Metab, 280*(2), E378-381.

Bianco, P., Robey, P. G., & Simmons, P. J. (2008). Mesenchymal stem cells: revisiting history, concepts, and assays. *Cell Stem Cell, 2*(4), 313-319. doi: 10.1016/j.stem.2008.03.002

Boulais, P. E., & Frenette, P. S. (2015). Making sense of hematopoietic stem cell niches. *Blood, 125*(17), 2621-2629. doi: 10.1182/blood-2014-09-570192

Bowie, M. B., McKnight, K. D., Kent, D. G., McCaffrey, L., Hoodless, P. A., & Eaves, C. J. (2006). Hematopoietic stem cells proliferate until after birth and show a reversible phase-specific engraftment defect. *J Clin Invest, 116*(10), 2808-2816. doi: 10.1172/JCI28310

Branen, L., Hovgaard, L., Nitulescu, M., Bengtsson, E., Nilsson, J., & Jovinge, S. (2004). Inhibition of tumor necrosis factor-alpha reduces atherosclerosis in apolipoprotein E knockout mice. *Arterioscler Thromb Vasc Biol, 24*(11), 2137-2142. doi: 10.1161/01.ATV.0000143933.20616.1b

Brennecke, P., Anders, S., Kim, J. K., Kolodziejczyk, A. A., Zhang, X., Proserpio, V., . . . Heisler, M. G. (2013). Accounting for technical noise in single-cell RNA-seq experiments. *Nat Methods, 10*(11), 1093-1095. doi: 10.1038/nmeth.2645

Bruns, I., Lucas, D., Pinho, S., Ahmed, J., Lambert, M. P., Kunisaki, Y., . . . Frenette, P. S. (2014). Megakaryocytes regulate hematopoietic stem cell quiescence through CXCL4 secretion. *Nat Med, 20*(11), 1315-1320. doi: 10.1038/nm.3707

Buchholz, B., Donato, M., Perez, V., Deutsch, A. C., Hocht, C., Del Mauro, J. S., . . . Gelpi, R. J. (2015). Changes in the loading conditions induced by vagal stimulation modify the myocardial infarct size through sympathetic-parasympathetic interactions. *Pflugers Arch, 467*(7), 1509-1522. doi: 10.1007/s00424-014-1591-2

Buijs, R. M., van der Vliet, J., Garidou, M. L., Huitinga, I., & Escobar, C. (2008). Spleen vagal denervation inhibits the production of antibodies to circulating antigens. *PLoS One, 3*(9), e3152. doi: 10.1371/journal.pone.0003152

Burnstock, G. (1981). Review lecture. Neurotransmitters and trophic factors in the autonomic nervous system. *J Physiol, 313*, 1-35.

Byron, J. W. (1972). Evidence for a -adrenergic receptor initiating DNA synthesis in haemopoietic stem cells. *Exp Cell Res, 71*(1), 228-232.

Calvi, L. M., Adams, G. B., Weibrecht, K. W., Weber, J. M., Olson, D. P., Knight, M. C., . . . Scadden, D. T. (2003). Osteoblastic cells regulate the haematopoietic stem cell niche. *Nature, 425*(6960), 841-846. doi: 10.1038/nature02040

Calvo, W. (1968). The innervation of the bone marrow in laboratory animals. *Am J Anat, 123*(2), 315-328. doi: 10.1002/aja.1001230206

Calvo, W., & Haas, R. J. (1969). [On the histogenesis of the bone marrow in the rat. Innervation, stroma and their relations to hemopoiesis]. *Z Zellforsch Mikrosk Anat, 95*(3), 377-395.

Cano, G., Sved, A. F., Rinaman, L., Rabin, B. S., & Card, J. P. (2001). Characterization of the central nervous system innervation of the rat spleen using viral transneuronal tracing. *J Comp Neurol, 439*(1), 1-18. doi: 10.1002/cne.1331

Ciuculescu, M. F., Park, S. Y., Canty, K., Mathieu, R., Silberstein, L. E., & Williams, D. A. (2015). Perivascular deletion of murine Rac reverses the ratio of marrow arterioles and sinusoid vessels and alters hematopoiesis in vivo. *Blood, 125*(20), 3105-3113. doi: 10.1182/blood-2014-10-604892

Cordeiro Gomes, A., Hara, T., Lim, V. Y., Herndler-Brandstetter, D., Nevius, E., Sugiyama, T., . . . Pereira, J. P. (2016). Hematopoietic Stem Cell Niches Produce Lineage-Instructive Signals to Control Multipotent Progenitor Differentiation. *Immunity, 45*(6), 1219-1231. doi: 10.1016/j.immuni.2016.11.004

Corselli, M., Chin, C. J., Parekh, C., Sahaghian, A., Wang, W., Ge, S., . . . Peault, B. (2013). Perivascular support of human hematopoietic stem/progenitor cells. *Blood, 121*(15), 2891-2901. doi: 10.1182/blood-2012-08-451864

Chambers, S. M., Boles, N. C., Lin, K. Y., Tierney, M. P., Bowman, T. V., Bradfute, S. B., . . . Goodell, M. A. (2007). Hematopoietic fingerprints: an expression database of stem cells and their progeny. *Cell Stem Cell, 1*(5), 578-591. doi: 10.1016/j.stem.2007.10.003

Chan, C. K., Seo, E. Y., Chen, J. Y., Lo, D., McArdle, A., Sinha, R., . . . Longaker, M. T. (2015). Identification and specification of the mouse skeletal stem cell. *Cell, 160*(1-2), 285-298. doi: 10.1016/j.cell.2014.12.002

Chang, E., Forsberg, E. C., Wu, J., Bingyin, W., Prohaska, S. S., Allsopp, R., . . . Cooke, J. P. (2010). Cholinergic activation of hematopoietic stem cells: role in tobacco-related disease? *Vasc Med, 15*(5), 375-385. doi: 10.1177/1358863X10378377

Chen, J., Larochelle, A., Fricker, S., Bridger, G., Dunbar, C. E., & Abkowitz, J. L. (2006). Mobilization as a preparative regimen for hematopoietic stem cell transplantation. *Blood, 107*(9), 3764-3771. doi: 10.1182/blood-2005-09-3593

Chen, X. H., Itoh, M., Sun, W., Miki, T., & Takeuchi, Y. (1996). Localization of sympathetic and parasympathetic neurons innervating pancreas and spleen in the cat. *J Auton Nerv Syst, 59*(1-2), 12-16.

Cheng, T., Rodrigues, N., Shen, H., Yang, Y., Dombkowski, D., Sykes, M., & Scadden, D. T. (2000). Hematopoietic stem cell quiescence maintained by p21cip1/waf1. *Science, 287*(5459), 1804-1808.

Cheshier, S. H., Morrison, S. J., Liao, X., & Weissman, I. L. (1999). In vivo proliferation and cell cycle kinetics of long-term self-renewing hematopoietic stem cells. *Proc Natl Acad Sci U S A, 96*(6), 3120-3125.

Chevendra, V., & Weaver, L. C. (1992). Distributions of neuropeptide Y, vasoactive intestinal peptide and somatostatin in populations of postganglionic neurons innervating the rat kidney, spleen and intestine. *Neuroscience, 50*(3), 727-743.

De Boer, S. F., & Van der Gugten, J. (1987). Daily variations in plasma noradrenaline, adrenaline and corticosterone concentrations in rats. *Physiol Behav, 40*(3), 323-328.

De Potter, W. P., Kurzawa, R., Miserez, B., & Coen, E. P. (1995). Evidence against differential release of noradrenaline, neuropeptide Y, and dopamine-beta-hydroxylase from adrenergic nerves in the isolated perfused sheep spleen. *Synapse, 19*(2), 67-76. doi: 10.1002/syn.890190202

Dexter, T. M., Wright, E. G., Krizsa, F., & Lajtha, L. G. (1977). Regulation of haemopoietic stem cell proliferation in long term bone marrow cultures. *Biomedicine, 27*(9-10), 344-349.

Ding, L., & Morrison, S. J. (2013). Haematopoietic stem cells and early lymphoid progenitors occupy distinct bone marrow niches. *Nature, 495*(7440), 231-235. doi: 10.1038/nature11885

Ding, L., Saunders, T. L., Enikolopov, G., & Morrison, S. J. (2012). Endothelial and perivascular cells maintain haematopoietic stem cells. *Nature, 481*(7382), 457-462. doi: 10.1038/nature10783

Dzierzak, E., & Speck, N. A. (2008). Of lineage and legacy: the development of mammalian hematopoietic stem cells. *Nat Immunol, 9*(2), 129-136. doi: 10.1038/ni1560

Ehninger, A., & Trumpp, A. (2011). The bone marrow stem cell niche grows up: mesenchymal stem cells and macrophages move in. *J Exp Med, 208*(3), 421-428. doi: 10.1084/jem.20110132

Elefteriou, F., Ahn, J. D., Takeda, S., Starbuck, M., Yang, X., Liu, X., . . . Karsenty, G. (2005). Leptin regulation of bone resorption by the sympathetic nervous system and CART. *Nature, 434*(7032), 514-520. doi: 10.1038/nature03398

Ericsson, A., Schalling, M., McIntyre, K. R., Lundberg, J. M., Larhammar, D., Seroogy, K., . . . Persson, H. (1987). Detection of neuropeptide Y and its mRNA in megakaryocytes: enhanced levels in certain autoimmune mice. *Proc Natl Acad Sci U S A, 84*(16), 5585-5589.

Espinosa-Medina, I., Saha, O., Boismoreau, F., Chettouh, Z., Rossi, F., Richardson, W. D., & Brunet, J. F. (2016). The sacral autonomic outflow is sympathetic. *Science, 354*(6314), 893-897. doi: 10.1126/science.aah5454

Felten, D. L., Ackerman, K. D., Wiegand, S. J., & Felten, S. Y. (1987). Noradrenergic sympathetic innervation of the spleen: I. Nerve fibers associate with lymphocytes and macrophages in specific compartments of the splenic white pulp. *J Neurosci Res, 18*(1), 28-36, 118-121. doi: 10.1002/jnr.490180107

Fitch, S. R., Kimber, G. M., Wilson, N. K., Parker, A., Mirshekar-Syahkal, B., Gottgens, B., . . . Ottersbach, K. (2012). Signaling from the sympathetic nervous system regulates hematopoietic stem cell emergence during embryogenesis. *Cell Stem Cell, 11*(4), 554-566. doi: 10.1016/j.stem.2012.07.002

Fleming, M. S., Vysochan, A., Paixao, S., Niu, J., Klein, R., Savitt, J. M., & Luo, W. (2015). Cis and trans RET signaling control the survival and central projection growth of rapidly adapting mechanoreceptors. *Elife, 4*, e06828. doi: 10.7554/eLife.06828

Florian, M. C., Nattamai, K. J., Dorr, K., Marka, G., Uberle, B., Vas, V., . . . Geiger, H. (2013). A canonical to non-canonical Wnt signalling switch in haematopoietic stem-cell ageing. *Nature, 503*(7476), 392-396. doi: 10.1038/nature12631

Fonseca-Pereira, D., Arroz-Madeira, S., Rodrigues-Campos, M., Barbosa, I. A., Domingues, R. G., Bento, T., . . . Veiga-Fernandes, H. (2014). The neurotrophic factor receptor RET drives haematopoietic stem cell survival and function. *Nature, 514*(7520), 98-101. doi: 10.1038/nature13498

Forsberg, E. C., Passegue, E., Prohaska, S. S., Wagers, A. J., Koeva, M., Stuart, J. M., & Weissman, I. L. (2010). Molecular signatures of quiescent, mobilized and leukemia-initiating hematopoietic stem cells. *PLoS One, 5*(1), e8785. doi: 10.1371/journal.pone.0008785

Francis, N. J., Asmus, S. E., & Landis, S. C. (1997). CNTF and LIF are not required for the target-directed acquisition of cholinergic and peptidergic properties by sympathetic neurons in vivo. *Dev Biol, 182*(1), 76-87. doi: 10.1006/dbio.1996.8464

Francis, N. J., & Landis, S. C. (1999). Cellular and molecular determinants of sympathetic neuron development. *Annu Rev Neurosci, 22*, 541-566. doi: 10.1146/annurev.neuro.22.1.541

Frenette, P. S., Subbarao, S., Mazo, I. B., von Andrian, U. H., & Wagner, D. D. (1998). Endothelial selectins and vascular cell adhesion molecule-1 promote hematopoietic progenitor homing to bone marrow. *Proc Natl Acad Sci U S A, 95*(24), 14423-14428.

Fried, G., Terenius, L., Brodin, E., Efendic, S., Dockray, G., Fahrenkrug, J., . . . Hokfelt, T. (1986). Neuropeptide Y, enkephalin and noradrenaline coexist in sympathetic neurons innervating the bovine spleen. Biochemical and immunohistochemical evidence. *Cell Tissue Res, 243*(3), 495-508.

Friedenstein, A. J., Chailakhjan, R. K., & Lalykina, K. S. (1970). The development of fibroblast colonies in monolayer cultures of guinea-pig bone marrow and spleen cells. *Cell Tissue Kinet, 3*(4), 393-403.

Fu, L., Patel, M. S., Bradley, A., Wagner, E. F., & Karsenty, G. (2005). The molecular clock mediates leptin-regulated bone formation. *Cell, 122*(5), 803-815. doi: 10.1016/j.cell.2005.06.028

Furshpan, E. J., Landis, S. C., Matsumoto, S. G., & Potter, D. D. (1986). Synaptic functions in rat sympathetic neurons in microcultures. I. Secretion of norepinephrine and acetylcholine. *J Neurosci, 6*(4), 1061-1079.

Gahring, L. C., Enioutina, E. Y., Myers, E. J., Spangrude, G. J., Efimova, O. V., Kelley, T. W., . . . Rogers, S. W. (2013). Nicotinic receptor alpha7 expression identifies a novel hematopoietic progenitor lineage. *PLoS One, 8*(3), e57481. doi: 10.1371/journal.pone.0057481

Gajda, M., Adriaensen, D., & Cichocki, T. (2000). Development of the innervation of long bones: expression of the growth-associated protein 43. *Folia Histochem Cytobiol, 38*(3), 103-110.

Gajda, M., Litwin, J. A., Tabarowski, Z., Zagolski, O., Cichocki, T., Timmermans, J. P., & Adriaensen, D. (2010). Development of rat tibia innervation: colocalization of autonomic nerve fiber markers with growth-associated protein 43. *Cells Tissues Organs, 191*(6), 489-499. doi: 10.1159/000276591

Gautron, L., Rutkowski, J. M., Burton, M. D., Wei, W., Wan, Y., & Elmquist, J. K. (2013). Neuronal and nonneuronal cholinergic structures in the mouse gastrointestinal tract and spleen. *J Comp Neurol, 521*(16), 3741-3767. doi: 10.1002/cne.23376

Gavioli, M., Lara, A., Almeida, P. W., Lima, A. M., Damasceno, D. D., Rocha-Resende, C., . . . Guatimosim, S. (2014). Cholinergic signaling exerts protective effects in models of sympathetic hyperactivity-induced cardiac dysfunction. *PLoS One, 9*(7), e100179. doi: 10.1371/journal.pone.0100179

Gong, J. K. (1978). Endosteal marrow: a rich source of hematopoietic stem cells. *Science, 199*(4336), 1443-1445.

Grassinger, J., & Nilsson, S. K. (2011). Methods to analyze the homing efficiency and spatial distribution of hematopoietic stem and progenitor cells and their relationship to the bone marrow endosteum and vascular endothelium. *Methods Mol Biol, 750*, 197-214. doi: 10.1007/978-1-61779-145-1_14

Green, D. E., & Rubin, C. T. (2014). Consequences of irradiation on bone and marrow phenotypes, and its relation to disruption of hematopoietic precursors. *Bone, 63*, 87-94. doi: 10.1016/j.bone.2014.02.018

Greenbaum, A., Hsu, Y. M., Day, R. B., Schuettpelz, L. G., Christopher, M. J., Borgerding, J. N., . . . Link, D. C. (2013). CXCL12 in early mesenchymal progenitors is required for haematopoietic stem-cell maintenance. *Nature, 495*(7440), 227-230. doi: 10.1038/nature11926

Guidry, G., & Landis, S. C. (1998). Target-dependent development of the vesicular acetylcholine transporter in rodent sweat gland innervation. *Dev Biol, 199*(2), 175-184. doi: 10.1006/dbio.1998.8929

Habecker, B. A., & Landis, S. C. (1994). Noradrenergic regulation of cholinergic differentiation. *Science, 264*(5165), 1602-1604.

Hasan, W., & Smith, P. G. (2014). Decreased adrenoceptor stimulation in heart failure rats reduces NGF expression by cardiac parasympathetic neurons. *Auton Neurosci, 181*, 13-20. doi: 10.1016/j.autneu.2013.11.001

Henderson, C. E. (1996). Role of neurotrophic factors in neuronal development. *Curr Opin Neurobiol, 6*(1), 64-70.

Herskovits, M. S., & Singh, I. J. (1984). Effect of guanethidine-induced sympathectomy on osteoblastic activity in the rat femur evaluated by 3H-proline autoradiography. *Acta Anat (Basel), 120*(3), 151-155.

Heuckeroth, R. O., Enomoto, H., Grider, J. R., Golden, J. P., Hanke, J. A., Jackman, A., . . . Milbrandt, J. (1999). Gene targeting reveals a critical role for neurturin in the

development and maintenance of enteric, sensory, and parasympathetic neurons. *Neuron, 22*(2), 253-263.

Hiltunen, P. H., & Airaksinen, M. S. (2004). Sympathetic cholinergic target innervation requires GDNF family receptor GFR alpha 2. *Mol Cell Neurosci, 26*(3), 450-457. doi: 10.1016/j.mcn.2004.04.003

Hoane, M. R., Gulwadi, A. G., Morrison, S., Hovanesian, G., Lindner, M. D., & Tao, W. (1999). Differential in vivo effects of neurturin and glial cell-line-derived neurotrophic factor. *Exp Neurol, 160*(1), 235-243. doi: 10.1006/exnr.1999.7175

Hohmann, E. L., Elde, R. P., Rysavy, J. A., Einzig, S., & Gebhard, R. L. (1986). Innervation of periosteum and bone by sympathetic vasoactive intestinal peptide-containing nerve fibers. *Science, 232*(4752), 868-871.

Hooper, A. T., Butler, J. M., Nolan, D. J., Kranz, A., Iida, K., Kobayashi, M., . . . Rafii, S. (2009). Engraftment and reconstitution of hematopoiesis is dependent on VEGFR2-mediated regeneration of sinusoidal endothelial cells. *Cell Stem Cell, 4*(3), 263-274. doi: 10.1016/j.stem.2009.01.006

Huang, T., Hu, J., Wang, B., Nie, Y., Geng, J., & Cheng, L. (2013). Tlx3 controls cholinergic transmitter and Peptide phenotypes in a subset of prenatal sympathetic neurons. *J Neurosci, 33*(26), 10667-10675. doi: 10.1523/JNEUROSCI.0192-13.2013

Huston, J. M., Ochani, M., Rosas-Ballina, M., Liao, H., Ochani, K., Pavlov, V. A., . . . Ulloa, L. (2006). Splenectomy inactivates the cholinergic antiinflammatory pathway during lethal endotoxemia and polymicrobial sepsis. *J Exp Med, 203*(7), 1623-1628. doi: 10.1084/jem.20052362

Isern, J., Garcia-Garcia, A., Martin, A. M., Arranz, L., Martin-Perez, D., Torroja, C., . . . Mendez-Ferrer, S. (2014). The neural crest is a source of mesenchymal stem cells with specialized hematopoietic stem cell niche function. *Elife, 3*, e03696. doi: 10.7554/eLife.03696

Isern, J., Martin-Antonio, B., Ghazanfari, R., Martin, A. M., Lopez, J. A., del Toro, R., . . . Mendez-Ferrer, S. (2013). Self-renewing human bone marrow mesenspheres promote hematopoietic stem cell expansion. *Cell Rep, 3*(5), 1714-1724. doi: 10.1016/j.celrep.2013.03.041

Itkin, T., Gur-Cohen, S., Spencer, J. A., Schajnovitz, A., Ramasamy, S. K., Kusumbe, A. P., . . . Lapidot, T. (2016). Distinct bone marrow blood vessels differentially regulate haematopoiesis. *Nature, 532*(7599), 323-328. doi: 10.1038/nature17624

Katayama, Y., Battista, M., Kao, W. M., Hidalgo, A., Peired, A. J., Thomas, S. A., & Frenette, P. S. (2006). Signals from the sympathetic nervous system regulate hematopoietic stem cell egress from bone marrow. *Cell, 124*(2), 407-421. doi: 10.1016/j.cell.2005.10.041

Katayama, Y., Hidalgo, A., Furie, B. C., Vestweber, D., Furie, B., & Frenette, P. S. (2003). PSGL-1 participates in E-selectin-mediated progenitor homing to bone marrow: evidence for cooperation between E-selectin ligands and alpha4 integrin. *Blood, 102*(6), 2060-2067. doi: 10.1182/blood-2003-04-1212

Kawakami, M., Kimura, T., Kishimoto, Y., Tatekawa, T., Baba, Y., Nishizaki, T., . . . Soma, T. (2004). Preferential expression of the vasoactive intestinal peptide (VIP) receptor VPAC1 in human cord blood-derived CD34+CD38- cells: possible role of VIP as a growth-promoting factor for hematopoietic stem/progenitor cells. *Leukemia, 18*(5), 912-921. doi: 10.1038/sj.leu.2403330

Kiel, M. J., & Morrison, S. J. (2008). Uncertainty in the niches that maintain haematopoietic stem cells. *Nat Rev Immunol, 8*(4), 290-301. doi: 10.1038/nri2279

Kiel, M. J., Yilmaz, O. H., Iwashita, T., Yilmaz, O. H., Terhorst, C., & Morrison, S. J. (2005). SLAM family receptors distinguish hematopoietic stem and progenitor cells and reveal endothelial niches for stem cells. *Cell, 121*(7), 1109-1121. doi: 10.1016/j.cell.2005.05.026

Kinney, K. S., Cohen, N., & Felten, S. Y. (1994). Noradrenergic and peptidergic innervation of the amphibian spleen: comparative studies. *Dev Comp Immunol, 18*(6), 511-521.

Kollet, O., Dar, A., Shivtiel, S., Kalinkovich, A., Lapid, K., Sztainberg, Y., . . . Lapidot, T. (2006). Osteoclasts degrade endosteal components and promote mobilization of hematopoietic progenitor cells. *Nat Med, 12*(6), 657-664. doi: 10.1038/nm1417

Kooijman, S., Meurs, I., van Beek, L., Khedoe, P. P., Giezekamp, A., Pike-Overzet, K., . . . Rensen, P. C. (2015). Splenic autonomic denervation increases inflammatory status but does not aggravate atherosclerotic lesion development. *Am J Physiol Heart Circ Physiol, 309*(4), H646-654. doi: 10.1152/ajpheart.00787.2014

Krivtsov, A. V., Twomey, D., Feng, Z., Stubbs, M. C., Wang, Y., Faber, J., . . . Armstrong, S. A. (2006). Transformation from committed progenitor to leukaemia stem cell initiated by MLL-AF9. *Nature, 442*(7104), 818-822. doi: 10.1038/nature04980

Kunisaki, Y., Bruns, I., Scheiermann, C., Ahmed, J., Pinho, S., Zhang, D., . . . Frenette, P. S. (2013). Arteriolar niches maintain haematopoietic stem cell quiescence. *Nature, 502*(7473), 637-643. doi: 10.1038/nature12612

Kusumbe, A. P., Ramasamy, S. K., & Adams, R. H. (2014). Coupling of angiogenesis and osteogenesis by a specific vessel subtype in bone. *Nature, 507*(7492), 323-328. doi: 10.1038/nature13145

Kusumbe, A. P., Ramasamy, S. K., Itkin, T., Mae, M. A., Langen, U. H., Betsholtz, C., . . . Adams, R. H. (2016). Age-dependent modulation of vascular niches for haematopoietic stem cells. *Nature, 532*(7599), 380-384. doi: 10.1038/nature17638

Landis, S. C. (1976). Rat sympathetic neurons and cardiac myocytes developing in microcultures: correlation of the fine structure of endings with neurotransmitter function in single neurons. *Proc Natl Acad Sci U S A, 73*(11), 4220-4224.

Landis, S. C. (1996). The development of cholinergic sympathetic neurons: a role for neuropoietic cytokines? *Perspect Dev Neurobiol, 4*(1), 53-63.

Lapidot, T., Dar, A., & Kollet, O. (2005). How do stem cells find their way home? *Blood, 106*(6), 1901-1910. doi: 10.1182/blood-2005-04-1417

Lapidot, T., & Kollet, O. (2010). The brain-bone-blood triad: traffic lights for stem-cell homing and mobilization. *Hematology Am Soc Hematol Educ Program, 2010*, 1-6. doi: 10.1182/asheducation-2010.1.1

Lee, N. J., Nguyen, A. D., Enriquez, R. F., Luzuriaga, J., Bensellam, M., Laybutt, R., . . . Herzog, H. (2015). NPY signalling in early osteoblasts controls glucose homeostasis. *Mol Metab, 4*(3), 164-174. doi: 10.1016/j.molmet.2014.12.010

Levesque, J. P., Hendy, J., Takamatsu, Y., Simmons, P. J., & Bendall, L. J. (2003). Disruption of the CXCR4/CXCL12 chemotactic interaction during hematopoietic stem cell mobilization induced by GCSF or cyclophosphamide. *J Clin Invest, 111*(2), 187-196. doi: 10.1172/JCI15994

Levesque, J. P., Liu, F., Simmons, P. J., Betsuyaku, T., Senior, R. M., Pham, C., & Link, D. C. (2004). Characterization of hematopoietic progenitor mobilization in protease-deficient mice. *Blood, 104*(1), 65-72. doi: 10.1182/blood-2003-05-1589

Li, H., Ghazanfari, R., Zacharaki, D., Ditzel, N., Isern, J., Ekblom, M., . . . Scheding, S. (2014). Low/negative expression of PDGFR-alpha identifies the candidate primary mesenchymal stromal cells in adult human bone marrow. *Stem Cell Reports, 3*(6), 965-974. doi: 10.1016/j.stemcr.2014.09.018

Liu, F., Poursine-Laurent, J., & Link, D. C. (2000). Expression of the G-CSF receptor on hematopoietic progenitor cells is not required for their mobilization by G-CSF. *Blood, 95*(10), 3025-3031.

Lo Celso, C., Fleming, H. E., Wu, J. W., Zhao, C. X., Miake-Lye, S., Fujisaki, J., . . . Scadden, D. T. (2009). Live-animal tracking of individual haematopoietic stem/progenitor cells in their niche. *Nature, 457*(7225), 92-96. doi: 10.1038/nature07434

Lohse, M. J., Benovic, J. L., Codina, J., Caron, M. G., & Lefkowitz, R. J. (1990). beta-Arrestin: a protein that regulates beta-adrenergic receptor function. *Science, 248*(4962), 1547-1550.

Lord, B. I., Testa, N. G., & Hendry, J. H. (1975). The relative spatial distributions of CFUs and CFUc in the normal mouse femur. *Blood, 46*(1), 65-72.

Lucas, D., Battista, M., Shi, P. A., Isola, L., & Frenette, P. S. (2008). Mobilized hematopoietic stem cell yield depends on species-specific circadian timing. *Cell Stem Cell, 3*(4), 364-366. doi: 10.1016/j.stem.2008.09.004

Lundberg, P., Allison, S. J., Lee, N. J., Baldock, P. A., Brouard, N., Rost, S., . . . Herzog, H. (2007). Greater bone formation of Y2 knockout mice is associated with increased osteoprogenitor numbers and altered Y1 receptor expression. *J Biol Chem, 282*(26), 19082-19091. doi: 10.1074/jbc.M609629200

Luther, J. A., & Birren, S. J. (2009). Neurotrophins and target interactions in the development and regulation of sympathetic neuron electrical and synaptic properties. *Auton Neurosci, 151*(1), 46-60. doi: 10.1016/j.autneu.2009.08.009

Lv, F. J., Tuan, R. S., Cheung, K. M., & Leung, V. Y. (2014). Concise review: the surface markers and identity of human mesenchymal stem cells. *Stem Cells, 32*(6), 1408-1419. doi: 10.1002/stem.1681

Mach, D. B., Rogers, S. D., Sabino, M. C., Luger, N. M., Schwei, M. J., Pomonis, J. D., . . . Mantyh, P. W. (2002). Origins of skeletal pain: sensory and sympathetic innervation of the mouse femur. *Neuroscience, 113*(1), 155-166.

Madisen, L., Mao, T., Koch, H., Zhuo, J. M., Berenyi, A., Fujisawa, S., . . . Zeng, H. (2012). A toolbox of Cre-dependent optogenetic transgenic mice for light-induced activation and silencing. *Nat Neurosci, 15*(5), 793-802. doi: 10.1038/nn.3078

Maestroni, G. J., & Conti, A. (1990). The pineal neurohormone melatonin stimulates activated CD4+, Thy-1+ cells to release opioid agonist(s) with immunoenhancing and anti-stress properties. *J Neuroimmunol, 28*(2), 167-176.

Maestroni, G. J., & Conti, A. (1994a). Modulation of hematopoiesis via alpha 1-adrenergic receptors on bone marrow cells. *Exp Hematol, 22*(3), 313-320.

Maestroni, G. J., & Conti, A. (1994b). Noradrenergic modulation of lymphohematopoiesis. *Int J Immunopharmacol, 16*(2), 117-122.

Maestroni, G. J., Conti, A., & Pedrinis, E. (1992). Effect of adrenergic agents on hematopoiesis after syngeneic bone marrow transplantation in mice. *Blood, 80*(5), 1178-1182.

Maestroni, G. J., Conti, A., & Pierpaoli, W. (1988). Pineal melatonin, its fundamental immunoregulatory role in aging and cancer. *Ann N Y Acad Sci, 521*, 140-148.

Maestroni, G. J., Cosentino, M., Marino, F., Togni, M., Conti, A., Lecchini, S., & Frigo, G. (1998). Neural and endogenous catecholamines in the bone marrow. Circadian association of norepinephrine with hematopoiesis? *Exp Hematol, 26*(12), 1172-1177.

Maestroni, G. J., Togni, M., & Covacci, V. (1997). Norepinephrine protects mice from acute lethal doses of carboplatin. *Exp Hematol, 25*(6), 491-494.

Massberg, S., Schaerli, P., Knezevic-Maramica, I., Kollnberger, M., Tubo, N., Moseman, E. A., . . . von Andrian, U. H. (2007). Immunosurveillance by hematopoietic progenitor cells trafficking through blood, lymph, and peripheral tissues. *Cell, 131*(5), 994-1008. doi: 10.1016/j.cell.2007.09.047

Mendez-Ferrer, S., Battista, M., & Frenette, P. S. (2010). Cooperation of beta(2)- and beta(3)-adrenergic receptors in hematopoietic progenitor cell mobilization. *Ann N Y Acad Sci, 1192*, 139-144. doi: 10.1111/j.1749-6632.2010.05390.x

Mendez-Ferrer, S., Lucas, D., Battista, M., & Frenette, P. S. (2008). Haematopoietic stem cell release is regulated by circadian oscillations. *Nature, 452*(7186), 442-447. doi: 10.1038/nature06685

Mendez-Ferrer, S., Michurina, T. V., Ferraro, F., Mazloom, A. R., Macarthur, B. D., Lira, S. A., . . . Frenette, P. S. (2010). Mesenchymal and haematopoietic stem cells form a unique bone marrow niche. *Nature, 466*(7308), 829-834. doi: 10.1038/nature09262

Miller, M. L., & McCuskey, R. S. (1973). Innervation of bone marrow in the rabbit. *Scand J Haematol, 10*(1), 17-23.

Miyashita, Y., Furukawa, Y., Nakajima, K., Hirose, M., Kurogouchi, F., & Chiba, S. (1999). Parasympathetic inhibition of sympathetic effects on pacemaker location and rate in hearts of anesthetized dogs. *J Cardiovasc Electrophysiol, 10*(8), 1066-1076.

Molineux, G., Pojda, Z., Hampson, I. N., Lord, B. I., & Dexter, T. M. (1990). Transplantation potential of peripheral blood stem cells induced by granulocyte colony-stimulating factor. *Blood, 76*(10), 2153-2158.

Morrison, S. J., & Scadden, D. T. (2014). The bone marrow niche for haematopoietic stem cells. *Nature, 505*(7483), 327-334. doi: 10.1038/nature12984

Nagasawa, T., Hirota, S., Tachibana, K., Takakura, N., Nishikawa, S., Kitamura, Y., . . . Kishimoto, T. (1996). Defects of B-cell lymphopoiesis and bone-marrow myelopoiesis in mice lacking the CXC chemokine PBSF/SDF-1. *Nature, 382*(6592), 635-638. doi: 10.1038/382635a0

Nagatsu, T., Levitt, M., & Udenfriend, S. (1964). Tyrosine Hydroxylase. The Initial Step in Norepinephrine Biosynthesis. *J Biol Chem, 239*, 2910-2917.

Nakamura-Ishizu, A., Takubo, K., Fujioka, M., & Suda, T. (2014). Megakaryocytes are essential for HSC quiescence through the production of thrombopoietin. *Biochem Biophys Res Commun, 454*(2), 353-357. doi: 10.1016/j.bbrc.2014.10.095

Nakayama, S., Iida, K., Tsuzuki, T., Iwashita, T., Murakami, H., Asai, N., . . . Takahashi, M. (1999). Implication of expression of GDNF/Ret signalling components in differentiation of bone marrow haemopoietic cells. *Br J Haematol, 105*(1), 50-57.

Nam, C., Case, A. J., Hostager, B. S., & O'Dorisio, M. S. (2009). The role of vasoactive intestinal peptide (VIP) in megakaryocyte proliferation. *J Mol Neurosci, 37*(2), 160-167. doi: 10.1007/s12031-008-9119-x

Nance, D. M., & Sanders, V. M. (2007). Autonomic innervation and regulation of the immune system (1987-2007). *Brain Behav Immun, 21*(6), 736-745. doi: 10.1016/j.bbi.2007.03.008

Niijima, A., Nagai, K., Nagai, N., & Nakagawa, H. (1992). Light enhances sympathetic and suppresses vagal outflows and lesions including the suprachiasmatic nucleus eliminate these changes in rats. *J Auton Nerv Syst, 40*(2), 155-160.

Nilsson, S. K., Johnston, H. M., & Coverdale, J. A. (2001). Spatial localization of transplanted hemopoietic stem cells: inferences for the localization of stem cell niches. *Blood, 97*(8), 2293-2299.

Nilsson, S. K., Johnston, H. M., Whitty, G. A., Williams, B., Webb, R. J., Denhardt, D. T., . . . Haylock, D. N. (2005). Osteopontin, a key component of the hematopoietic stem cell niche and regulator of primitive hematopoietic progenitor cells. *Blood, 106*(4), 1232-1239. doi: 10.1182/blood-2004-11-4422

Oguro, H., Ding, L., & Morrison, S. J. (2013). SLAM family markers resolve functionally distinct subpopulations of hematopoietic stem cells and multipotent progenitors. *Cell Stem Cell, 13*(1), 102-116. doi: 10.1016/j.stem.2013.05.014

Olofsson, P. S., Rosas-Ballina, M., Levine, Y. A., & Tracey, K. J. (2012). Rethinking inflammation: neural circuits in the regulation of immunity. *Immunol Rev, 248*(1), 188-204. doi: 10.1111/j.1600-065X.2012.01138.x

Omatsu, Y., Sugiyama, T., Kohara, H., Kondoh, G., Fujii, N., Kohno, K., & Nagasawa, T. (2010). The essential functions of adipo-osteogenic progenitors as the hematopoietic stem and progenitor cell niche. *Immunity, 33*(3), 387-399. doi: 10.1016/j.immuni.2010.08.017

Papayannopoulou, T., Priestley, G. V., Nakamoto, B., Zafiropoulos, V., & Scott, L. M. (2001). Molecular pathways in bone marrow homing: dominant role of alpha(4)beta(1) over beta(2)-integrins and selectins. *Blood, 98*(8), 2403-2411.

Park, M. H., Jin, H. K., Min, W. K., Lee, W. W., Lee, J. E., Akiyama, H., . . . Bae, J. S. (2015). Neuropeptide Y regulates the hematopoietic stem cell microenvironment and prevents nerve injury in the bone marrow. *EMBO J, 34*(12), 1648-1660. doi: 10.15252/embj.201490174

Park, M. H., Lee, J. K., Kim, N., Min, W. K., Lee, J. E., Kim, K. T., . . . Bae, J. S. (2016). Neuropeptide Y Induces Hematopoietic Stem/Progenitor Cell Mobilization by Regulating Matrix Metalloproteinase-9 Activity Through Y1 Receptor in Osteoblasts. *Stem Cells, 34*(8), 2145-2156. doi: 10.1002/stem.2383

Park, S. K., Olson, T. A., Ercal, N., Summers, M., & O'Dorisio, M. S. (1996). Characterization of vasoactive intestinal peptide receptors on human megakaryocytes and platelets. *Blood, 87*(11), 4629-4635.

Patt, H. M., & Maloney, M. A. (1975). Bone marrow regeneration after local injury: a review. *Exp Hematol, 3*(2), 135-148.

Pelayo, R., Miyazaki, K., Huang, J., Garrett, K. P., Osmond, D. G., & Kincade, P. W. (2006). Cell cycle quiescence of early lymphoid progenitors in adult bone marrow. *Stem Cells, 24*(12), 2703-2713. doi: 10.1634/stemcells.2006-0217

Pendry, Y. D., & Maclagan, J. (1991). Evidence for prejunctional inhibitory muscarinic receptors on sympathetic nerves innervating guinea-pig trachealis muscle. *Br J Pharmacol, 103*(1), 1165-1171.

Pierce, H., Zhang, D., Magnon, C., Lucas, D., Christin, J. R., Huggins, M., . . . Frenette, P. S. (2017). Cholinergic Signals from the CNS Regulate G-CSF-Mediated HSC Mobilization from Bone Marrow via a Glucocorticoid Signaling Relay. *Cell Stem Cell*. doi: 10.1016/j.stem.2017.01.002

Pinho, S., Lacombe, J., Hanoun, M., Mizoguchi, T., Bruns, I., Kunisaki, Y., & Frenette, P. S. (2013). PDGFRalpha and CD51 mark human nestin+ sphere-forming mesenchymal stem cells capable of hematopoietic progenitor cell expansion. *J Exp Med, 210*(7), 1351-1367. doi: 10.1084/jem.20122252

Pongratz, G., & Straub, R. H. (2014). The sympathetic nervous response in inflammation. *Arthritis Res Ther, 16*(6), 504.

Rameshwar, P., Gascon, P., Oh, H. S., Denny, T. N., Zhu, G., & Ganea, D. (2002). Vasoactive intestinal peptide (VIP) inhibits the proliferation of bone marrow progenitors through the VPAC1 receptor. *Exp Hematol, 30*(9), 1001-1009.

Reya, T., Duncan, A. W., Ailles, L., Domen, J., Scherer, D. C., Willert, K., . . . Weissman, I. L. (2003). A role for Wnt signalling in self-renewal of haematopoietic stem cells. *Nature, 423*(6938), 409-414. doi: 10.1038/nature01593

Richins, C. A., & Kuntz, A. (1953). The autonomic nervous system. *Prog Neurol Psychiatry, 8*, 197-227.

Romano, T. A., Felten, S. Y., Felten, D. L., & Olschowka, J. A. (1991). Neuropeptide-Y innervation of the rat spleen: another potential immunomodulatory neuropeptide. *Brain Behav Immun, 5*(1), 116-131.

Rosas-Ballina, M., Ochani, M., Parrish, W. R., Ochani, K., Harris, Y. T., Huston, J. M., . . . Tracey, K. J. (2008). Splenic nerve is required for cholinergic antiinflammatory pathway control of TNF in endotoxemia. *Proc Natl Acad Sci U S A, 105*(31), 11008-11013. doi: 10.1073/pnas.0803237105

Rosas-Ballina, M., Olofsson, P. S., Ochani, M., Valdes-Ferrer, S. I., Levine, Y. A., Reardon, C., . . . Tracey, K. J. (2011). Acetylcholine-synthesizing T cells relay neural signals in a vagus nerve circuit. *Science, 334*(6052), 98-101. doi: 10.1126/science.1209985

Rossi, J., Luukko, K., Poteryaev, D., Laurikainen, A., Sun, Y. F., Laakso, T., . . . Airaksinen, M. S. (1999). Retarded growth and deficits in the enteric and parasympathetic nervous system in mice lacking GFR alpha2, a functional neurturin receptor. *Neuron, 22*(2), 243-252.

Sacchetti, B., Funari, A., Michienzi, S., Di Cesare, S., Piersanti, S., Saggio, I., . . . Bianco, P. (2007). Self-renewing osteoprogenitors in bone marrow sinusoids can organize a hematopoietic microenvironment. *Cell, 131*(2), 324-336. doi: 10.1016/j.cell.2007.08.025

Saito, H. (1990). Innervation of the guinea pig spleen studied by electron microscopy. *Am J Anat, 189*(3), 213-235. doi: 10.1002/aja.1001890305

Sanchez-Aguilera, A., Arranz, L., Martin-Perez, D., Garcia-Garcia, A., Stavropoulou, V., Kubovcakova, L., . . . Mendez-Ferrer, S. (2014). Estrogen signaling selectively induces apoptosis of hematopoietic progenitors and myeloid neoplasms without harming steady-state hematopoiesis. *Cell Stem Cell, 15*(6), 791-804. doi: 10.1016/j.stem.2014.11.002

Sanchez-Aguilera, A., Lee, Y. J., Lo Celso, C., Ferraro, F., Brumme, K., Mondal, S., . . . Williams, D. A. (2011). Guanine nucleotide exchange factor Vav1 regulates perivascular homing and bone marrow retention of hematopoietic stem and progenitor cells. *Proc Natl Acad Sci U S A, 108*(23), 9607-9612. doi: 10.1073/pnas.1102018108

Sauerbier, I., & von Mayersbach, H. (1977). Circadian variation of catecholamines in human blood. *Horm Metab Res, 9*(6), 529-530. doi: 10.1055/s-0028-1095589

Schajnovitz, A., Itkin, T., D'Uva, G., Kalinkovich, A., Golan, K., Ludin, A., . . . Lapidot, T. (2011). CXCL12 secretion by bone marrow stromal cells is dependent on cell contact and mediated by connexin-43 and connexin-45 gap junctions. *Nat Immunol, 12*(5), 391-398. doi: 10.1038/ni.2017

Scheiermann, C., Kunisaki, Y., Lucas, D., Chow, A., Jang, J. E., Zhang, D., . . . Frenette, P. S. (2012). Adrenergic nerves govern circadian leukocyte recruitment to tissues. *Immunity, 37*(2), 290-301. doi: 10.1016/j.immuni.2012.05.021

Schepers, K., Hsiao, E. C., Garg, T., Scott, M. J., & Passegue, E. (2012). Activated Gs signaling in osteoblastic cells alters the hematopoietic stem cell niche in mice. *Blood, 120*(17), 3425-3435. doi: 10.1182/blood-2011-11-395418

Schofield, R. (1978). The relationship between the spleen colony-forming cell and the haemopoietic stem cell. *Blood Cells, 4*(1-2), 7-25.

Schutz, B., Jurastow, I., Bader, S., Ringer, C., von Engelhardt, J., Chubanov, V., . . . Weihe, E. (2015). Chemical coding and chemosensory properties of cholinergic brush cells in the mouse gastrointestinal and biliary tract. *Front Physiol, 6*, 87. doi: 10.3389/fphys.2015.00087

Shi, Y., Oury, F., Yadav, V. K., Wess, J., Liu, X. S., Guo, X. E., . . . Karsenty, G. (2010). Signaling through the M(3) muscarinic receptor favors bone mass accrual by decreasing sympathetic activity. *Cell Metab, 11*(3), 231-238. doi: 10.1016/j.cmet.2010.01.005

Smaaland, R., Sothern, R. B., Laerum, O. D., & Abrahamsen, J. F. (2002). Rhythms in human bone marrow and blood cells. *Chronobiol Int, 19*(1), 101-127.

Smith-White, M. A., Wallace, D., & Potter, E. K. (1999). Sympathetic-parasympathetic interactions at the heart in the anaesthetised rat. *J Auton Nerv Syst, 75*(2-3), 171-175.

Smith, L. G., Weissman, I. L., & Heimfeld, S. (1991). Clonal analysis of hematopoietic stem-cell differentiation in vivo. *Proc Natl Acad Sci U S A, 88*(7), 2788-2792.

Spiegel, A., Shivtiel, S., Kalinkovich, A., Ludin, A., Netzer, N., Goichberg, P., . . . Lapidot, T. (2007). Catecholaminergic neurotransmitters regulate migration and repopulation of immature human CD34+ cells through Wnt signaling. *Nat Immunol, 8*(10), 1123-1131. doi: 10.1038/ni1509

Stier, S., Ko, Y., Forkert, R., Lutz, C., Neuhaus, T., Grunewald, E., . . . Scadden, D. T. (2005). Osteopontin is a hematopoietic stem cell niche component that negatively regulates stem cell pool size. *J Exp Med, 201*(11), 1781-1791. doi: 10.1084/jem.20041992

Sugiyama, T., Kohara, H., Noda, M., & Nagasawa, T. (2006). Maintenance of the hematopoietic stem cell pool by CXCL12-CXCR4 chemokine signaling in bone marrow stromal cell niches. *Immunity, 25*(6), 977-988. doi: 10.1016/j.immuni.2006.10.016

Tabarowski, Z., Gibson-Berry, K., & Felten, S. Y. (1996). Noradrenergic and peptidergic innervation of the mouse femur bone marrow. *Acta Histochem, 98*(4), 453-457. doi: 10.1016/S0065-1281(96)80013-4

Takeda, S., Elefteriou, F., Levasseur, R., Liu, X., Zhao, L., Parker, K. L., . . . Karsenty, G. (2002). Leptin regulates bone formation via the sympathetic nervous system. *Cell, 111*(3), 305-317.

Takeda, S., & Karsenty, G. (2008). Molecular bases of the sympathetic regulation of bone mass. *Bone, 42*(5), 837-840. doi: 10.1016/j.bone.2008.01.005

Teixeira, L., Sousa, D. M., Nunes, A. F., Sousa, M. M., Herzog, H., & Lamghari, M. (2009). NPY revealed as a critical modulator of osteoblast function in vitro: new insights into the role of Y1 and Y2 receptors. *J Cell Biochem, 107*(5), 908-916. doi: 10.1002/jcb.22194

Terazono, H., Mutoh, T., Yamaguchi, S., Kobayashi, M., Akiyama, M., Udo, R., . . . Shibata, S. (2003). Adrenergic regulation of clock gene expression in mouse liver. *Proc Natl Acad Sci U S A, 100*(11), 6795-6800. doi: 10.1073/pnas.0936797100

Tormin, A., Li, O., Brune, J. C., Walsh, S., Schutz, B., Ehinger, M., . . . Scheding, S. (2011). CD146 expression on primary nonhematopoietic bone marrow stem cells is correlated with in situ localization. *Blood, 117*(19), 5067-5077. doi: 10.1182/blood-2010-08-304287

Travlos, G. S. (2006). Normal structure, function, and histology of the bone marrow. *Toxicol Pathol, 34*(5), 548-565. doi: 10.1080/01926230600939856

Trumpp, A., Essers, M., & Wilson, A. (2010). Awakening dormant haematopoietic stem cells. *Nat Rev Immunol, 10*(3), 201-209. doi: 10.1038/nri2726

Vega, J. A., Garcia-Suarez, O., Hannestad, J., Perez-Perez, M., & Germana, A. (2003). Neurotrophins and the immune system. *J Anat, 203*(1), 1-19.

Vida, G., Pena, G., Deitch, E. A., & Ulloa, L. (2011). alpha7-cholinergic receptor mediates vagal induction of splenic norepinephrine. *J Immunol, 186*(7), 4340-4346. doi: 10.4049/jimmunol.1003722

Visnjic, D., Kalajzic, Z., Rowe, D. W., Katavic, V., Lorenzo, J., & Aguila, H. L. (2004). Hematopoiesis is severely altered in mice with an induced osteoblast deficiency. *Blood, 103*(9), 3258-3264. doi: 10.1182/blood-2003-11-4011

Walkley, C. R., Olsen, G. H., Dworkin, S., Fabb, S. A., Swann, J., McArthur, G. A., . . . Purton, L. E. (2007). A microenvironment-induced myeloproliferative syndrome caused by retinoic acid receptor gamma deficiency. *Cell, 129*(6), 1097-1110. doi: 10.1016/j.cell.2007.05.014

Weihe, E., Tao-Cheng, J. H., Schafer, M. K., Erickson, J. D., & Eiden, L. E. (1996). Visualization of the vesicular acetylcholine transporter in cholinergic nerve terminals and its targeting to a specific population of small synaptic vesicles. *Proc Natl Acad Sci U S A, 93*(8), 3547-3552.

Wilson, A., Laurenti, E., Oser, G., van der Wath, R. C., Blanco-Bose, W., Jaworski, M., . . . Trumpp, A. (2008). Hematopoietic stem cells reversibly switch from dormancy to self-renewal during homeostasis and repair. *Cell, 135*(6), 1118-1129. doi: 10.1016/j.cell.2008.10.048

Williams, D. A., Xu, H., & Cancelas, J. A. (2006). Children are not little adults: just ask their hematopoietic stem cells. *J Clin Invest, 116*(10), 2593-2596. doi: 10.1172/JCI30083

Winkler, I. G., Sims, N. A., Pettit, A. R., Barbier, V., Nowlan, B., Helwani, F., . . . Levesque, J. P. (2010). Bone marrow macrophages maintain hematopoietic stem cell (HSC) niches and their depletion mobilizes HSCs. *Blood, 116*(23), 4815-4828. doi: 10.1182/blood-2009-11-253534

Wolber, F. M., Leonard, E., Michael, S., Orschell-Traycoff, C. M., Yoder, M. C., & Srour, E. F. (2002). Roles of spleen and liver in development of the murine hematopoietic system. *Exp Hematol, 30*(9), 1010-1019.

Wolinsky, E., & Patterson, P. H. (1983). Tyrosine hydroxylase activity decreases with induction of cholinergic properties in cultured sympathetic neurons. *J Neurosci, 3*(7), 1495-1500.

Xie, Y., Yin, T., Wiegraebe, W., He, X. C., Miller, D., Stark, D., . . . Li, L. (2009). Detection of functional haematopoietic stem cell niche using real-time imaging. *Nature, 457*(7225), 97-101. doi: 10.1038/nature07639

Yamazaki, K., & Allen, T. D. (1990). Ultrastructural morphometric study of efferent nerve terminals on murine bone marrow stromal cells, and the recognition of a novel anatomical unit: the "neuro-reticular complex". *Am J Anat, 187*(3), 261-276. doi: 10.1002/aja.1001870306

Yamazaki, S., Ema, H., Karlsson, G., Yamaguchi, T., Miyoshi, H., Shioda, S., . . . Nakauchi, H. (2011). Nonmyelinating Schwann cells maintain hematopoietic stem cell hibernation in the bone marrow niche. *Cell, 147*(5), 1146-1158. doi: 10.1016/j.cell.2011.09.053

Yang, B., Slonimsky, J. D., & Birren, S. J. (2002). A rapid switch in sympathetic neurotransmitter release properties mediated by the p75 receptor. *Nat Neurosci, 5*(6), 539-545. doi: 10.1038/nn853

Yoshihara, H., Arai, F., Hosokawa, K., Hagiwara, T., Takubo, K., Nakamura, Y., . . . Suda, T. (2007). Thrombopoietin/MPL signaling regulates hematopoietic stem cell quiescence and interaction with the osteoblastic niche. *Cell Stem Cell, 1*(6), 685-697. doi: 10.1016/j.stem.2007.10.020

Zanjani, E. D., Ascensao, J. L., & Tavassoli, M. (1993). Liver-derived fetal hematopoietic stem cells selectively and preferentially home to the fetal bone marrow. *Blood, 81*(2), 399-404.

Zhang, J., Niu, C., Ye, L., Huang, H., He, X., Tong, W. G., . . . Li, L. (2003). Identification of the haematopoietic stem cell niche and control of the niche size. *Nature, 425*(6960), 836-841. doi: 10.1038/nature02041

Zhao, M., Perry, J. M., Marshall, H., Venkatraman, A., Qian, P., He, X. C., . . . Li, L. (2014). Megakaryocytes maintain homeostatic quiescence and promote post-injury regeneration of hematopoietic stem cells. *Nat Med, 20*(11), 1321-1326. doi: 10.1038/nm.3706

Zhou, B. O., Ding, L., & Morrison, S. J. (2015). Hematopoietic stem and progenitor cells regulate the regeneration of their niche by secreting Angiopoietin-1. *Elife, 4*, e05521. doi: 10.7554/eLife.05521

Zhou, B. O., Yue, R., Murphy, M. M., Peyer, J. G., & Morrison, S. J. (2014). Leptin-receptor-expressing mesenchymal stromal cells represent the main source of bone formed by adult bone marrow. *Cell Stem Cell, 15*(2), 154-168. doi: 10.1016/j.stem.2014.06.008

Publications

García-García, A., Korn, C., García-Fernández, M., Fielding, F., Isern, J., Martín-Pérez, D., Lau, WW., Diamanti, E., Del Toro, R., Skepper, JN., Sendtner, R., Sendtner, M., Green, AR., Göttgens, B., Airaksinen, MS. & Méndez-Ferrer, S. Spatiotemporal regulation of blood stem cell niches by dual cholinergic signalling. *(Submitted)*

García-García, A., & Méndez-Ferrer, S. (2017). Chapter Three-The Role of the CNS in the Regulation of HSCs. *Advances in Stem Cells and their Niches*, *1*, 35-57.

Garcia-Garcia, A., de Castillejo, C. L., & Méndez-Ferrer, S. (2015). BMSCs and hematopoiesis. *Immunology letters, 168(2)*, 129-135.

Sánchez-Aguilera, A., Arranz, L., Martín-Pérez, D., García-García, A., Stavropoulou, V., Kubovcakova, L., ... & Schwaller, J. (2014). Estrogen signaling selectively induces apoptosis of hematopoietic progenitors and myeloid neoplasms without harming steady-state hematopoiesis. *Cell stem cell, 15(6)*, 791-804.

Isern, J., García-García, A., Martín, A. M., Arranz, L., Martín-Pérez, D., Torroja, C., ... & Méndez-Ferrer, S. (2014). The neural crest is a source of mesenchymal stem cells with specialized hematopoietic stem cell niche function. *Elife, 3*, e03696.